Engineering Dynamics

Lecture Notes
Draft, V 3.0

Daniel J. Rixen

Prof. Dr. Ir., MSc.

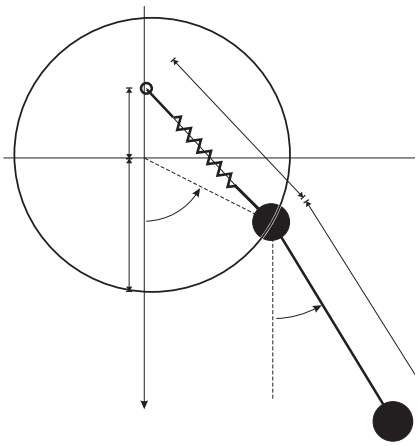

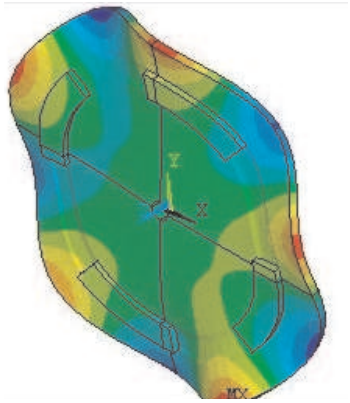

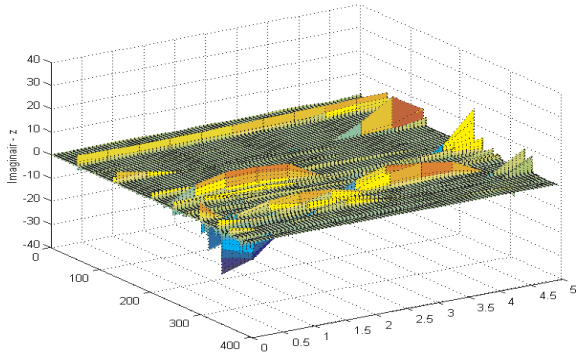

Delft University of Technology
Faculty of Mechanical, Maritime and Materials Engineering
Section of Engineering Dynamics

Sept 2008

Contents

List of Figures

Introduction

Dynamics of systems is at the heart of many engineering fields. In mechanical engineering, the dynamic description of structural and electro-mechanical is the starting point for the design and the control of advanced products. It is therefore a discipline that must be mastered by mechanical engineering students who want to specialize in system controls and in mechanical analysis and simulation.

In this lecture we intend to lay out the fundamental principles of dynamics and to bring the student to a level where he masters the essential concepts such as degrees of freedoms, constraints, vibration, mode superposition ... Hence we expect that the student will study to **understand** those essential concepts and not to memorize difficult formulas. Understanding is for the student's life, memorizing is just for the exam ... That is why during the exam the student will be asked to answer a theoretical question and to solve an exercise having access to his lecture notes. In that way he can demonstrate how much he really understands! Hopefully after having followed this course student will no longer think that engineering dynamics is a *religion* (see Calvin and Hobbes strip below), but will be enthusiastic about the different facets of engineering they are able to comprehend ... An ambitious program.

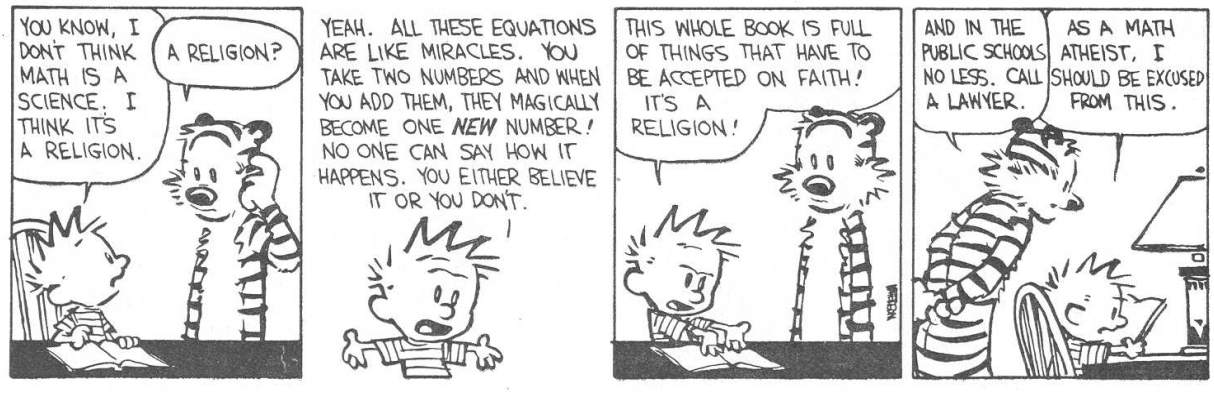

Figure 1: Sciences should not be a religion to our students, but become a way of thinking for themselves (strip extract from *Calvin and Hobbes, Attack of the deranged mutant killer monster snow goons, Bill Watterson, ed. Andrews and McMeel, Kansas City, 1992*)

The student is supposed to be acquainted with statics, engineering mechanics and basic dynamic principles (i.e. kinematics and Newton laws). We also assume the student has fundamental knowledge in vector theory, algebra and calculus. The numerical aspects involved in the solution of the dynamic formulations described in this course are not included here. Numerical issues are discussed in another course (wb1416) and can also be found in textbooks (see references).

Notations

In the text, we will use bold characters to denote matrices. Lower case bold symbols will represent uni-column matrices whereas upper case ones denote multi-column matrices. For instance,

$$\boldsymbol{a} = \begin{bmatrix} a_1 \\ a_2 \\ \vdots \end{bmatrix}$$

and

$$\boldsymbol{A} = \begin{bmatrix} a_{11} & a_{12} & a_{13} & \cdots \\ a_{21} & a_{22} & \cdots & \\ a_{31} & \vdots & \ddots & \\ \vdots & & & \end{bmatrix}$$

Non-bold symbols represent scalars.

Chapter 1

Analytical Dynamics of discrete systems

The analytical approach to mechanics, unlike vector mechanics, is based on the concepts of energy and work and therefore provides a better understanding of mechanical phenomena. It provides at the same time a very powerful tool for two main reasons:

- It considerably simplifies the analytical formulation of the motion equations for a complex mechanical system.
- It gives rise to approximate numerical methods for the solution of both discrete and continuous systems in the most natural manner.

The objective of this chapter is to recall to the reader, starting from the principle of virtual work, how the concept of degrees of freedom of a system is naturally introduced and how Lagrange equations are derived.

1.1 Principle of virtual work for a particle

Let us consider a particle of mass m, submitted to a force field $\overrightarrow{X}$ of components X_i in an inertial frame. The dynamic equilibrium of the particle can be expressed in d'Alembert's form

$$m\ddot{u}_i - X_i = 0 \qquad\qquad i = 1, 2, 3 \tag{1.1}$$

where u_i represents the displacement of the particle.

Let us next imagine that the particle follows during the time interval $[t_1, t_2]$ a motion trajectory ${u_i}^*$ distinct from the real one u_i. This allows us to define the virtual displacement of the particle by the relationship (figure 1.1)

$$\delta u_i = {u_i}^* - u_i \tag{1.2}$$

By its very definition, the virtual displacement δu_i is arbitrary for $t_1 < t < t_2$.

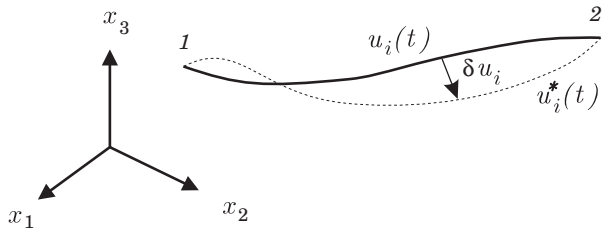

Figure 1.1: Virtual Displacement of a particle

Let us next multiply the dynamic equilibrium equations (1.1) by the associated virtual displacement and sum over the components: the virtual work expression results

$$\sum_{i=1}^{3}\big(m\ddot{u}_i - X_i\big)\delta u_i = 0 \tag{1.3}$$

This expression represents the scalar product between the forces acting on the particle and the virtual displacement $\overrightarrow{\delta u}$. It thus represents the *projection of the equilibrium along the direction* $\overrightarrow{\delta u}$. If (1.3) is satisfied for all variations δu_i, then the trajectory $u_i(t)$ satisfies the dynamic equilibrium in all directions.

If no kinematical constraint is imposed onto the particle, namely of no restriction is imposed on the possible displacement of the particle, the trajectory of the material point is determined by the equilibrium in all directions.

If kinematic constraints are specified for the particle, there exist reaction forces on top of the applied forces. These reaction forces ensure that the imposed kinematical constraints are satisfied and depend on the trajectory itself. Hence they are unknown *a priori*. Figure 1.2 describes a particle constrained to move along a plane curve and a spherical pendulum where a particle is constrained to have a constant distance with respect to a fixed point. On one hand, the presence of reaction forces acting in the direction of the constraint generally renders the equilibrium description more complex since those unknown forces must be determined along the entire trajectory such that kinematical constraints are satisfied. On the other hand, solving the equilibrium equations in the direction constrained by the kinematical conditions is not useful since, in that direction, the trajectory is prescribed by the constrained and thus known.

In the system described in figure 1.2.a only the motion along the direction tangent to the curve needs to be determined. In doing so, the reaction forces, which act in the direction normal to the curve, do not participate to the motion and thus need not to be determined. The position of the particle in the direction normal to the curve is obviously imposed by the constraint and does not require solving the equilibrium equation in that

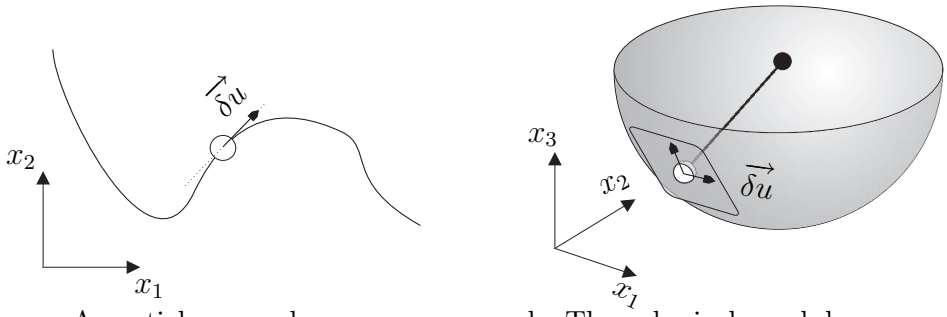

a. A particle on a plane curve b. The spherical pendulum

Figure 1.2: Kinematically admissible virtual displacements

direction. In the same way, if the equilibrium of the particle of the spherical pendulum is expressed in the plane tangent to the sphere (figure 1.2.b), only the forces actually applied participate to determine the trajectory.

Let us therefore decide that, in the presence of kinematical constraints, we consider only virtual displacements δu_i *compatible with the constraints* or, in other words, *kinematically admissible*. Equation (1.3) then describes the projection of the dynamic equilibrium in the space compatible with the constraints, namely in directions orthogonal to unknown reaction forces. The form (1.3) does thus involve only effectively applied forces and stipulates that

> *the virtual work produced by the effective forces acting on the particle during a virtual displacement δu_i compatible with the constraints is equal to zero.*

This is the virtual *work principle* for a particle. Also, equations (1.3) indicates that

> *if the trajectory u_i of the particle is such that the effectively applied forces produce no virtual work for any virtual displacement compatible with the constraints, the equilibrium is then satisfied.*

The usefulness of the virtual work principle comes from the fact that it allows to express the dynamic equilibrium in a simple manner along the directions compatible with the constraints.

1.2 Equations of motion for a system of N particles

1.2.1 Virtual work principle for N particles

Every particle k of a system of N particles with mass m_k satisfies the dynamic equilibrium

$$m_k \ddot{u}_{ik} - X_{ik} - R_{ik} = 0 \qquad \begin{matrix} i = 1,2,3 \\ k = 1,\ldots,N \end{matrix} \tag{1.4}$$

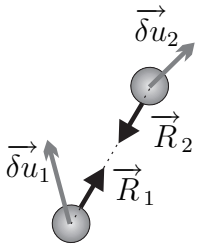

Figure 1.3: Virtual work of constraints between particles

where X_{ik} are the force components representing the known external forces and where R_{ik} are the unknown reactions resulting from the kinematic constraints imposed on the system.

For every particle k, one considers virtual displacements δu_{ik} such as

$$\delta u_{ik} = {u_{ik}}^* - u_{ik} \qquad\qquad i = 1, 2, 3 \tag{1.5}$$

The virtual work principle is obtained by projecting the dynamic equilibrium equations on the virtual displacements and by summing up over the particles:

$$\sum_{k=1}^{N} \sum_{i=1}^{3} \Big(m_k \ddot{u}_{ik} - X_{ik} - R_{ik} \Big) \delta u_{ik} = 0 \tag{1.6}$$

As for the case of one particle, we decide to consider only virtual displacement *compatible with the constraints*. Hence, the virtual displacements must satisfy constraints imposed on one particle as well as constraints imposed between particles. The situation where two points are rigidly linked to one another is an important example of such constraints. In that case, the reaction forces linking the particles are equal and opposite (figure 1.3):

$$\overrightarrow{R}_1 + \overrightarrow{R}_2 = 0$$

and the virtual work associated to a virtual displacement $(\overrightarrow{\delta u_1}, \overrightarrow{\delta u_2})$ is

$$\delta\tau = \sum_{i=1}^{3} \big(R_{i1} \delta u_{i1} + R_{i2} \delta u_{i2} \big) = \overrightarrow{R}_1 \cdot \overrightarrow{\delta u_1} + \overrightarrow{R}_2 \cdot \overrightarrow{\delta u_2} = \overrightarrow{R}_1 \cdot \Big(\overrightarrow{\delta u_1} - \overrightarrow{\delta u_2} \Big) = 0$$

since the compatible virtual displacements must be equal in the direction of the rigid link. Projecting the equations onto the kinematically admissible displacements thus consists in summing up the equilibrium equations in the constrained direction such that the unknown linking forces vanish.

Since the reaction forces do vanish when projecting the equations of motion onto kinematically admissible displacement directions, the virtual work principle (1.6) writes

$$\boxed{\sum_{k=1}^{N} \sum_{i=1}^{3} \Big(m_k \ddot{u}_{ik} - X_{ik} \Big) \delta u_{ik} = 0} \tag{1.7}$$

As for the case of a single particle, the virtual work principle thus states that

the virtual work of the forces effectively applied onto a system of particles is zero with respect to any kinematically compatible virtual displacement ***if and only if*** *the system is in dynamic equilibrium.*

Again, the principle of virtual work corresponds to the projection of the equilibrium equations in the directions compatible with the kinematical constraints. The resulting equations are then easier to solve since the constraining forces are no longer unknowns in the problem.

1.2.2 Kinematic constraints

Figure 1.4: Talking about constraints ....

Without kinematic constraints, the state of the system would be completely defined by the $3N$ displacement components u_{ik} since, starting from a reference configuration x_{ik}, they represent the instantaneous configuration

$$\xi_{ik}(t) = x_{ik} + u_{ik}(x_{jk}, t) \qquad \begin{matrix} i,j = 1,2,3 \\ k = 1,\ldots,N \end{matrix} \tag{1.8}$$

The system is then said to possess $3N$ degrees of freedom.

In most mechanical systems, however, the particles are submitted to kinematic constraints which restrain their motion and define dependency relationships between particles.

Holonomic constraints Holonomic constraints[1] are defined as constraints that can be expressed as implicit relationships of the type

$$f\big(\xi_{ik}, t\big) = 0 \tag{1.9}$$

which relate particle positions. If the relationship (1.9) is not dependent on time, the constraints are said to be *scleronomic*. Otherwise they are said to be *rheonomic*.

Equations of the type of (1.9) define a direct relationship between possible displacements. They can therefore be accounted for when expressing admissible displacements. Hence,

> *a holonomic constraint reduces by one the number of degrees of freedom of the system.*

Example 1: rigid link

Let us consider the case of two mass particles connected by a rigid bar of length ℓ. Their instantaneous positions ξ_{i1} and ξ_{i2} verify the relationship

$$f\big(\xi_{ik}, t\big) = \sum_{i=1}^{3} \big(\xi_{i2} - \xi_{i1}\big)^2 - \ell^2 = 0$$

Taking the variation of the constraint with respect to virtual displacements,

$$\delta f = \sum_{i=1}^{3} \big((\xi_{i1} - \xi_{i2})\delta u_{i1} - (\xi_{i1} - \xi_{i2})\delta u_{i2}\big) = 0$$

indicating that virtual displacements must satisfy

$$\Big(\overrightarrow{\xi}_1 - \overrightarrow{\xi}_2\Big) \cdot \overrightarrow{\delta u}_1 = \Big(\overrightarrow{\xi}_1 - \overrightarrow{\xi}_2\Big) \cdot \overrightarrow{\delta u}_2$$

Hence virtual displacements must be equal in the direction of the link (see figure 1.3). A system of 2 particles that are rigidly linked has $6 - 1 = 5$ degrees of freedom.

Example 2: rigid bodies

Let us consider a system of N particles rigidly linked and forming a rigid body in space. Every individual particle has 3 degrees of freedom if it would not be rigidly linked. By definition, the particles forming a rigid body, the distance between any pair of particles is constant. If the system is made of 2 particles ($N = 2$), one constraint can be defined. If a particle is then added to the system of 2 particles, 2 additional constraints must be defined in order to ensure that the third particle has a constant distance with respect to the 2 previous. For any additional particle in the system, 3 additional non-redundant constraints must be defined in order to ensure that the particle is rigidly connected to the system. Hence, for a system of N particles rigidly linked, $1 + 2 + 3(N - 3)$ non-redundant holonomic constraints can be defined so that the system has $3N - (1 + 2 + 3(N - 3)) = 6$ degrees of freedom.

[1] from the Greek words *holos*, "entire", and *nemein*, "to govern", hence "'which governs the behavior entirely".

Non-holonomic constraints Constraints are said to be *non-holonomic* if they can not be put in the form (1.9). In particular, non-holonomic constraints are most often expressed as a differential relation of the form

$$f^{nh}\big(\dot{\xi}_{ik}, \xi_{ik}, t\big) = 0 \tag{1.10}$$

Unlike holonomic constraints, these relationships can not be integrated and therefore do not allow to write an explicit relation between virtual displacements. Therefore

> *non-holonomic constraints do not reduce the number of degrees of freedom of the system.*

In fact, non-holonomic constraints act as constraints on the behavior of the system. Thus *they do not restrain the possible configurations of the system but rather the manner in which those configurations can be realized.*

Example : the thin wheel

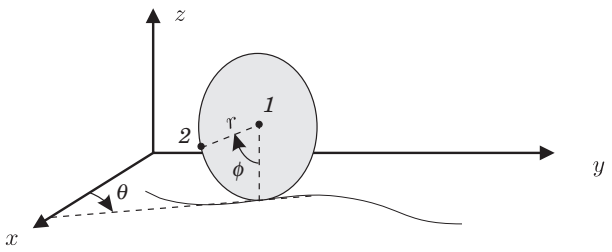

Figure 1.5: Non-holonomic constraints

Let us consider a rigid wheel of radius r, rolling without slipping on a plane (figure 1.5). We assume that the rotation axis of the wheel remains parallel to the rolling plane. Let us then consider a particle on the rim of the wheel. The rolling without splipping condition can be expressed as

$$\begin{aligned} \dot{x}_1 + r\dot{\phi}\cos\theta &= 0 \qquad (a.) \\ \dot{y}_1 - r\dot{\phi}\sin\theta &= 0 \qquad (b.) \end{aligned}$$

where ϕ and θ are the angles such that

$$\begin{aligned} x_2 - x_1 &= r\sin\phi\cos\theta \qquad (c.) \\ y_2 - y_1 &= -r\sin\phi\sin\theta \qquad (d.) \end{aligned}$$

These four relations define two implicit non-holonomic constraints between x_i and y_i. Finally, the kinematic constraints of the system also stipulate that

$$\begin{aligned} z_2 - z_1 &= -r\cos\phi \qquad (e.) \\ z_1 &= r \qquad (f.) \end{aligned}$$

One observes that the system is described by 8 variables

$$x_1, y_1, z_1, x_2, y_2, z_2, \phi, \theta$$

and is subjected to

- 2 non-holonomic constraints (a.) and (b.) ;
- 4 holonomic constraints (c.), (d.), (e.) and (f.).

Only the holonomic constraints restrain the degrees of freedom of the wheel. The 4 remaining degrees of freedom are represented by 2 translations of the center of the wheel in the plane, the rotation of the wheel around its axis and the rotation of the wheel around an axis perpendicular to the plane. The non-holonomic constraints act as constraints on the instantaneous trajectory, but not on the possible configuration of the system.

1.2.3 Generalized coordinates and equations of motion

If R kinematic constraints exist between the $3N$ displacement components of the system, the number of degrees of freedom is reduced to $3N - R$. It is then necessary to define $n = 3N - R$ configuration parameters, or *generalized coordinates*, denoted $(q_1, \ldots, q_n)$ in terms of which the displacements of the system particles are expressed in the form

$$u_{ik}(x_{jk}, t) = U_{ik}(q_1, \ldots, q_n, t) \tag{1.11}$$

When only holonomic constraints are applied to the system, the generalized coordinates q_s are independent and may be varied in an arbitrary manner without violating the kinematic constraints. The virtual displacements δu_{ik} compatible with the holonomic constraints may be expressed in the form

$$\delta u_{ik} = \sum_{s=1}^{n} \frac{\partial U_{ik}}{\partial q_s} \delta q_s \tag{1.12}$$

The virtual work equation becomes

$$\boxed{\sum_{s=1}^{n} \left[\sum_{k=1}^{N} \sum_{i=1}^{3} \left(m_k \ddot{u}_{ik} - X_{ik}\right) \frac{\partial U_{ik}}{\partial q_s} \right] \delta q_s = 0} \tag{1.13}$$

The coefficients $\frac{\partial U_{ik}}{\partial q_s}$ define the displacement directions of mass k when the generalized coordinate q_s is varied. The variations δq_s are totally independent by definition, meaning that they can be chosen arbitrarily without violating any kinematic constraint. The identity (1.13) being satisfied for any virtual displacement, it follows that each associated term in the virtual work (1.13) principal must be zero. These terms correspond to the equilibrium projected onto the direction of the generalized coordinate q_s and writes

$$\boxed{\sum_{k=1}^{N} \sum_{i=1}^{3} \left(m_k \frac{d^2 U_{ik}(q_1, \ldots, q_n, t)}{dt^2} - X_{ik} \right) \frac{\partial U_{ik}}{\partial q_s} = 0 \qquad s = 1, \cdots n} \tag{1.14}$$

The second term in this equation corresponds to the *generalized force* conjugate to the degree of freedom q_s:

$$Q_s = \sum_{k=1}^{N} \sum_{i=1}^{3} X_{ik} \frac{\partial U_{ik}}{\partial q_s} \tag{1.15}$$

The first term in (1.14) has the meaning of a generalized inertia force.

Example 1: the pendulum

Figure 1.6 depicts a simple two-dimensional pendulum. The system has $2 - 1 = 1$

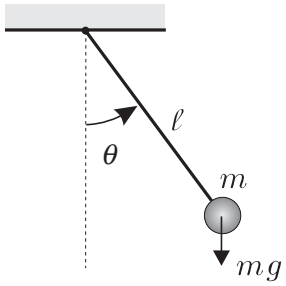

Figure 1.6: The pendulum

degrees of freedom and we choose θ as generalized coordinate so that equation (1.11) for the pendulum is

$$\begin{aligned} u_1 &= \ell\cos\theta - \ell \\ u_2 &= \ell\sin\theta \end{aligned}$$

so the compatible virtual displacements are

$$\begin{aligned} \delta u_1 &= (-\ell\sin\theta)\ \delta\theta \\ \delta u_2 &= (\ell\cos\theta)\ \delta\theta \end{aligned}$$

The virtual work equation then writes

$$(m\ddot{u}_1 - mg)(-\ell\sin\theta) + (m\ddot{u}_2)(\ell\cos\theta) = 0$$

The accelerations can be expressed as

$$\begin{aligned} \ddot{u}_1 &= -\ell\ddot{\theta}\sin\theta - \ell\dot{\theta}^2\cos\theta \\ \ddot{u}_2 &= \ell\ddot{\theta}\cos\theta - \ell\dot{\theta}^2\sin\theta \end{aligned}$$

and thus the equation of motion is

$$m\ell^2\ddot{\theta} + mg\ell\sin\theta = 0$$

Example 2: the double pendulum

Let us consider the double pendulum of figure 1.7. The system is made of two mass particles. The motion is restricted to 2-D motion, so that its kinematics is described by the four instantaneous position components ξ_{ik}. The two holonomic constraints applied to the system express the length invariance of the members:

$$\begin{aligned} \xi_{11}^2 + \xi_{21}^2 &= \ell_1^2 \\ \left(\xi_{12} - \xi_{11}\right)^2 + \left(\xi_{22} - \xi_{21}\right)^2 &= \ell_2^2 \end{aligned}$$

The system kinematics may thus be described in terms of $4 - 2 = 2$ generalized

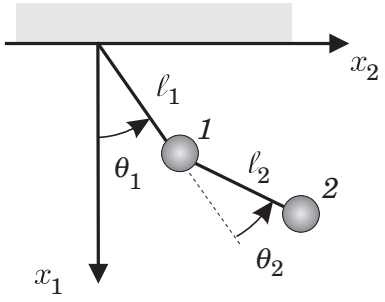

Figure 1.7: The double pendulum

coordinates. One may adopt the two rotation angles of the pendulum θ_1 and θ_2:

$$\begin{aligned}
\xi_{11} &= \ell_1 \cos\theta_1 \\
\xi_{21} &= \ell_1 \sin\theta_1 \\
\xi_{12} &= \xi_{11} + \ell_2 \cos(\theta_1+\theta_2) = \ell_1 \cos\theta_1 + \ell_2 \cos(\theta_1+\theta_2) \\
\xi_{22} &= \xi_{21} + \ell_2 \sin(\theta_1+\theta_2) = \ell_1 \sin\theta_1 + \ell_2 \sin(\theta_1+\theta_2)
\end{aligned}$$

These equations define the relation (1.11) for the double pendulum. Taking the variation of these relations

$$\begin{aligned}
\begin{bmatrix}\delta u_{11}\\ \delta u_{21}\end{bmatrix} &= \begin{bmatrix}-\ell_1\sin\theta_1 & 0\\ \ell_1\cos\theta_1 & 0\end{bmatrix}\begin{bmatrix}\delta\theta_1\\ \delta\theta_2\end{bmatrix} \\
\begin{bmatrix}\delta u_{12}\\ \delta u_{22}\end{bmatrix} &= \begin{bmatrix}-\ell_1\sin\theta_1 - \ell_2\sin(\theta_1+\theta_2) & -\ell_2\sin(\theta_1+\theta_2)\\ \ell_1\cos\theta_1 + \ell_2\cos(\theta_1+\theta_2) & \ell_2\cos(\theta_1+\theta_2)\end{bmatrix}\begin{bmatrix}\delta\theta_1\\ \delta\theta_2\end{bmatrix}
\end{aligned}$$

Comparing to (1.12), the matrices here above correspond to $\frac{\partial U_{ik}}{\partial q_s}$ and the reader can verify on figure 1.7 that their columns define the displacement directions associated to $\delta\theta_1$ and $\delta\theta_2$. Calling $\overrightarrow{F}_1$ and $\overrightarrow{F}_2$ the forces effectively applied on mass 1 and 2 respectively, the virtual work principle (1.13) then writes $\overrightarrow{\delta u}_1 \cdot \overrightarrow{F}_1 + \overrightarrow{\delta u}_2 \cdot \overrightarrow{F}_2 = 0$. Hence

$$\begin{aligned}
&\begin{bmatrix}\delta\theta_1 & \delta\theta_2\end{bmatrix}\begin{bmatrix}-\ell_1\sin\theta_1 & \ell_1\cos\theta_1\\ 0 & 0\end{bmatrix}\begin{bmatrix}m_1\ddot{u}_{11} - mg\\ m_1\ddot{u}_{21}\end{bmatrix} \\
&+\begin{bmatrix}\delta\theta_1 & \delta\theta_2\end{bmatrix}\begin{bmatrix}-\ell_1\sin\theta_1 - \ell_2\sin(\theta_1+\theta_2) & \ell_1\cos\theta_1 + \ell_2\cos(\theta_1+\theta_2)\\ -\ell_2\sin(\theta_1+\theta_2) & \ell_2\cos(\theta_1+\theta_2)\end{bmatrix}\begin{bmatrix}m_2\ddot{u}_{12} - mg\\ m_2\ddot{u}_{22}\end{bmatrix} = 0
\end{aligned}$$

This relation being satisfied for any variation $\delta\theta_1$ and $\delta\theta_2$, we obtain the equations of motion

$$\begin{aligned}
&\begin{bmatrix}-\ell_1\sin\theta_1 & \ell_1\cos\theta_1\\ 0 & 0\end{bmatrix}\begin{bmatrix}m_1\ddot{u}_{11} - mg\\ m_1\ddot{u}_{21}\end{bmatrix} \\
&+\begin{bmatrix}-\ell_1\sin\theta_1 - \ell_2\sin(\theta_1+\theta_2) & \ell_1\cos\theta_1 + \ell_2\cos(\theta_1+\theta_2)\\ -\ell_2\sin(\theta_1+\theta_2) & \ell_2\cos(\theta_1+\theta_2)\end{bmatrix}\begin{bmatrix}m_2\ddot{u}_{12} - mg\\ m_2\ddot{u}_{22}\end{bmatrix} = 0
\end{aligned}$$

Expressing then the accelerations in terms of the degrees of freedom θ_1 and θ_2 using the kinematic relations above, one obtains the two equations of motion to determine the generalized displacements.

Example 3: the plane rigid body

Let us consider a group of N particles on a plane and let us assume that their motion is constrained to be in the plane (figure 1.8). If we also assume that the particles are rigidly linked, 3 degrees of freedom exist for the system. These degrees of freedom are chosen to be the 2 translations along orthogonal inertial axis of a point O on the rigid body and the rotation around a rotation axis perpendicular to the plane and passing through the point O.

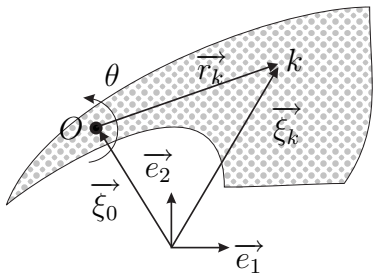

Figure 1.8: System of particles on a two-dimensional rigid body

The position of mass k can thus be expressed as

$$\overrightarrow{\xi_k} = \overrightarrow{\xi_O} + \overrightarrow{r_k}(\theta)$$

where θ is the rotation angle and $\overrightarrow{r_k}$ is the vector describing the position of particle k with respect to O. The virtual displacement compatible with the rigid constraints is thus

$$\delta\overrightarrow{u_k} = \delta\overrightarrow{u_O} + \delta\overrightarrow{r_k} = \delta\overrightarrow{u_O} + \overrightarrow{e_3} \times \overrightarrow{r_k}\delta\theta$$

where $\overrightarrow{e_3}$ is the unit vector out of plane. The equilibrium equations for a particle writes

$$m_k\ddot{\overrightarrow{u_k}} - \overrightarrow{X_k} - \overrightarrow{R_k} = 0$$

where $\overrightarrow{X_k}$ are the applied forces and $\overrightarrow{R_k}$ are the reaction forces associated to the rigid link constraints. Projecting these equations on the virtual displacements and summing over the particles,

$$\sum_{k=1}^{N} \left(m_k\ddot{\overrightarrow{u_k}} - \overrightarrow{X_k} - \overrightarrow{R_k} \right) \cdot \delta\overrightarrow{u_k} = 0$$

Noting that $\sum_{k=1}^{N} \overrightarrow{R_k} \cdot \delta\overrightarrow{u_k} = 0$ for virtual displacements compatible with the rigid link constraints, we find

$$\sum_{k=1}^{N} \left(m_k\ddot{\overrightarrow{u_k}} - \overrightarrow{X_k} \right) \cdot (\delta\overrightarrow{u_O} + \overrightarrow{e_3} \times \overrightarrow{r_k}\delta\theta) = 0$$

which is the virtual work principle. Since this relation is true for any arbitrary variation, one obtains

$$\begin{aligned} \sum_{k=1}^{N} m_k \ddot{\overrightarrow{u_k}} &= \sum_{k=1}^{N} \overrightarrow{X_k} && (a) \\ \sum_{k=1}^{N} m_k \overrightarrow{r_k} \times \ddot{\overrightarrow{u_k}} &= \sum_{k=1}^{N} \overrightarrow{r_k} \times \overrightarrow{X_k} && (b) \end{aligned}$$

These equations state the translation and rotation equilibrium of the rigid body under the action of inertia and applied forces. The velocity of a particle is obtained from

$$\begin{aligned} \dot{\overrightarrow{u_k}} &= \dot{\overrightarrow{u_O}} + \dot{\overrightarrow{r_k}} \\ &= \dot{\overrightarrow{u_O}} + \dot{\theta}\overrightarrow{e_3} \times \overrightarrow{r_k} \end{aligned}$$

and the acceleration is then obtained as

$$\begin{aligned} \ddot{\overrightarrow{u_k}} &= \ddot{\overrightarrow{u_O}} + \ddot{\theta}\overrightarrow{e_3} \times \overrightarrow{r_k} + \dot{\theta}\overrightarrow{e_3} \times \dot{\overrightarrow{r_k}} \\ &= \ddot{\overrightarrow{u_O}} + \ddot{\theta}\overrightarrow{e_3} \times \overrightarrow{r_k} + \dot{\theta}^2\overrightarrow{e_3} \times (\overrightarrow{e_3} \times \overrightarrow{r_k}) \\ &= \ddot{\overrightarrow{u_O}} + \ddot{\theta}\overrightarrow{e_3} \times \overrightarrow{r_k} - \dot{\theta}^2\overrightarrow{r_k} \qquad (c) \end{aligned}$$

Let us call $\overrightarrow{r_C}$ the position of the center of mass such that

$$\sum_{k=1}^{N} m_k \overrightarrow{r_k} = m_{tot}\overrightarrow{r_C}$$

where $m_{tot} = \sum_{k=1}^{N} m_k$ is the total mass. Substituting then the expression for the accelerations (c) in the motion equations (a) and (b) one finds

$$\begin{aligned} m_{tot}\ddot{\overrightarrow{u_O}} + m_{tot}\overrightarrow{e_3} \times \overrightarrow{r_C}\ddot{\theta} - m_{tot}\overrightarrow{r_C}\dot{\theta}^2 &= \sum_{k=1}^{N} \overrightarrow{X_k} \\ m_{tot}\overrightarrow{r_C} \times \ddot{\overrightarrow{u_O}} + \sum_{k=1}^{N} m_k \overrightarrow{r_k} \times (\overrightarrow{e_3} \times \overrightarrow{r_k})\,\ddot{\theta} &= \sum_{k=1}^{N} \overrightarrow{r_k} \times \overrightarrow{X_k} \end{aligned}$$

Finally, since $\overrightarrow{r_k} \times (\overrightarrow{e_3} \times \overrightarrow{r_k}) = \|\overrightarrow{r_k}\|^2\overrightarrow{e_3}$, we define the rotational inertia $J_O = \sum_{k=1}^{N} m_k\|\overrightarrow{r_k}\|^2$ so that the equations of motion take the form

$$\begin{aligned} m_{tot}\ddot{\overrightarrow{u_O}} + m_{tot}\overrightarrow{e_3} \times \overrightarrow{r_C}\ddot{\theta} - m_{tot}\overrightarrow{r_C}\dot{\theta}^2 &= \sum_{k=1}^{N} \overrightarrow{X_k} \\ m_{tot}\overrightarrow{r_C} \times \ddot{\overrightarrow{u_O}} + J_0\overrightarrow{e_3}\ddot{\theta} &= \sum_{k=1}^{N} \overrightarrow{r_k} \times \overrightarrow{X_k} \end{aligned}$$

1.3 Lagrange equations

The virtual work principle discussed in the previous chapter defines a procedure to obtain the equations of motion where all the unknown forces due to kinematical constraints vanish. The basic idea of the virtual work principle is to project the equation of motions of all individual particles onto a direction compatible with the constraints. However, as seen in the examples of the double pendulum, applying the virtual work principal still requires lengthy mathematical manipulations.

Therefore, we introduce in this section a different, though equivalent, way to derive the equation of motions in terms of the generalized coordinates: the Lagrange equations. These equations involve the energy of the system which often facilitates the set up of the equation of motions. However, in the energy description of the system and when applying the Lagrange equations, the physical interpretation in the sense of Newton's law is often lost.

Photo taken in Turino (courtesy of D. LoConte 2009): Joseph-Louis Lagrange, born as Giuseppe Lodovico Lagrangia, in Turino, Italy, in 1736. Mathematician and astronomer who worked in France and Prussia. He died in Paris on 1813.)

We define the kinetic energy of a system of N particle as

$$\mathcal{T} \triangleq \frac{1}{2} \sum_{k=1}^{N} \sum_{i=1}^{3} m_k \dot{u}_{ik}^2 \tag{1.16}$$

As a consequence, the inertia forces associated to the displacement u_{ik} can be derived from

$$\frac{d}{dt}\left(\frac{\partial \mathcal{T}}{\partial \dot{u}_{ik}}\right) = m_k \ddot{u}_{ik} \tag{1.17}$$

Let us then substitute (1.17) in the equations of motion (1.14) derived from the virtual work principle:

$$\sum_{k=1}^{N} \sum_{i=1}^{3} \left(\frac{d}{dt}\left(\frac{\partial \mathcal{T}}{\partial \dot{u}_{ik}}\right) - X_{ik}\right) \frac{\partial u_{ik}}{\partial q_s} = 0 \qquad s = 1, \cdots n \tag{1.18}$$

We then note that

$$\frac{d}{dt}\left(\frac{\partial \mathcal{T}}{\partial \dot{u}_{ik}}\frac{\partial u_{ik}}{\partial q_s}\right) = \frac{d}{dt}\left(\frac{\partial \mathcal{T}}{\partial \dot{u}_{ik}}\right)\frac{\partial u_{ik}}{\partial q_s} + \frac{\partial \mathcal{T}}{\partial \dot{u}_{ik}}\frac{d}{dt}\left(\frac{\partial u_{ik}}{\partial q_s}\right) \tag{1.19}$$

The equation (1.18) thus writes

$$\sum_{k=1}^{N}\sum_{i=1}^{3}\left(\frac{d}{dt}\left(\frac{\partial \mathcal{T}}{\partial \dot{u}_{ik}}\frac{\partial u_{ik}}{\partial q_s}\right) - \frac{\partial \mathcal{T}}{\partial \dot{u}_{ik}}\frac{d}{dt}\left(\frac{\partial u_{ik}}{\partial q_s}\right) - X_{ik}\frac{\partial u_{ik}}{\partial q_s}\right) = 0 \qquad s = 1, \cdots n \tag{1.20}$$

Also, since according to (1.11)

$$\dot{u}_{ik} = \frac{\partial u_{ik}}{\partial t} + \sum_{s=1}^{n}\frac{\partial u_{ik}}{\partial q_s}\dot{q}_s \tag{1.21}$$

we have

$$\frac{\partial \dot{u}_{ik}}{\partial \dot{q}_s} = \frac{\partial u_{ik}}{\partial q_s} \tag{1.22}$$

Substituting this result into the first term of (1.20) and recalling the chain rule for derivation, the equation of motion associated to the degree of freedom q_s now takes the form

$$\frac{d}{dt}\frac{\partial \mathcal{T}}{\partial \dot{q}_s} - \frac{\partial \mathcal{T}}{\partial q_s} - Q_s = 0 \qquad s = 1, \cdots n \tag{1.23}$$

where Q_s is, as defined in (1.15), the generalized force associated to q_s.

In the case where a potential $\mathcal{V}$ can be defined such that the forces are derived as

$$X_{ik} = -\frac{\partial \mathcal{V}}{\partial u_{ik}} \tag{1.24}$$

the forces are called *conservative* since it can be shown that the total energy is then conserved (see section 3.2.1). The generalized conservative forces can be obtained as

$$Q_s^{cons} = -\sum_{k=1}^{N}\sum_{i=1}^{3}\frac{\partial \mathcal{V}}{\partial u_{ik}}\frac{\partial u_{ik}}{\partial q_s} = -\frac{\partial \mathcal{V}}{\partial q_s} \tag{1.25}$$

Finally, in the case where conservative and non-conservative forces Q_s^{ncons} are applied on a system, the Lagrange equations state that the dynamic equilibrium of the system is expressed in terms of its generalized coordinates by the n equations

$$\boxed{\frac{d}{dt}\frac{\partial \mathcal{T}}{\partial \dot{q}_s} - \frac{\partial \mathcal{T}}{\partial q_s} + \frac{\partial \mathcal{V}}{\partial q_s} - Q_s^{ncons} = 0 \qquad s = 1, \cdots n} \tag{1.26}$$

Using the Lagrange equations, the construction of the equation of motions from the energy expression can be automated using symbolic computation software.

Example 1: the pendulum

Consider the simple two-dimensional pendulum described in figure 1.6. As found before we can choose the angle θ as degree of freedom so that

$$\begin{aligned} u_1 &= \ell\cos\theta - \ell \\ u_2 &= \ell\sin\theta \end{aligned}$$

and

$$\begin{aligned} \dot{u}_1 &= (-\ell\sin\theta)\,\dot{\theta} \\ \dot{u}_2 &= (\ell\cos\theta)\,\dot{\theta} \end{aligned}$$

The kinetic and potential energy of the system are then written for θ:

$$\begin{aligned} \mathcal{T} &= \frac{1}{2}m(\dot{u}_1^2 + \dot{u}_2^2) = \frac{1}{2}m\ell^2\dot{\theta}^2 \\ \mathcal{V} &= -mgu_1 = mg\ell(1-\cos\theta) \end{aligned}$$

We verify that the definition of the potential energy is such that $-\partial V/\partial u_1$ yields the applied force in direction of u_1.

One computes

$$\begin{aligned} \frac{d}{dt}\frac{\partial\mathcal{T}}{\partial\dot{\theta}} &= \frac{d}{dt}\left(m\ell^2\dot{\theta}\right) = m\ell^2\ddot{\theta} \\ \frac{\partial\mathcal{T}}{\partial\theta} &= 0 \\ \frac{\partial\mathcal{V}}{\partial\theta} &= mg\ell\sin\theta \end{aligned}$$

The Lagrange equation thus yields

$$m\ell^2\ddot{\theta} + mg\ell\sin\theta = 0$$

Example 2: the double pendulum

Let us once more consider the double pendulum described in figure 1.7 where the angles θ_1 and θ_2 are chosen as generalized degrees of freedom. In order to derive the equations of motion from the Lagrange equations, we must first express the kinetic energy of the system in terms of the generalized coordinates. Using the kinematic relations

$$\begin{aligned} \xi_{11} &= \ell_1\cos\theta_1 \\ \xi_{21} &= \ell_1\sin\theta_1 \\ \xi_{12} &= \xi_{11} + \ell_2\cos(\theta_1+\theta_2) = \ell_1\cos\theta_1 + \ell_2\cos(\theta_1+\theta_2) \\ \xi_{22} &= \xi_{21} + \ell_2\sin(\theta_1+\theta_2) = \ell_1\sin\theta_1 + \ell_2\sin(\theta_1+\theta_2) \end{aligned}$$

we compute the velocities

$$\begin{aligned}
\dot{u}_{11} &= -\ell_1\dot{\theta}_1\sin\theta_1 \\
\dot{u}_{21} &= \ell_1\dot{\theta}_1\cos\theta_1 \\
\dot{u}_{12} &= -\ell_1\dot{\theta}_1\sin\theta_1 - \ell_2(\dot{\theta}_1+\dot{\theta}_2)\sin(\theta_1+\theta_2) \\
\dot{u}_{22} &= \ell_1\dot{\theta}_1\cos\theta_1 + \ell_2(\dot{\theta}_1+\dot{\theta}_2)\cos(\theta_1+\theta_2)
\end{aligned}$$

The kinetic energy is then expressed as

$$\begin{aligned}
\mathcal{T} &= \frac{1}{2}\left(m_1(\dot{u}_{11}^2+\dot{u}_{21}^2)+m_2(\dot{u}_{12}^2+\dot{u}_{22}^2)\right) \\
&= \frac{1}{2}\left(m_1\ell_1^2\dot{\theta}_1^2 + m_2\left(\ell_1^2\dot{\theta}_1^2+\ell_2^2(\dot{\theta}_1+\dot{\theta}_2)^2+2\ell_1\ell_2\dot{\theta}_1(\dot{\theta}_1+\dot{\theta}_2)\cos\theta_2\right)\right)
\end{aligned}$$

The potential energy of the system due to gravity forces is

$$\mathcal{V} = -m_1 g u_{11} - m_2 g u_{12}$$

which, in terms of the generalized coordinates is

$$\mathcal{V} = m_1 g\ell_1(1-\cos\theta_1) + m_2 g\left(\ell_1(1-\cos\theta_1)+\ell_2(1-\cos(\theta_1+\theta_2))\right)$$

Let us then compute the different terms of the Lagrange equations (1.26):

- for s=1, namely $q_s = \theta_1$,

$$\begin{aligned}
\frac{d}{dt}\frac{\partial\mathcal{T}}{\partial\dot{\theta}_1} &= \frac{d}{dt}\left(m_1\ell_1^2\dot{\theta}_1 + m_2\left(\ell_1^2\dot{\theta}_1+\ell_2^2(\dot{\theta}_1+\dot{\theta}_2)+\ell_1\ell_2(2\dot{\theta}_1+\dot{\theta}_2)\cos\theta_2\right)\right) \\
&= m_1\ell_1^2\ddot{\theta}_1 \\
&\quad + m_2\left(\ell_1^2\ddot{\theta}_1+\ell_2^2(\ddot{\theta}_1+\ddot{\theta}_2)+\ell_1\ell_2(2\ddot{\theta}_1+\ddot{\theta}_2)\cos\theta_2 - \ell_1\ell_2(2\dot{\theta}_1+\dot{\theta}_2)\dot{\theta}_2\sin\theta_2\right) \\
\frac{\partial\mathcal{T}}{\partial\theta_1} &= 0 \\
\frac{\partial\mathcal{V}}{\partial\theta_1} &= m_1 g\ell_1\sin\theta_1 + m_2 g\left(\ell_1\sin\theta_1+\ell_2\sin(\theta_1+\theta_2)\right)
\end{aligned}$$

- for s=2, namely $q_s = \theta_2$,

$$\begin{aligned}
\frac{d}{dt}\frac{\partial\mathcal{T}}{\partial\dot{\theta}_2} &= \frac{d}{dt}\left(m_2\left(\ell_2^2(\dot{\theta}_1+\dot{\theta}_2)+\ell_1\ell_2\dot{\theta}_1\cos\theta_2\right)\right) \\
&= m_2\left(\ell_2^2(\ddot{\theta}_1+\ddot{\theta}_2)+\ell_1\ell_2\ddot{\theta}_1\cos\theta_2 - \ell_1\ell_2\dot{\theta}_1\dot{\theta}_2\sin\theta_2\right) \\
\frac{\partial\mathcal{T}}{\partial\theta_2} &= -m_2\ell_1\ell_2\dot{\theta}_1(\dot{\theta}_1+\dot{\theta}_2)\sin\theta_2 \\
\frac{\partial\mathcal{V}}{\partial\theta_2} &= m_2 g\ell_2\sin(\theta_1+\theta_2)
\end{aligned}$$

Substituting these results in the Lagrange equations

$$\begin{aligned}
\frac{d}{dt}\frac{\partial\mathcal{T}}{\partial\dot{\theta}_1} - \frac{\partial\mathcal{T}}{\partial\theta_1} + \frac{\partial\mathcal{V}}{\partial\theta_1} &= 0 \\
\frac{d}{dt}\frac{\partial\mathcal{T}}{\partial\dot{\theta}_2} - \frac{\partial\mathcal{T}}{\partial\theta_2} + \frac{\partial\mathcal{V}}{\partial\theta_2} &= 0
\end{aligned}$$

then yields the equations of motion.

Example 3: a guided double pendulum

Let us consider the double pendulum described in figure 1.9. The mass m_1 slides without friction along a circle of radius r. The spring with stiffness k is fixed at a distance e from the center of the circle and ℓ is its undeformed length. Gravity g acts along the X axis. Using the angles θ_1 and θ_2 as defined in figure 1.9, the energy of the system can be found to be

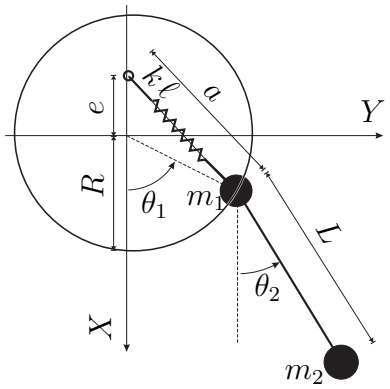

Figure 1.9: Guided double pendulum

$$\mathcal{T} = \frac{1}{2}\left(\left(m_1+m_2\right)R^2\dot{\theta}_1^2 + m_2L^2\dot{\theta}_2^2 + 2RLm_2\dot{\theta}_1\dot{\theta}_2\cos(\theta_1-\theta_2)\right)$$
$$\mathcal{V} = -\left(m_1+m_2\right)gR\cos\theta_1 - m_2gL\cos\theta_2 + \frac{1}{2}k(a-\ell)^2$$

where $a = \sqrt{R^2+e^2+2Re\cos\theta_1}$. Expressing the Lagrange equations then yields the following equations of motion:

$$\begin{cases} \left(m_1+m_2\right)R^2\ddot{\theta}_1 + RLm_2\ddot{\theta}_2\cos(\theta_1-\theta_2) + RLm_2\dot{\theta}_2^2\sin(\theta_1-\theta_2) \\ \qquad\qquad + \left(m_1+m_2\right)gR\sin\theta_1 - k\left(1-\dfrac{\ell}{a}\right)Re\sin\theta_1 \;=\; 0 \\ m_2L^2\ddot{\theta}_2 + RLm_2\ddot{\theta}_1\cos(\theta_1-\theta_2) - RLm_2\dot{\theta}_1^2\sin(\theta_1-\theta_2) + m_2gL\sin\theta_2 \;=\; 0 \end{cases}$$

Let us note that if we set $k = 0$, the system is equivalent to the double pendulum described in figure 1.7. The equations obtained here are then the equations of motion of the double pendulum in terms of absolute angles, whereas the equations derived in the previous example correspond to the equations of motion when the relative angle of the second pendulum is taken as degree of freedom. Indeed, setting $k = 0$ and $\theta_2 = \theta_1 + \theta_2^{rel}$, we find

$$\begin{cases} \left(m_1+m_2\right)R^2\ddot{\theta}_1 + RLm_2(\ddot{\theta}_1+\ddot{\theta}_2^{rel})\cos(\theta_2^{rel}) + RLm_2(\dot{\theta}_1+\dot{\theta}_2^{rel})^2\sin(-\theta_2^{rel}) \\ \qquad\qquad + \left(m_1+m_2\right)gR\sin\theta_1 \;=\; 0 \\ m_2L^2(\ddot{\theta}_1+\ddot{\theta}_2^{rel}) + RLm_2\ddot{\theta}_1\cos(\theta_2^{rel}) - RLm_2\dot{\theta}_1^2\sin(-\theta_2^{rel}) + m_2gL\sin(\theta_1+\theta_2^{rel}) \;=\; 0 \end{cases}$$

The last equation is equivalent to the second equation obtained in the previous example. The first equation of motion of the previous example is obtained by summing the two equations here above.

1.4 Lagrange multipliers

Lagrange equations involve only the forces effectively applied onto the systems thanks to the choice of kinematically admissible coordinates q_s. The Lagrange equations thus express the equilibrium in a subspace orthogonal to the constraints so that reaction forces do not appear in the equations of motion.

In some cases it is nevertheless useful or easier to make the reaction forces appear explicitly in the expression of the equilibrium and to choose generalized coordinates that do not satisfy the kinematic constraints.

1.4.1 Constrained equations and Lagrange multipliers

Let us consider a holonomic constraint (1.9) and lets take its variation:

$$\delta f = \sum_{k=1}^{N} \sum_{i=1}^{3} \frac{\partial f}{\partial u_{ik}} \delta u_{ik} = 0 \tag{1.27}$$

This relation indicates that if the displacements are varied (δu_{ik}) the constraint f is still verified if and only if the δu_{ik} define a motion orthogonal to the direction determined by $\frac{\partial f}{\partial u_{ik}}$. Thus the derivatives $\frac{\partial f}{\partial u_{ik}}$ define the constrained directions and the reaction forces can be expressed as

$$R_{ik} = \lambda \frac{\partial f}{\partial u_{ik}} \tag{1.28}$$

where λ describes the unknown intensity of the reaction and is called *Lagrange multiplier*. Using (1.27) and (1.28), the virtual work associated to the reaction forces is

$$\sum_{k=1}^{N} \sum_{i=1}^{3} R_{ik} \delta u_{ik} = \sum_{k=1}^{N} \sum_{i=1}^{3} \lambda \frac{\partial f}{\partial u_{ik}} \delta u_{ik} = \lambda \delta f \tag{1.29}$$

If we choose generalized coordinates q_s that do not automatically satisfy the constraints $f = 0$, the equation of motions deducted from the virtual work principle (1.14) writes

$$\sum_{k=1}^{N} \sum_{i=1}^{3} \left(m_k \frac{d^2 U(_{ik}(q_1, \ldots, q_n, t)}{dt^2} - X_{ik} - \lambda \frac{\partial f}{\partial u_{ik}} \right) \frac{\partial U_{ik}}{\partial q_s} = 0 \tag{1.30}$$

and the reaction force intensity is determined to satisfy the condition

$$f(\xi_{ik}, t) = f(x_{ik} + U_{ik}(q_s, t), t) = 0 \tag{1.31}$$

The Lagrange equations and the complementary kinematic condition are

$$\begin{cases} \dfrac{d}{dt}\left(\dfrac{\partial \mathcal{T}}{\partial \dot{q}_s}\right) - \dfrac{\partial \mathcal{T}}{\partial q_s} - Q_s - \lambda \dfrac{\partial f}{\partial q_s} = 0 \\ \\ f(x_{ik} + U_{ik}(q_s, t), t) = 0 \qquad\qquad s = 1, \dots\ n \end{cases} \tag{1.32}$$

This approach can easily be extended to the case where several holonomic constraints are not satisfied. One Lagrange multiplier per constraint is then introduced.

1.4.2 From constrained equations to minimum set of degrees of freedom

In order to illustrate the relation between constrained equations and the non-constrained equations obtained when a minimum set of degrees of freedom is used, let us start from the Newton equations for a system of N masses. The governing relations are the Newton equations (1.4) where the reaction forces are related by the derivatives of the constraints. Assuming that R holonomic constraints exist on the system

$$\begin{cases} m_k \ddot{u}_{ik} - X_{ik} - \displaystyle\sum_{c=1}^{R} \lambda_c \frac{\partial f_c}{\partial u_{ik}} = 0 \\ f_c(u_{ik}, t) = 0 \end{cases} \tag{1.33}$$

$$\begin{aligned} i &= 1, 2, 3 \\ k &= 1, \dots, N \\ c &= 1, \dots\ R \end{aligned}$$

If we then choose $n = N - R$ degrees of freedom q_s such that

$$f_c(U_{ik}(q_s, t), t) = 0 \qquad \text{for any value of } \ q_s \tag{1.34}$$

then we have for any variation of q_s that

$$\delta_{q_s} f_c = 0 \qquad \text{for all } \ \delta q_s \qquad\qquad \begin{aligned} c &= 1, \dots, R \\ s &= 1, \dots, n \end{aligned} \tag{1.35}$$

Hence we can write

$$\delta_{q_s} f_c = \frac{\partial f_c}{\partial q_s} \delta q_s = \sum_{i=1}^{3} \sum_{k=1}^{N} \frac{\partial f_c}{\partial u_{ik}} \frac{\partial U_{ik}}{\partial q_s} \delta q_s = 0 \tag{1.36}$$

Since this is true for any δq_s, we have that

$$\sum_{i=1}^{3} \sum_{k=1}^{N} \frac{\partial f_c}{\partial u_{ik}} \frac{\partial U_{ik}}{\partial q_s} = 0 \tag{1.37}$$

which indicates, as seen in section 1.2.1, that when projecting the reaction forces in the directions obtained by the variation of the degrees of freedom (i.e. of the virtual displacements kinematically admissible), they vanish. Hence, the constrained equations (1.33) can be transformed into

$$\begin{cases} \displaystyle\sum_{i=1}^{3}\sum_{k=1}^{N}\left(m_k\ddot{u}_{ik} - X_{ik} - \sum_{c=1}^{R}\lambda_c\frac{\partial f_c}{\partial u_{ik}}\right)\frac{\partial U_{ik}}{\partial q_s} = 0 \\ \\ f_c(U_{ik}(q_s,t),t) = 0 \end{cases} \tag{1.38}$$

The constraining forces thus cancel out and the second equation is automatically satisfied. Hence we find the equations of motion (1.14) obtained from the virtual work principle.

Example: the pendulum

Let us reconsider the simple pendulum described in Figure 1.6, but now let us try to write the constrained equations of motion using the cartesian displacement as unknowns. The constraint of the system can be written as

$$f = \sqrt{(\ell+u_1)^2+u_2^2} - \ell = 0$$

Taking the derivatives of the constrain with respect to u_1 and u_2, one finds the direction of the the reaction forces, namely

$$\overrightarrow{R} = \lambda\begin{bmatrix} \frac{\partial f}{\partial u_1} \\ \frac{\partial f}{\partial u_2} \end{bmatrix} = \lambda\begin{bmatrix} \frac{(\ell+u_1)}{\sqrt{(\ell+u_1)^2+u_2^2}} \\ \frac{u_2}{\sqrt{(\ell+u_1)^2+u_2^2}} \end{bmatrix} = \lambda\begin{bmatrix} \frac{(\ell+u_1)}{\ell} \\ \frac{u_2}{\ell} \end{bmatrix}$$

The constrained equations can thus be written us

$$\begin{cases} m\ddot{u}_1 - mg - \lambda\dfrac{(\ell+u_1)}{\ell} = 0 \\ m\ddot{u}_2 - \lambda\dfrac{u_2}{\ell} = 0 \\ \sqrt{(\ell+u_1)^2+u_2^2} - \ell = 0 \end{cases}$$

If we choose the degree of freedom θ such that

$$\begin{aligned} u_1 &= \ell\cos\theta - \ell \\ u_2 &= \ell\sin\theta \end{aligned}$$

the constraint is always satisfied. Using these relations the reaction forces can be expressed as

$$\overrightarrow{R} = \lambda\begin{bmatrix} \frac{(\ell+u_1)}{\ell} \\ \frac{u_2}{\ell} \end{bmatrix} = \lambda\begin{bmatrix} \frac{\ell\cos\theta}{\ell} \\ \frac{\ell\sin\theta}{\ell} \end{bmatrix} = \lambda\begin{bmatrix} \cos\theta \\ \sin\theta \end{bmatrix}$$

and as seen on page 10, projecting this force in the direction compatible with the constraint leads to the unconstrained equation of motion for the pendulum.

1.4.3 Equations constrained by non-holonomic constraints

Also, the Lagrange multiplier approach can be used in the presence of non-holonomic constraints. In that case, the non-holonomic kinematic conditions (1.10) can not be used to reduce the number of degrees of freedom in the description of the system dynamics, but it provides an explicit relation between the kinematically admissible virtual displacements such as

$$\sum_{i=1}^{3}\sum_{k=1}^{N} A_{ik}^{nh}\delta u_{ik} = 0 \tag{1.39}$$

In that case, the Lagrange equations write

$$\begin{cases} -\dfrac{d}{dt}\left(\dfrac{\partial \mathcal{T}}{\partial \dot{q}_s}\right) + \dfrac{\partial \mathcal{T}}{\partial q_s} + Q_s + \displaystyle\sum_{i=1}^{3}\sum_{s=1}^{N} \lambda A_{ik}^{nh}\dfrac{\partial u_{ik}}{\partial q_s} = 0 \\ f^{nh}(\dot{U}_{ik}(q_s,t),t) = 0 \qquad\qquad s = 1,\dots\ n \end{cases} \tag{1.40}$$

Exercise

1.1 Let us consider the guided double pendulum of figure 1.10.a where a mass m_1 is prescribed to move without friction on a bar making an angle α with respect to the vertical direction. The spring of stiffness k is attached to a fixed point and its undeformed length is ℓ. Gravity g is acting along X. Using the degrees of freedom z and θ, write the energy of the system and find its equations of motion.

$$\begin{aligned}\mathcal{T} &= \frac{1}{2}m_1\dot{z}^2 + \frac{1}{2}m_2\left(\dot{z}^2 + L^2\dot{\theta}^2 + 2L\dot{z}\dot{\theta}\sin(\alpha-\theta)\right)\\ \mathcal{V} &= -m_1 g z\cos\alpha - m_2 g\left(z\cos\alpha + L\cos\theta\right) + \frac{1}{2}k(a-\ell)^2\\ &\quad \text{where } a^2 = (e+z\cos\alpha)^2 + (z\sin\alpha)^2\end{aligned}$$

$$\left\{\begin{array}{l}(m_1+m_2)\,\ddot{z} + m_2 L\ddot{\theta}\sin(\alpha-\theta) - m_2 L\dot{\theta}^2\cos(\alpha-\theta)\\ \qquad -(m_1+m_2)\,g\cos\alpha - k(\ell-a)\dfrac{z+e\cos\alpha}{a} = 0\\ m_2 L\sin(\alpha-\theta)\ddot{z} + m_2 L^2\ddot{\theta} + m_2 gL\sin\theta = 0\end{array}\right.$$

1.2 For the coupled pendulum of figure 1.10.b, write the energy of the system. The undeformed length of the spring D is equal to the distance between the attachment points of the pendulums.

$$\begin{aligned}\mathcal{T} &= \frac{1}{2}m\ell^2\left(\dot{\theta_1}^2 + \dot{\theta_2}^2\right)\\ \mathcal{V} &= mg\ell(1-\cos\theta_1) + mg\ell(1-\cos\theta_2) + \frac{1}{2}k\zeta^2\end{aligned}$$

where

$$\zeta(\theta_1,\theta_2) = L - D \quad \text{and} \quad L(\theta_1,\theta_2) = \sqrt{a^2(\cos\theta_2-\cos\theta_1)^2 + (a\sin\theta_2 - a\sin\theta_1 + D)^2}$$

1.3 Consider the rotating system of figure 1.10.c. Its rotating speed Ω is imposed. Two masses m_1 and m_2 slide without friction into the orthogonal grooves. The mass points are linked through a rigid bar of length e. Find the equation of motion in terms of the displacements d_1 and d_2 of the masses along the grooves. The inertia of the rigid bar is neglected and the the rotating speed of the system is kept constant. If $m_1 = m_2 = m$ and if no force is applied to the system, show that the reaction force in the rigid link is constant and that the bar is always under traction.

$$f = \sqrt{d_1^2 + d_2^2} - e$$

$$\left\{\begin{array}{rcl} m_1\ddot{d}_1 - \lambda\dfrac{d_1}{e} &=& d_1 m_1\Omega^2\\ m_2\ddot{d}_2 - \lambda\dfrac{d_2}{e} &=& d_2 m_2\Omega^2\end{array}\right.$$

If $m_1 = m_2 = m$,

$$d_1 = e\cos\theta \qquad\qquad d_2 = e\sin\theta$$

is the general solution if $\dot{\theta}$ is constant. The reaction force in the link is then $\lambda = -em(\Omega^2 + \dot{\theta}^2) < 0$.

1.4 Write the equations of motion for the double pendulum of figure 1.7 using the absolute angles as degrees of freedom.

1.5 Write the equations of motion for the double pendulum of figure 1.7 in the case when the upper attachment point has a constant horizontal acceleration a.

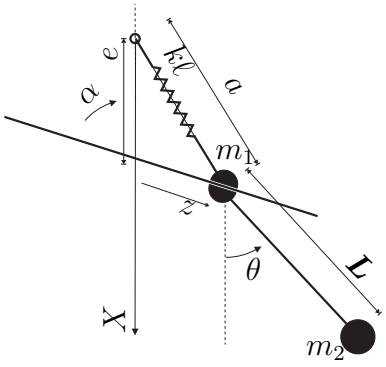

a.

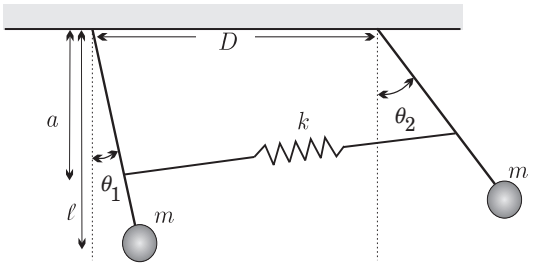

b.

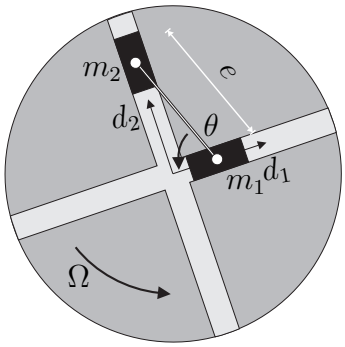

c.

Figure 1.10: Exercise

Chapter 2

Linearized equations of motion around an equilibrium position

In Chapter 1, we have discussed how the equations of motion of a system of discrete particles (possibly with constraints) can be written in terms of generalized degrees of freedom. From the examples treated in that chapter, it should be clear to the reader that the equations of motion arising from the virtual work approach or, equivalently, from Lagrange's equations are most often non-linear (see e.g. the pendulum equation page 16). Solving these equations to compute the response of the system in time generally requires the application of numerical integration techniques.

In many cases however, the system undergoes only small displacements and its configuration remains very close to some equilibrium configuration in which the system remains if no external perturbation is applied. In that case, the system is said to *oscillate* around an equilibrium configuration and, the displacements remaining small, its analysis can be performed by considering linearized equations of motions. The analysis of oscillations is classically referred to as *vibration analysis*. Vibration analysis of structures covers many practical cases where system undergo small displacements. It also provides the framework to evaluate the stability of equilibrium positions.

In this chapter we will define equilibrium positions and discuss how the equations of motion (written in the Lagrange equations form) can be linearized around such configurations.

2.1 Concepts of equilibrium configurations and linearized dynamics

Let us call *equilibrium configuration of a system* described by its n generalized degrees of freedom q_s a *time-independent configuration*, namely a configuration that can be achieved by the system with

$$\boldsymbol{q}(t) = \boldsymbol{q}(t=0) = \boldsymbol{q}_{eq} \qquad \text{and thus} \qquad \left\{ \begin{array}{l} \dot{\boldsymbol{q}}(t) = \boldsymbol{0} \\ \ddot{\boldsymbol{q}}(t) = \boldsymbol{0} \end{array} \right. \qquad \forall t \tag{2.1}$$

where

$$\boldsymbol{q} = \begin{bmatrix} q_1 \\ q_2 \\ \vdots \\ q_n \end{bmatrix}$$

Let us note that, in an equilibrium position, the system is not necessarily at rest for an observer in an inertial frame. Indeed, if a transport motion is forced onto the system through rheonomic constraints, the system might exhibit equilibrium states for which the generalized degrees of freedom are constant in time, but where, due to transport motion imposed on the system, the system undergoes a prescribed motion in an inertial frame. In other word, considering the kinematic relation (1.11)

$$u_{ik}(x_{jk}, t) = U_{ik}(q_1, \ldots, q_n, t) \tag{1.11}$$

between Cartesian displacements in an inertial frame and generalized degrees of freedom chosen so as to satisfy the constraints of the system, the system will not be at rest if U_{ik} explicitly depends on time t, even if all q_s are constant. As an example consider the simple system of a mass forced to move along a massless rod rotating at an imposed constant speed (Figure 2.1). Clearly, as will be discussed later, there is an equilibrium position where the restoring force of the spring equals the centrifugal force so that the mass does not move along the guide. However, an overall motion exist for the equilibrium position. Hence in our discussion of equilibrium and linearized equations of motion we must consider

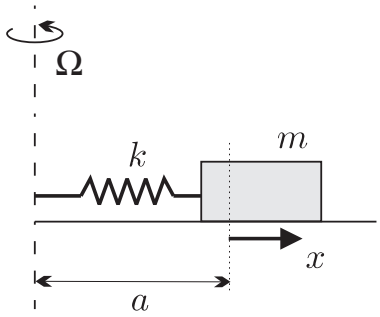

Figure 2.1: Spring–mass system under rotation

separately the case when only scleronomic constraints exist and the case when the system undergoes a global motion, that is when rheonomic constraints are applied or, yet in other words, when U_{ik} explicitly depends on time.

Let us note $\boldsymbol{f}(\ddot{\boldsymbol{q}}, \dot{\boldsymbol{q}}, \boldsymbol{q})$ the total forces implied in the Lagrange equations of motion, namely

$$f_s = \frac{d}{dt}\frac{\partial \mathcal{T}}{\partial \dot{q}_s} - \frac{\partial \mathcal{T}}{\partial q_s} + \frac{\partial \mathcal{V}}{\partial q_s} - Q_s \qquad s = 1, \cdots n \tag{2.2}$$

This set of n equations can be written in matrix notation as follows

$$\boldsymbol{f} = \frac{d}{dt}\frac{\partial \mathcal{T}}{\partial \dot{\boldsymbol{q}}} - \frac{\partial \mathcal{T}}{\partial \boldsymbol{q}} + \frac{\partial \mathcal{V}}{\partial \boldsymbol{q}} - \boldsymbol{Q} \tag{2.3}$$

if we take as convention that the derivation operators applied on a scalar yield

$$\frac{\partial}{\partial \boldsymbol{q}} = \begin{bmatrix} \frac{\partial}{\partial q_1} \\ \frac{\partial}{\partial q_2} \\ \vdots \\ \frac{\partial}{\partial q_n} \end{bmatrix} \qquad \text{and} \qquad \frac{\partial}{\partial \dot{\boldsymbol{q}}} = \begin{bmatrix} \frac{\partial}{\partial \dot{q}_1} \\ \frac{\partial}{\partial \dot{q}_2} \\ \vdots \\ \frac{\partial}{\partial \dot{q}_n} \end{bmatrix}$$

The equation for an equilibrium configuration is thus, according to (2.1),

$$\boxed{\boldsymbol{f}(\ddot{\boldsymbol{q}} = \boldsymbol{0}, \dot{\boldsymbol{q}} = \boldsymbol{0}, \boldsymbol{q} = \boldsymbol{q}_{eq}) = \boldsymbol{0}} \tag{2.4}$$

Once equilibrium positions are found, one can write linearized dynamic equations by writing the equations of motion (e.g. the Lagrange equations) for small perturbations around an equilibrium position. We call $\tilde{q}_s$ small deviations of the generalized degrees of freedom around an equilibrium configuration $\boldsymbol{q}_{eq}$ such that

$$\begin{aligned} \boldsymbol{q} &= \boldsymbol{q}_{eq} + \tilde{\boldsymbol{q}} \\ \dot{\boldsymbol{q}} &= \dot{\tilde{\boldsymbol{q}}} \\ \ddot{\boldsymbol{q}} &= \ddot{\tilde{\boldsymbol{q}}} \end{aligned}$$

The dynamic equations around an equilibrium can then be linearized by writing

$$\begin{aligned} \boldsymbol{f}(\ddot{\boldsymbol{q}} = \ddot{\tilde{\boldsymbol{q}}}, \dot{\boldsymbol{q}} = \dot{\tilde{\boldsymbol{q}}}, \boldsymbol{q} = \boldsymbol{q}_{eq} + \tilde{\boldsymbol{q}}) &\simeq \boldsymbol{f}(\ddot{\boldsymbol{q}} = \boldsymbol{0}, \dot{\boldsymbol{q}} = \boldsymbol{0}, \boldsymbol{q}_{eq}) \\ &\quad + \left.\frac{\partial \boldsymbol{f}}{\partial \ddot{\boldsymbol{q}}}\right|_{\substack{\boldsymbol{q}=\boldsymbol{q}_{eq} \\ \dot{\boldsymbol{q}}=\boldsymbol{0} \\ \ddot{\boldsymbol{q}}=\boldsymbol{0}}} \ddot{\tilde{\boldsymbol{q}}} + \left.\frac{\partial \boldsymbol{f}}{\partial \dot{\boldsymbol{q}}}\right|_{\substack{\boldsymbol{q}=\boldsymbol{q}_{eq} \\ \dot{\boldsymbol{q}}=\boldsymbol{0} \\ \ddot{\boldsymbol{q}}=\boldsymbol{0}}} \dot{\tilde{\boldsymbol{q}}} + \left.\frac{\partial \boldsymbol{f}}{\partial \boldsymbol{q}}\right|_{\substack{\boldsymbol{q}=\boldsymbol{q}_{eq} \\ \dot{\boldsymbol{q}}=\boldsymbol{0} \\ \ddot{\boldsymbol{q}}=\boldsymbol{0}}} \tilde{\boldsymbol{q}} \\ &= \boldsymbol{0} \end{aligned} \tag{2.5}$$

where our convention is that the derivation operators applied on a uni-column matrix results in matrices such that the element in row r and column s is

$$\left[\frac{\partial \boldsymbol{f}}{\partial \boldsymbol{q}}\right]_{rs} = \frac{\partial f_r}{\partial q_s}$$

The first term in the series (2.5) is null by definition of the equilibrium (see (2.4)), so that (2.3) now writes around an equilibrium equation:

$$\boldsymbol{M}\ddot{\tilde{\boldsymbol{q}}} + \boldsymbol{C}\dot{\tilde{\boldsymbol{q}}} + \boldsymbol{K}\tilde{\boldsymbol{q}} = \boldsymbol{0} \tag{2.6}$$

where the coefficients of the mass, damping and stiffness matrices around the equilibrium position are obtained as

$$m_{sr} = \left.\frac{\partial f_s}{\partial \ddot{q}_r}\right|_{\substack{\boldsymbol{q}=\boldsymbol{q}_{eq}\\ \dot{\boldsymbol{q}}=\boldsymbol{0}\\ \ddot{\boldsymbol{q}}=\boldsymbol{0}}} \tag{2.7}$$

$$c_{sr} = \left.\frac{\partial f_s}{\partial \dot{q}_r}\right|_{\substack{\boldsymbol{q}=\boldsymbol{q}_{eq}\\ \dot{\boldsymbol{q}}=\boldsymbol{0}\\ \ddot{\boldsymbol{q}}=\boldsymbol{0}}} \tag{2.8}$$

$$k_{sr} = \left.\frac{\partial f_s}{\partial q_r}\right|_{\substack{\boldsymbol{q}=\boldsymbol{q}_{eq}\\ \dot{\boldsymbol{q}}=\boldsymbol{0}\\ \ddot{\boldsymbol{q}}=\boldsymbol{0}}} \tag{2.9}$$

In what follows we will further analyze the equilibrium position and the linearized matrices both for the case of systems without and with overall motion due to rheonomic constraints. We will call $\boldsymbol{f}_{\mathcal{T}}$ and $\boldsymbol{f}_{\mathcal{V}}$ respectively the force contributions of the kinetic and potential energy to the equations of motion, namely[1]

$$\boldsymbol{f}_{\mathcal{T}}(\ddot{\boldsymbol{q}},\dot{\boldsymbol{q}},\boldsymbol{q}) \triangleq \frac{d}{dt}\frac{\partial \mathcal{T}(\dot{\boldsymbol{q}},\boldsymbol{q})}{\partial \dot{\boldsymbol{q}}} - \frac{\partial \mathcal{T}(\dot{\boldsymbol{q}},\boldsymbol{q})}{\partial \boldsymbol{q}} \qquad \text{and} \qquad \boldsymbol{f}_{\mathcal{V}}(\boldsymbol{q}) \triangleq \frac{\partial \mathcal{V}(\boldsymbol{q})}{\partial \boldsymbol{q}} \tag{2.10}$$

With these notations, the dynamic equations, the equilibrium configuration and the linearized matrices can be written as

$$\boldsymbol{f}_{\mathcal{T}}(\ddot{\boldsymbol{q}},\dot{\boldsymbol{q}},\boldsymbol{q}) + \boldsymbol{f}_{\mathcal{V}}(\boldsymbol{q}) - \boldsymbol{Q}(\dot{\boldsymbol{q}},\boldsymbol{q}) = \boldsymbol{0} \tag{2.11}$$

$$\boldsymbol{f}_{\mathcal{T}}(\ddot{\boldsymbol{q}}=\boldsymbol{0},\dot{\boldsymbol{q}}=\boldsymbol{0},\boldsymbol{q}=\boldsymbol{q}_{eq}) + \boldsymbol{f}_{\mathcal{V}}(\boldsymbol{q}=\boldsymbol{q}_{eq}) - \boldsymbol{Q}(\dot{\boldsymbol{q}}=\boldsymbol{0},\boldsymbol{q}=\boldsymbol{q}_{eq}) = \boldsymbol{0} \tag{2.12}$$

$$\boldsymbol{M} = \left.\frac{\partial \boldsymbol{f}}{\partial \ddot{\boldsymbol{q}}}\right|_{\substack{\boldsymbol{q}=\boldsymbol{q}_{eq}\\ \dot{\boldsymbol{q}}=\boldsymbol{0}\\ \ddot{\boldsymbol{q}}=\boldsymbol{0}}} = \left.\frac{\partial \boldsymbol{f}_{\mathcal{T}}}{\partial \ddot{\boldsymbol{q}}}\right|_{\substack{\boldsymbol{q}=\boldsymbol{q}_{eq}\\ \dot{\boldsymbol{q}}=\boldsymbol{0}\\ \ddot{\boldsymbol{q}}=\boldsymbol{0}}} \tag{2.13}$$

$$\boldsymbol{C} = \left.\frac{\partial \boldsymbol{f}}{\partial \dot{\boldsymbol{q}}}\right|_{\substack{\boldsymbol{q}=\boldsymbol{q}_{eq}\\ \dot{\boldsymbol{q}}=\boldsymbol{0}\\ \ddot{\boldsymbol{q}}=\boldsymbol{0}}} = \left.\frac{\partial(\boldsymbol{f}_{\mathcal{T}} - \boldsymbol{Q})}{\partial \dot{\boldsymbol{q}}}\right|_{\substack{\boldsymbol{q}=\boldsymbol{q}_{eq}\\ \dot{\boldsymbol{q}}=\boldsymbol{0}\\ \ddot{\boldsymbol{q}}=\boldsymbol{0}}} \tag{2.14}$$

$$\boldsymbol{K} = \left.\frac{\partial \boldsymbol{f}}{\partial \boldsymbol{q}}\right|_{\substack{\boldsymbol{q}=\boldsymbol{q}_{eq}\\ \dot{\boldsymbol{q}}=\boldsymbol{0}\\ \ddot{\boldsymbol{q}}=\boldsymbol{0}}} = \left.\frac{\partial(\boldsymbol{f}_{\mathcal{T}} + \boldsymbol{f}_{\mathcal{V}} - \boldsymbol{Q})}{\partial \boldsymbol{q}}\right|_{\substack{\boldsymbol{q}=\boldsymbol{q}_{eq}\\ \dot{\boldsymbol{q}}=\boldsymbol{0}\\ \ddot{\boldsymbol{q}}=\boldsymbol{0}}} \tag{2.15}$$

In the following sections the different force contributions will be analyzed. We will assume that generalized forces $\boldsymbol{Q}$ that do not derive from a potential (e.g. damping forces) are not present.

[1] Note that as defined here the forces $\boldsymbol{f}_{\mathcal{V}}$ are internal forces and therefore the minus sign does not appear when comparing to (1.24) where X_{ik} was defined as an external force.

2.2 Systems undergoing no overall motion

2.2.1 Equilibrium configuration

Let us assume that the system is described by generalized degrees of freedom such that U_{ik} does not depend explicitly on time (typically when only scleronomic kinematic constraints are imposed). In that case, the system does not undergo an imposed overall motion and

$$\dot{u}_{ik} = \frac{\partial U_{ik}}{\partial t} + \sum_{s=1}^{n} \frac{\partial U_{ik}}{\partial q_s} \dot{q}_s = \sum_{s=1}^{n} \frac{\partial U_{ik}}{\partial q_s} \dot{q}_s \tag{2.16}$$

or in matrix notations

$$\dot{\boldsymbol{u}}_k = \frac{\partial \boldsymbol{U}_k}{\partial \boldsymbol{q}} \dot{\boldsymbol{q}} \tag{2.17}$$

where $\boldsymbol{u}_k$ is the three-dimensional displacement of mass k, namely

$$\boldsymbol{u}_k = \begin{bmatrix} u_{1k} \\ u_{2k} \\ u_{3k} \end{bmatrix}$$

The kinetic energy of the system writes

$$\begin{aligned} \mathcal{T} &= \frac{1}{2} \sum_{k=1}^{N} \sum_{i=1}^{3} m_k \dot{u}_{ik}^2 = \frac{1}{2} \sum_{k=1}^{N} m_k \dot{\boldsymbol{u}}_k^T \dot{\boldsymbol{u}}_k \\ &= \frac{1}{2} \sum_{k=1}^{N} m_k \dot{\boldsymbol{q}}^T \left(\frac{\partial \boldsymbol{U}_k}{\partial \boldsymbol{q}} \right)^T \frac{\partial \boldsymbol{U}_k}{\partial \boldsymbol{q}} \dot{\boldsymbol{q}} \end{aligned} \tag{2.18}$$

which indicates that the kinetic energy is *quadratic* in the generalized velocities $\dot{q}_s$ and therefore

$$\boldsymbol{f}_{\mathcal{T}}(\ddot{\boldsymbol{q}} = \boldsymbol{0}, \dot{\boldsymbol{q}} = \boldsymbol{0}, \boldsymbol{q} = \boldsymbol{q}_{eq}) = \left(\frac{d}{dt} \frac{\partial \mathcal{T}}{\partial \dot{\boldsymbol{q}}} - \frac{\partial \mathcal{T}}{\partial \boldsymbol{q}} \right)_{\ddot{\boldsymbol{q}}=\boldsymbol{0}, \dot{\boldsymbol{q}}=\boldsymbol{0}, \boldsymbol{q}=\boldsymbol{q}_{eq}} = \boldsymbol{0}$$

The contributions of the forces $\boldsymbol{f}_{\mathcal{T}}$ to the equilibrium configuration is thus null and the equilibrium position is a solution of the equilibrium between all generalized applied forces only:

$$\boxed{\boldsymbol{f}_{\mathcal{V}}(\boldsymbol{q} = \boldsymbol{q}_{eq}) = \left. \frac{\partial \mathcal{V}}{\partial \boldsymbol{q}} \right|_{\boldsymbol{q}=\boldsymbol{q}_{eq}} = \boldsymbol{0}} \tag{2.19}$$

Note that typically the generalized forces in a system are non-linear and thus more then one equilibrium position may exist.

2.2.2 Linearized equations of motion

Stiffness matrix The stiffness matrix is obtained by observing that

$$\boldsymbol{K} = \left.\frac{\partial(\boldsymbol{f}_{\mathcal{T}} + \boldsymbol{f}_{\mathcal{V}})}{\partial \boldsymbol{q}}\right|_{\substack{\boldsymbol{q}=\boldsymbol{q}_{eq}\\ \dot{\boldsymbol{q}}=\boldsymbol{0}\\ \ddot{\boldsymbol{q}}=\boldsymbol{0}}} = \left.\frac{\partial \boldsymbol{f}_{\mathcal{V}}}{\partial \boldsymbol{q}}\right|_{\boldsymbol{q}=\boldsymbol{q}_{eq}} \tag{2.20}$$

since $\mathcal{T}$ is quadratic in the generalized velocities. Recalling then that the potential forces are obtained by derivation of a potential $\mathcal{V}$ as indicated in (2.10), we can write

$$\boxed{\boldsymbol{K} = \left.\frac{\partial^2 \mathcal{V}}{\partial \boldsymbol{q}\partial \boldsymbol{q}}\right|_{\boldsymbol{q}=\boldsymbol{q}_{eq}} \quad \text{or} \quad k_{sr} = k_{rs} = \left(\frac{\partial^2 \mathcal{V}}{\partial q_s \partial q_r}\right)_{\boldsymbol{q}=\boldsymbol{q}_{eq}}} \tag{2.21}$$

where $\mathcal{V}$ is assumed to have C_2 continuity at $\boldsymbol{q}_{eq}$ and where k_{sr} are the linearize stiffness coefficients. It is observed that, by construction, the stiffness matrix is *symmetric*.

In terms of the perturbations, the potential is approximated by the quadratic form

$$\mathcal{V}(\tilde{\boldsymbol{q}}) \simeq \frac{1}{2}\sum_{s=1}^{n}\sum_{r=1}^{n} k_{sr}\tilde{q}_s\tilde{q}_r = \frac{1}{2}\tilde{\boldsymbol{q}}^T\boldsymbol{K}\tilde{\boldsymbol{q}} \tag{2.22}$$

Damping matrix Since the kinetic energy is quadratic in the generalized speeds it is readily observed that

$$\boxed{\boldsymbol{C} = \left.\frac{\partial \boldsymbol{f}_{\mathcal{T}}}{\partial \dot{\boldsymbol{q}}}\right|_{\substack{\boldsymbol{q}=\boldsymbol{q}_{eq}\\ \dot{\boldsymbol{q}}=\boldsymbol{0}\\ \ddot{\boldsymbol{q}}=\boldsymbol{0}}} = \boldsymbol{0}} \tag{2.23}$$

Thus no damping-like term exists for the linearized equations of systems with no overall motion and when non-potential forces $\boldsymbol{Q}$ are absent.

Mass matrix From the definition (2.10) of $\boldsymbol{f}_{\mathcal{T}}$ and from the expression (2.18) of the kinetic energy for systems on which no overall motion is imposed, it is seen that

$$\begin{aligned}\boldsymbol{f}_{\mathcal{T}} = \frac{d}{dt}\frac{\partial \mathcal{T}}{\partial \dot{\boldsymbol{q}}} - \frac{\partial \mathcal{T}}{\partial \boldsymbol{q}} \;=\; & \sum_{k=1}^{N} m_k \frac{d}{dt}\left(\left(\frac{\partial \boldsymbol{U}_k}{\partial \boldsymbol{q}}\right)^T \frac{\partial \boldsymbol{U}_k}{\partial \boldsymbol{q}}\right)\dot{\boldsymbol{q}} \\ & + \sum_{k=1}^{N} m_k \left(\frac{\partial \boldsymbol{U}_k}{\partial \boldsymbol{q}}\right)^T \frac{\partial \boldsymbol{U}_k}{\partial \boldsymbol{q}}\ddot{\boldsymbol{q}} \\ & - \frac{\partial}{\partial \boldsymbol{q}}\left(\frac{1}{2}\sum_{k=1}^{N} m_k \dot{\boldsymbol{q}}^T \left(\frac{\partial \boldsymbol{U}_k}{\partial \boldsymbol{q}}\right)^T \frac{\partial \boldsymbol{U}_k}{\partial \boldsymbol{q}}\dot{\boldsymbol{q}}\right)\end{aligned} \tag{2.24}$$

Therefore the mass matrix as defined in (2.13) can be written as

$$\begin{aligned} \boldsymbol{M} &= \left.\frac{\partial \boldsymbol{f}_{\mathcal{T}}}{\partial \ddot{\boldsymbol{q}}}\right|_{\substack{\boldsymbol{q}=\boldsymbol{q}_{eq} \\ \dot{\boldsymbol{q}}=\boldsymbol{0} \\ \ddot{\boldsymbol{q}}=\boldsymbol{0}}} \\ &= \left(\sum_{k=1}^{N} m_k \left(\frac{\partial \boldsymbol{U}_k}{\partial \boldsymbol{q}}\right)^T \frac{\partial \boldsymbol{U}_k}{\partial \boldsymbol{q}}\right)_{\boldsymbol{q}=\boldsymbol{q}_{eq}} \end{aligned}$$

Observing that those terms are in fact the coefficients of the quadratic form (2.18) of the kinetic energy, we can directly compute the mass matrix as

$$\boxed{\boldsymbol{M} = \left.\frac{\partial^2 \mathcal{T}}{\partial \dot{\boldsymbol{q}} \partial \dot{\boldsymbol{q}}}\right|_{\boldsymbol{q}=\boldsymbol{q}_{eq}}} \tag{2.25}$$

or componentwise

$$m_{sr} = m_{rs} = \left(\frac{\partial^2 \mathcal{T}}{\partial \dot{q}_s \partial \dot{q}_r}\right)_{\boldsymbol{q}=\boldsymbol{q}_{eq}} = \sum_{k=1}^{N} m_k \sum_{i=1}^{3} \left(\frac{\partial U_{ik}}{\partial q_s}\right)_{\boldsymbol{q}=\boldsymbol{q}_{eq}} \left(\frac{\partial U_{ik}}{\partial q_r}\right)_{\boldsymbol{q}=\boldsymbol{q}_{eq}} \tag{2.26}$$

where m_{rs} are the *linearized inertia coefficients*

The kinetic energy is approximated in terms of the perturbations around the equilibrium by

$$\mathcal{T}(\dot{\boldsymbol{q}}) \simeq \frac{1}{2} \sum_{s=1}^{n} \sum_{r=1}^{n} m_{sr} \dot{q}_s \dot{q}_r = \frac{1}{2} \sum_{s=1}^{n} \sum_{r=1}^{n} m_{sr} \dot{\tilde{q}}_s \dot{\tilde{q}}_r \tag{2.27}$$

Thus, in matrix form, the kinetic energy is a positive definite quadratic form of the velocities

$$\mathcal{T}(\dot{\tilde{\boldsymbol{q}}}) = \frac{1}{2} \dot{\tilde{\boldsymbol{q}}}^T \boldsymbol{M} \dot{\tilde{\boldsymbol{q}}} > 0 \quad \text{for } \dot{\tilde{\boldsymbol{q}}} \neq \boldsymbol{0} \tag{2.28}$$

where the mass matrix $\boldsymbol{M}$ is *symmetric and positive definite.*

Example 1: the double pendulum (relative angles)

Let us again consider the double pendulum and choose as degrees of freedom the relative angles as described in Figure 1.7. Its kinetic and potential energies were found to be (see page 17)

$$\begin{aligned} \mathcal{T} &= \frac{1}{2}\left(m_1 \ell_1^2 \dot{\theta}_1^2 + m_2 \left(\ell_1^2 \dot{\theta}_1^2 + \ell_2^2 (\dot{\theta}_1 + \dot{\theta}_2)^2 + 2\ell_1 \ell_2 \dot{\theta}_1 (\dot{\theta}_1 + \dot{\theta}_2) \cos\theta_2\right)\right) \\ \mathcal{V} &= m_1 g \ell_1 (1 - \cos\theta_1) + m_2 g \left(\ell_1 (1 - \cos\theta_1) + \ell_2 (1 - \cos(\theta_1 + \theta_2))\right) \end{aligned}$$

Equilibrium positions of the double pendulum are defined by (2.1). For the double pendulum, it means that equilibrium positions are solution of

$$\begin{cases} (m_1 g + m_2 g)\ell_1 \sin\theta_1 + m_2 g \ell_2 \sin(\theta_1 + \theta_2) = 0 \\ m_2 g \ell_2 \sin(\theta_1 + \theta_2) = 0 \end{cases}$$

Clearly, equilibrium positions are found for

$$\begin{aligned}\theta_1 &= 0 \text{ or } \pi \\ \theta_2 &= 0 \text{ or } \pi\end{aligned}$$

indicating that there are four equilibrium configurations for the system.

Let us then find the linearized equations of motion around the equilibrium position corresponding to $\theta_1 = \theta_2 = 0$. We compute the stiffness and inertia coefficients as defined by (2.21) and (2.26):

$$\begin{aligned}k_{11} &= \Big(\frac{\partial^2 \mathcal{V}}{\partial\theta_1\partial\theta_1}\Big)_{\theta_1=\theta_2=0} = (m_1+m_2)g\ell_1 + m_2 g\ell_2 \\ k_{12} &= k_{21} = \Big(\frac{\partial^2 \mathcal{V}}{\partial\theta_1\partial\theta_2}\Big)_{\theta_1=\theta_2=0} = m_2 g\ell_2 \\ k_{22} &= \Big(\frac{\partial^2 \mathcal{V}}{\partial\theta_2\partial\theta_2}\Big)_{\theta_1=\theta_2=0} = m_2 g\ell_2\end{aligned}$$

$$\begin{aligned}m_{11} &= \Big(\frac{\partial^2 \mathcal{T}}{\partial\dot\theta_1\partial\dot\theta_1}\Big)_{\theta_1=\theta_2=0} = m_1\ell_1^2 + m_2(\ell_1+\ell_2)^2 \\ m_{12} &= m_{21} = \Big(\frac{\partial^2 \mathcal{T}}{\partial\dot\theta_1\partial\dot\theta_2}\Big)_{\theta_1=\theta_2=0} = m_2(\ell_2^2 + \ell_1\ell_2) \\ m_{22} &= \Big(\frac{\partial^2 \mathcal{T}}{\partial\dot\theta_2\partial\dot\theta_2}\Big)_{\theta_1=\theta_2=0} = m_2\ell_2^2\end{aligned}$$

Hence the equations of motion of the double pendulum are

$$\begin{bmatrix} m_1\ell_1^2 + m_2(\ell_1+\ell_2)^2 & m_2(\ell_2^2+\ell_1\ell_2) \\ m_2(\ell_2^2+\ell_1\ell_2) & m_2\ell_2^2 \end{bmatrix} \begin{bmatrix}\ddot{\tilde\theta}_1 \\ \ddot{\tilde\theta}_2\end{bmatrix} + \begin{bmatrix} (m_1+m_2)g\ell_1 + m_2 g\ell_2 & m_2 g\ell_2 \\ m_2 g\ell_2 & m_2 g\ell_2 \end{bmatrix} \begin{bmatrix}\tilde\theta_1 \\ \tilde\theta_2\end{bmatrix} = \boldsymbol{0}$$

Let us now write the linearized equations of motion for the equilibrium configuration corresponding to $\theta_1 = \pi$, $\theta_2 = 0$. Computing then the stiffness and inertia coefficients around this equilibrium yields the linearized equations of motion

$$\begin{bmatrix} m_1\ell_1^2 + m_2(\ell_1+\ell_2)^2 & m_2(\ell_2^2+\ell_1\ell_2) \\ m_2(\ell_2^2+\ell_1\ell_2) & m_2\ell_2^2 \end{bmatrix} \begin{bmatrix}\ddot{\tilde\theta}_1 \\ \ddot{\tilde\theta}_2\end{bmatrix} + \begin{bmatrix} -(m_1+m_2)g\ell_1 - m_2 g\ell_2 & -m_2 g\ell_2 \\ -m_2 g\ell_2 & -m_2 g\ell_2 \end{bmatrix} \begin{bmatrix}\tilde\theta_1 \\ \tilde\theta_2\end{bmatrix} = \boldsymbol{0}$$

Finally, if we consider the equilibrium position corresponding to $\theta_1 = \theta_2 = \pi$, the linearized equations of motion are

$$\begin{bmatrix} m_1\ell_1^2 + m_2(\ell_1-\ell_2)^2 & m_2(\ell_2^2-\ell_1\ell_2) \\ m_2(\ell_2^2-\ell_1\ell_2) & m_2\ell_2^2 \end{bmatrix} \begin{bmatrix}\ddot{\tilde\theta}_1 \\ \ddot{\tilde\theta}_2\end{bmatrix} + \begin{bmatrix} -(m_1+m_2)g\ell_1 + m_2 g\ell_2 & m_2 g\ell_2 \\ m_2 g\ell_2 & m_2 g\ell_2 \end{bmatrix} \begin{bmatrix}\tilde\theta_1 \\ \tilde\theta_2\end{bmatrix} = \boldsymbol{0}$$

Example 2: the double pendulum (absolute angles)

In case absolute angles are chosen as degrees of freedom for the double pendulum of Figure 1.7, the kinetic and potential energies are equal to the ones of the guided double pendulum of Figure 1.9 (see expression on page 18, with $k = 0$), namely

$$\mathcal{T} = \frac{1}{2}\left((m_1+m_2)\,\ell_1^2\dot{\theta}_1^2 + m_2\ell_2^2\dot{\theta}_2^2 + 2\ell_1\ell_2 m_2\dot{\theta}_1\dot{\theta}_2\cos(\theta_1-\theta_2)\right)$$
$$\mathcal{V} = -\,(m_1+m_2)\,g\ell_1\cos\theta_1 - m_2 g\ell_2\cos\theta_2$$

The equilibrium position are found to be

$$\begin{aligned}\theta_1 &= 0 \text{ or } \pi\\ \theta_2 &= 0 \text{ or } \pi\end{aligned}$$

Analyzing the oscillations around the equilibrium configuration $\theta_1 = \theta_2 = 0$, the linear equations of motion are

$$\begin{bmatrix}(m_1+m_2)\ell_1^2 & m_2\ell_1\ell_2\\ m_2\ell_1\ell_2 & m_2\ell_2^2\end{bmatrix}\begin{bmatrix}\ddot{\tilde{\theta}}_1\\ \ddot{\tilde{\theta}}_2\end{bmatrix} + \begin{bmatrix}(m_1+m_2)g\ell_1 & 0\\ 0 & m_2 g\ell_2\end{bmatrix}\begin{bmatrix}\tilde{\theta}_1\\ \tilde{\theta}_2\end{bmatrix} = \boldsymbol{0}$$

Let us note that, compared to the linear equations found for that equilibrium position in the previous example (page 32), using absolute angles leads to uncoupling of the stiffness contribution and to a different mass coupling. We note that if we substitute in these vibration equations the relation $\tilde{\theta}_2 = \tilde{\theta}_1 + \tilde{\theta}_2^{rel}$ where $\tilde{\theta}_2^{rel}$ is the relative angle of the second pendulum used as degree of freedom in the previous example, we find

$$\begin{bmatrix}(m_1+m_2)\ell_1^2 + m_2\ell_1\ell_2 & m_2\ell_1\ell_2\\ m_2\ell_1\ell_2 + m_2\ell_2^2 & m_2\ell_2^2\end{bmatrix}\begin{bmatrix}\ddot{\tilde{\theta}}_1\\ \ddot{\tilde{\theta}}_2^{rel}\end{bmatrix} + \begin{bmatrix}(m_1+m_2)g\ell_1 & 0\\ m_2 g\ell_2 & m_2 g\ell_2\end{bmatrix}\begin{bmatrix}\tilde{\theta}_1\\ \tilde{\theta}_2^{rel}\end{bmatrix} = \boldsymbol{0}$$

and one observes that adding the first and second equations in the above system yields the equilibrium equation as found in the previous example (page 32).

Example 3: the coupled pendulums

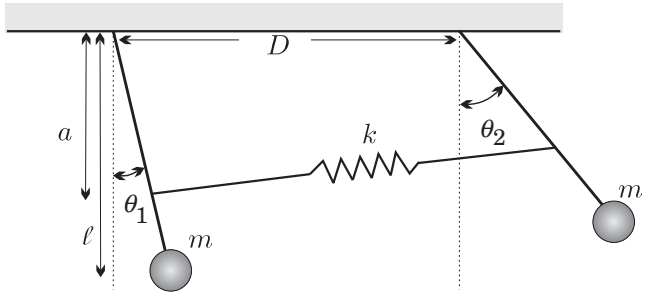

Figure 2.2: Coupled pendulums

Let us consider two pendulums coupled by a spring (figure 2.2). The natural length of the spring is equal to the distance D between the attachment points. In terms of the angles θ_1 and θ_2 adopted as generalized coordinates, the system energies take the form

$$\begin{aligned} \mathcal{T} &= \frac{1}{2} m\ell^2 \left(\dot{\theta_1}^2 + \dot{\theta_2}^2\right) \\ \mathcal{V} &= mg\ell(1-\cos\theta_1) + mg\ell(1-\cos\theta_2) + \frac{1}{2}k\zeta^2 \end{aligned}$$

where

$$\begin{aligned} \zeta(\theta_1,\theta_2) &= L - D \\ L(\theta_1,\theta_2) &= \sqrt{a^2(\cos\theta_2-\cos\theta_1)^2 + (a\sin\theta_2 - a\sin\theta_1 + D)^2} \end{aligned}$$

The equilibrium positions of the system has to satisfy the equations

$$\frac{\partial \mathcal{V}}{\partial \theta_s} = mg\ell\sin\theta_s + k\zeta\frac{\partial L}{\partial \theta_s} = 0$$

It is easy to verify that the configuration $\theta_1 = \theta_2 = 0$ is one of the equilibrium states. To find the linearized equations of motion around that equilibrium configuration, we compute the following stiffness coefficients:

$$\begin{aligned} k_{rs} = k_{sr} &= \left(\frac{\partial^2 \mathcal{V}}{\partial\theta_s \partial\theta_r}\right)_{0,0} = mg\ell\delta_{rs} + k\left(\frac{\partial L}{\partial\theta_s}\right)_{0,0}\left(\frac{\partial L}{\partial\theta_r}\right)_{0,0} + k\ \zeta(\theta_1=\theta_2=0)\left(\frac{\partial^2 L}{\partial\theta_r\partial\theta_s}\right)_{0,0} \\ &= mg\ell\delta_{rs} + k\left(\frac{\partial L}{\partial\theta_s}\right)_{0,0}\left(\frac{\partial L}{\partial\theta_r}\right)_{0,0} \end{aligned}$$

where

$$\left(\frac{\partial L}{\partial\theta_1}\right)_{0,0} = -a \quad \text{and} \quad \left(\frac{\partial L}{\partial\theta_2}\right)_{0,0} = a$$

Computing then the inertia coefficients, one finds the linearized stiffness and mass matrices

$$\boldsymbol{K} = \begin{bmatrix} mg\ell + ka^2 & -ka^2 \\ -ka^2 & mg\ell + ka^2 \end{bmatrix} \qquad \boldsymbol{M} = \begin{bmatrix} m\ell^2 & 0 \\ 0 & m\ell^2 \end{bmatrix}$$

Example 4: a guided double pendulum

Let us consider the guided double pendulum as described in Figure 1.9. Considering the absolute angles as degrees of freedom, the energies are expressed by

$$\begin{aligned} \mathcal{T} &= \frac{1}{2}\left((m_1+m_2)\,R^2\dot{\theta}_1^2 + m_2L^2\dot{\theta}_2^2 + 2RLm_2\dot{\theta}_1\dot{\theta}_2\cos(\theta_1-\theta_2)\right) \\ \mathcal{V} &= -(m_1+m_2)\,gR\cos\theta_1 - m_2gL\cos\theta_2 + \frac{1}{2}k(a-\ell)^2 \end{aligned}$$

where $a(\theta_1) = \sqrt{R^2 + e^2 + 2Re\cos\theta_1}$. Let us first find the equilibrium positions of the system. The equilibrium condition (2.1) in this example writes

$$\begin{cases} \dfrac{\partial \mathcal{V}}{\partial \theta_1} = \Big((m_1+m_2)g + k\dfrac{e}{a}(-a+\ell)\Big) R\sin\theta_1 = 0 \\ \dfrac{\partial \mathcal{V}}{\partial \theta_2} = m_2 g L \sin\theta_2 = 0 \end{cases}$$

The reader can graphically verify that the first equation indeed corresponds to the static equilibrium of mass m_1 in the direction tangent to the circle on which the first pendulum is constrained. Let us assume that

$$\ell = R \qquad e = R/2 \qquad L = R \qquad m_1 = m_2 = m \qquad mg = \frac{kR}{16}$$

so that the equilibrium conditions write

$$\begin{cases} \big(2mg + k\frac{R}{2a}(R-a)\big)\sin\theta_1 = 0 \\ mgL\sin\theta_2 = 0 \end{cases}$$

where $a(\theta_1) = \sqrt{\dfrac{5}{4}R^2 + R^2\cos\theta_1}$. In equilibrium we thus have

$$\theta_2 = 0 \text{ or } \pi$$

and for θ_1, the possible values at equilibrium are

$$\theta_1 = 0 \text{ or } \pi$$

or θ_1 solution of $2mg + k\frac{R}{2a(\theta_1)}(R - a(\theta_1)) = 0$. Rearranging and using the data $mg = \frac{kR}{16}$,

$$a(\theta_1) = \frac{k\frac{R^2}{2}}{k\frac{R}{2} - 2mg} = \frac{4}{3}R$$

Reminding that on the other hand $a(\theta_1) = \sqrt{\dfrac{5}{4}R^2 + R^2\cos\theta_1}$, θ_1 must be solution of

$$\cos\theta_1 = \frac{16}{9} - \frac{5}{4}$$

which finally means that there exists also equilibrium positions for

$$\theta_1 = \pm 1.0148 \text{ rad}$$

Let us now compute the stiffness coefficients for the linearized equations around the equilibrium position $\theta_1 = \theta_2 = 0$:

$$\begin{aligned} k_{11} &= \Big(\frac{\partial^2 \mathcal{V}}{\partial\theta_1\partial\theta_1}\Big)_{\theta_1=\theta_2=0} = 2mgR + k\frac{R^2}{2a}(R-a) = -\frac{kR^2}{24} \\ k_{12} &= k_{21} = \Big(\frac{\partial^2 \mathcal{V}}{\partial\theta_1\partial\theta_2}\Big)_{\theta_1=\theta_2=0} = 0 \\ k_{22} &= \Big(\frac{\partial^2 \mathcal{V}}{\partial\theta_2\partial\theta_2}\Big)_{\theta_1=\theta_2=0} = mgR \end{aligned}$$

Computing then the inertia coefficients, we find the linearized equations around $\theta_1 = \theta_2 = 0$:

$$\begin{bmatrix} 2mR^2 & mR^2 \\ mR^2 & mR^2 \end{bmatrix} \begin{bmatrix} \ddot{\tilde{\theta}}_1 \\ \ddot{\tilde{\theta}}_2 \end{bmatrix} + \begin{bmatrix} -\frac{kR^2}{24} & 0 \\ 0 & mgR \end{bmatrix} \begin{bmatrix} \tilde{\theta}_1 \\ \tilde{\theta}_2 \end{bmatrix} = \boldsymbol{0}$$

2.3 Systems undergoing overall motion

2.3.1 Equilibrium with respect to an overall motion

We now consider the case where rheonomic constraints are imposed onto the system so that the kinematic relations between Cartesian displacements and generalized displacements depend explicitly on time and thus

$$\dot{u}_{ik} = \frac{\partial U_{ik}}{\partial t} + \sum_{s=1}^{n} \frac{\partial U_{ik}}{\partial q_s} \dot{q}_s \tag{2.29}$$

where $\frac{\partial U_{ik}}{\partial t} \neq 0$. In matrix form this writes

$$\dot{\boldsymbol{u}}_k = \frac{\partial \boldsymbol{U}_k}{\partial t} + \frac{\partial \boldsymbol{U}_k}{\partial \boldsymbol{q}} \dot{\boldsymbol{q}} \tag{2.30}$$

The system described in Figure 2.1 is an example of such systems: if x, the displacement along the rod rotating at a constant speed Ω is taken as degree of freedom, the displacements and velocities of the mass are expressed as

$$\begin{aligned} u_1 &= (x+a)\cos(\Omega t) & \dot{u}_1 &= -(x+a)\Omega \sin(\Omega t) + \dot{x}\cos(\Omega t) \\ u_2 &= (x+a)\sin(\Omega t) & \dot{u}_2 &= (x+a)\Omega \cos(\Omega t) + \dot{x}\sin(\Omega t) \end{aligned}$$

Hence, in the case where rheonomic constraints are imposed, the kinetic energy has the general expression

$$\mathcal{T}(q, \dot{q}, t) = \frac{1}{2} \sum_{k=1}^{N} m_k \dot{\boldsymbol{u}}_k^T \dot{\boldsymbol{u}}_k = \mathcal{T}_0 + \mathcal{T}_1 + \mathcal{T}_2 \tag{2.31}$$

where $\mathcal{T}_0, \mathcal{T}_1$ and $\mathcal{T}_2$ are respectively homogeneous forms of degree 0, 1 or 2 in the generalized velocities $\dot{q}_s$:

- $$\mathcal{T}_0 = \frac{1}{2} \sum_{k=1}^{N} m_k \left(\frac{\partial \boldsymbol{U}_k}{\partial t} \right)^T \frac{\partial \boldsymbol{U}_k}{\partial t} = \mathcal{T}_0(\boldsymbol{q}, t) \tag{2.32}$$

  is the *transport kinetic energy* of the system since it corresponds to the remaining kinetic energy when the degrees of freedom $q_1, \ldots, q_n$ are frozen.

- $$\mathcal{T}_1 = \sum_{k=1}^{N} m_k \frac{\partial \boldsymbol{U}_k}{\partial t}^T \frac{\partial \boldsymbol{U}_k}{\partial \boldsymbol{q}} \dot{\boldsymbol{q}} \tag{2.33}$$

  is the *mutual* or *coupling kinetic energy.*

- $$\mathcal{T}_2 = \frac{1}{2} \sum_{k=1}^{N} m_k \dot{\boldsymbol{q}}^T \left(\frac{\partial \boldsymbol{U}_k}{\partial \boldsymbol{q}} \right)^T \frac{\partial \boldsymbol{U}_k}{\partial \boldsymbol{q}} \dot{\boldsymbol{q}} \tag{2.34}$$

  is the *relative kinetic energy* since it corresponds to what is left when the explicit dependence of velocities $\dot{\boldsymbol{u}}_k$ with respect to time is suppressed.

Let us now analyze what part of the kinetic energy contributes to the forces in an equilibrium configuration.Considering the force $\boldsymbol{f}_{\mathcal{T}}$ defined in (2.10), we find

$$\begin{aligned} \boldsymbol{f}_{\mathcal{T}}(\ddot{\boldsymbol{q}} = \boldsymbol{0}, \dot{\boldsymbol{q}} = \boldsymbol{0}, \boldsymbol{q} = \boldsymbol{q}_{eq}) &= \left(\frac{d}{dt} \frac{\partial \mathcal{T}(\dot{\boldsymbol{q}}, \boldsymbol{q})}{\partial \dot{\boldsymbol{q}}} - \frac{\partial \mathcal{T}(\dot{\boldsymbol{q}}, \boldsymbol{q})}{\partial \boldsymbol{q}} \right)_{\substack{\boldsymbol{q} = \boldsymbol{q}_{eq} \\ \dot{\boldsymbol{q}} = \boldsymbol{0} \\ \ddot{\boldsymbol{q}} = \boldsymbol{0}}} \\ &= \left(\frac{d}{dt} \frac{\partial (\mathcal{T}_2 + \mathcal{T}_1)}{\partial \dot{\boldsymbol{q}}} - \frac{\partial (\mathcal{T}_2 + \mathcal{T}_1 + \mathcal{T}_0)}{\partial \boldsymbol{q}} \right)_{\substack{\boldsymbol{q} = \boldsymbol{q}_{eq} \\ \dot{\boldsymbol{q}} = \boldsymbol{0} \\ \ddot{\boldsymbol{q}} = \boldsymbol{0}}} \\ &= \left(\frac{d}{dt} \frac{\partial (\mathcal{T}_1)}{\partial \dot{\boldsymbol{q}}} \right)_{\substack{\boldsymbol{q} = \boldsymbol{q}_{eq} \\ \dot{\boldsymbol{q}} = \boldsymbol{0}}} - \left(\frac{\partial (\mathcal{T}_0)}{\partial \boldsymbol{q}} \right)_{\boldsymbol{q} = \boldsymbol{q}_{eq}} \end{aligned} \tag{2.35}$$

Hence, compared to systems with no overall motion where the forces present in the equilibrium state are only the forces deriving from a potential (see (2.19)), the overall motion imposed to the system by the rheonomic constraints induces additional forces present in the equilibrium state. The equilibrium configuration must satisfy

$$\left(\frac{d}{dt} \frac{\partial \mathcal{T}_1}{\partial \dot{\boldsymbol{q}}} \right)_{\substack{\boldsymbol{q} = \boldsymbol{q}_{eq} \\ \dot{\boldsymbol{q}} = \boldsymbol{0}}} + \left(-\frac{\partial \mathcal{T}_0}{\partial \boldsymbol{q}} + \frac{\partial \mathcal{V}}{\partial \boldsymbol{q}} \right)_{\boldsymbol{q} = \boldsymbol{q}_{eq}} = \boldsymbol{0} \tag{2.36}$$

If we define

$$\mathcal{V}^* = \mathcal{V} - \mathcal{T}_0 \tag{2.37}$$

the modified potential obtained by subtracting from the potential of the system the transport kinetic energy, the equilibrium condition obtained from Lagrange's equations then write

$$\boxed{\left(\frac{d}{dt} \frac{\partial \mathcal{T}_1}{\partial \dot{\boldsymbol{q}}} \right)_{\substack{\boldsymbol{q} = \boldsymbol{q}_{eq} \\ \dot{\boldsymbol{q}} = \boldsymbol{0}}} + \left(\frac{\partial \mathcal{V}^*}{\partial \boldsymbol{q}} \right)_{\boldsymbol{q} = \boldsymbol{q}_{eq}} = \boldsymbol{0}} \tag{2.38}$$

Obviously an equilibrium solution in the sense of (2.1) will exist only if the additional forces due to relative motion effects in (2.38) do not depend on time. As will be shown in the examples below, this is the case for systems submitted to uniformly accelerated translations or forced to rotate with constant angular velocity.

Example of a passenger in a lift :

To illustrate the additional terms in the equilibrium equation (2.38), let us consider a mass in a lift with a prescribed constant linear acceleration a. If one chooses as degrees of freedom q the position of the mass in the direction of the linear acceleration but relative to the motion imposed to the lift, the absolute displacement is

$$u = a\frac{t^2}{2} + q$$

and the absolute velocity is

$$\dot{u} = at + \dot{q}$$

The kinetic energy is then

$$\mathcal{T} = \frac{1}{2}m(\dot{q}^2 + 2at\dot{q} + a^2t^2) = \mathcal{T}_2 + \mathcal{T}_1 + \mathcal{T}_0$$

The first term in (2.38) is thus

$$\frac{d}{dt}\frac{\partial(\mathcal{T}_1)}{\partial\dot{q}} = ma$$

whereas

$$\frac{\partial\mathcal{T}_0}{\partial q} = 0$$

Hence, for the case of linearly accelerated systems with constant imposed acceleration, the apparent force must be considered for finding the equilibrium position in terms of degrees of freedom relative to the overall motion.

Example of a rotating mass

Let us consider the system described in Figure 2.1 made of a mass m rotating about a fixed direction axis with given angular velocity Ω. A spring of natural length a connects the mass to the rotation axis. The absolute velocity of the mass is calculated as follows: calling u_1 and u_2 the displacement of the mass in a fixed reference and x the relative coordinate about the rotating axis,

$$\begin{aligned}
u_1 &= (a+x)\cos\Omega t \\
u_2 &= (a+x)\sin\Omega t \\
v^2 &= \dot{u_1}^2 + \dot{u_2}^2 \\
&= \left[-(a+x)\Omega\sin\Omega t + \dot{x}\cos\Omega t\right]^2 + \left[(a+x)\Omega\cos\Omega t + \dot{x}\sin\Omega t\right]^2 \\
&= (a+x)^2\Omega^2 + \dot{x}^2
\end{aligned}$$

where x is the only generalized coordinate of the system. The kinetic and potential energies are expressed by

$$\begin{aligned}\mathcal{V} &= \frac{1}{2}kx^2\\ \mathcal{T} &= \mathcal{T}_0 + \mathcal{T}_2\\ \mathcal{T}_0 &= \frac{\Omega^2}{2}m(x+a)^2\\ \mathcal{T}_2 &= \frac{1}{2}m\dot{x}^2\end{aligned}$$

If the angular velocity Ω is constant, the equilibrium configuration is obtained as the solution of

$$\left.\frac{\partial \mathcal{V}^*}{\partial x}\right|_{eq} = kx_{eq} - \Omega^2 m(x_{eq}+a) = 0$$

clearly stating the static equilibrium between the spring force and the centrifugal force along the rotating guide. Hence

$$x_{eq} = \frac{\Omega^2 ma}{k - \Omega^2 m}$$

2.3.2 Linearized equations of motion around an overall motion

Stiffness matrix To obtained the stiffness matrix as defined by (2.15) one observes that

$$\begin{aligned}\boldsymbol{K} &= \left.\frac{\partial(\boldsymbol{f}_{\mathcal{T}} + \boldsymbol{f}_{\mathcal{V}})}{\partial \boldsymbol{q}}\right|_{\substack{\boldsymbol{q}=\boldsymbol{q}_{eq}\\ \dot{\boldsymbol{q}}=\boldsymbol{0}\\ \ddot{\boldsymbol{q}}=\boldsymbol{0}}}\\ &= \left(\frac{\partial}{\partial \boldsymbol{q}}\left(\frac{d}{dt}\frac{\partial(\mathcal{T}_2+\mathcal{T}_1)}{\partial \dot{\boldsymbol{q}}} - \frac{\partial(\mathcal{T}_2+\mathcal{T}_1+\mathcal{T}_0)}{\partial \boldsymbol{q}}\right)\right)_{\substack{\boldsymbol{q}=\boldsymbol{q}_{eq}\\ \dot{\boldsymbol{q}}=\boldsymbol{0}\\ \ddot{\boldsymbol{q}}=\boldsymbol{0}}} + \left.\frac{\partial \boldsymbol{f}_{\mathcal{V}}}{\partial \boldsymbol{q}}\right|_{\boldsymbol{q}=\boldsymbol{q}_{eq}}\\ &= \left(-\frac{\partial^2(\mathcal{T}_0)}{\partial \boldsymbol{q}\partial \boldsymbol{q}} + \frac{\partial^2 \mathcal{V}}{\partial \boldsymbol{q}\partial \boldsymbol{q}}\right)_{\boldsymbol{q}=\boldsymbol{q}_{eq}}\end{aligned} \tag{2.39}$$

Hence recalling the definition of the modified potential (2.37), one finds

$$\boxed{\boldsymbol{K} = \left.\frac{\partial^2 \mathcal{V}^*}{\partial \boldsymbol{q}\partial \boldsymbol{q}}\right|_{\boldsymbol{q}=\boldsymbol{q}_{eq}}} \tag{2.40}$$

Again, by construction, it is *symmetric*.

Damping matrix According to the definition (2.14), the damping matrix is

$$\begin{aligned}
\boldsymbol{C} &= \left.\frac{\partial \boldsymbol{f}_{\mathcal{T}}}{\partial \dot{\boldsymbol{q}}}\right|_{\substack{\boldsymbol{q}=\boldsymbol{q}_{eq}\\ \dot{\boldsymbol{q}}=\boldsymbol{0}\\ \ddot{\boldsymbol{q}}=\boldsymbol{0}}} \\
&= \left(\frac{\partial}{\partial \dot{\boldsymbol{q}}}\left(\frac{d}{dt}\frac{\partial(\mathcal{T}_2+\mathcal{T}_1)}{\partial \dot{\boldsymbol{q}}} - \frac{\partial(\mathcal{T}_2+\mathcal{T}_1+\mathcal{T}_0)}{\partial \boldsymbol{q}}\right)\right)_{\substack{\boldsymbol{q}=\boldsymbol{q}_{eq}\\ \dot{\boldsymbol{q}}=\boldsymbol{0}\\ \ddot{\boldsymbol{q}}=\boldsymbol{0}}} \\
&= \left(\frac{\partial}{\partial \dot{\boldsymbol{q}}}\left(\frac{d}{dt}\frac{\partial \mathcal{T}_1}{\partial \dot{\boldsymbol{q}}} - \frac{\partial \mathcal{T}_1}{\partial \boldsymbol{q}}\right)\right)_{\substack{\boldsymbol{q}=\boldsymbol{q}_{eq}\\ \dot{\boldsymbol{q}}=\boldsymbol{0}\\ \ddot{\boldsymbol{q}}=\boldsymbol{0}}} \\
&= \left(\frac{\partial}{\partial \dot{\boldsymbol{q}}}\left(\frac{\partial}{\partial t}\frac{\partial(\mathcal{T}_1)}{\partial \dot{\boldsymbol{q}}} + \frac{\partial^2 \mathcal{T}_1}{\partial \boldsymbol{q}\partial \dot{\boldsymbol{q}}}\dot{\boldsymbol{q}} - \frac{\partial \mathcal{T}_1}{\partial \boldsymbol{q}}\right)\right)_{\substack{\boldsymbol{q}=\boldsymbol{q}_{eq}\\ \dot{\boldsymbol{q}}=\boldsymbol{0}\\ \ddot{\boldsymbol{q}}=\boldsymbol{0}}} \\
&= \left(\frac{\partial^2 \mathcal{T}_1}{\partial \boldsymbol{q}\partial \dot{\boldsymbol{q}}} - \frac{\partial^2 \mathcal{T}_1}{\partial \dot{\boldsymbol{q}}\partial \boldsymbol{q}}\right)_{\boldsymbol{q}=\boldsymbol{q}_{eq}}
\end{aligned} \tag{2.41}$$

Note that this is not null but, according to our notation convention,

$$c_{rs} = \left(\frac{\partial^2 \mathcal{T}_1}{\partial q_s \partial \dot{q}_r} - \frac{\partial^2 \mathcal{T}_1}{\partial \dot{q}_s \partial q_r}\right)_{\boldsymbol{q}=\boldsymbol{q}_{eq}} = -c_{sr} \tag{2.42}$$

Hence the damping matrix is a skew symmetric matrix which originates from inertia coupling effects and is generally called the *gyroscopic matrix* denoted by $\boldsymbol{G}$. The instantaneous power related to the gyroscopic force $\boldsymbol{G}\dot{\boldsymbol{q}}$ is null: $\dot{\boldsymbol{q}}^T\boldsymbol{G}\dot{\boldsymbol{q}} = 0$. This is clearly different from viscous damping forces which appear in linear equations as $\boldsymbol{C}\dot{\boldsymbol{q}}$, $\boldsymbol{C}$ being a symmetric damping matrix.

To summarize we have

$$\boxed{\boldsymbol{G} = \left(\frac{\partial^2 \mathcal{T}_1}{\partial \boldsymbol{q}\partial \dot{\boldsymbol{q}}} - \frac{\partial^2 \mathcal{T}_1}{\partial \dot{\boldsymbol{q}}\partial \boldsymbol{q}}\right)_{\boldsymbol{q}=\boldsymbol{q}_{eq}} \quad \text{or} \quad g_{rs} = \left(\frac{\partial^2 \mathcal{T}_1}{\partial q_s \partial \dot{q}_r} - \frac{\partial^2 \mathcal{T}_1}{\partial \dot{q}_s \partial q_r}\right)_{\boldsymbol{q}=\boldsymbol{q}_{eq}} = -g_{sr}} \tag{2.43}$$

Mass matrix For the mass matrix, we recall the definition (2.13) and find

$$\begin{aligned}
\boldsymbol{M} &= \left.\frac{\partial \boldsymbol{f}_{\mathcal{T}}}{\partial \ddot{\boldsymbol{q}}}\right|_{\substack{\boldsymbol{q}=\boldsymbol{q}_{eq}\\ \dot{\boldsymbol{q}}=\boldsymbol{0}\\ \ddot{\boldsymbol{q}}=\boldsymbol{0}}} \\
&= \left.\left(\frac{\partial}{\partial \ddot{\boldsymbol{q}}}\left(\frac{d}{dt}\frac{\partial(\mathcal{T}_2+\mathcal{T}_1)}{\partial \dot{\boldsymbol{q}}} - \frac{\partial(\mathcal{T}_2+\mathcal{T}_1+\mathcal{T}_0)}{\partial \boldsymbol{q}}\right)\right)\right|_{\substack{\boldsymbol{q}=\boldsymbol{q}_{eq}\\ \dot{\boldsymbol{q}}=\boldsymbol{0}\\ \ddot{\boldsymbol{q}}=\boldsymbol{0}}} \\
&= \left(\frac{\partial}{\partial \ddot{\boldsymbol{q}}}\left(\frac{d}{dt}\frac{\partial \mathcal{T}_2}{\partial \dot{\boldsymbol{q}}}\right)\right)_{\boldsymbol{q}=\boldsymbol{q}_{eq}} \\
&= \left.\frac{\partial^2 \mathcal{T}_2}{\partial \dot{\boldsymbol{q}}\partial \dot{\boldsymbol{q}}}\right|_{\boldsymbol{q}=\boldsymbol{q}_{eq}}
\end{aligned} \tag{2.44}$$

Hence, similarly to the case without overall motion the mass matrix is given by

$$\boxed{\boldsymbol{M} = \left.\frac{\partial^2 \mathcal{T}_2}{\partial \dot{\boldsymbol{q}} \partial \dot{\boldsymbol{q}}}\right|_{\boldsymbol{q}=\boldsymbol{q}_{eq}} = \left(\sum_{k=1}^{N} m_k \left(\frac{\partial \boldsymbol{U}_k}{\partial \boldsymbol{q}}\right)^T \frac{\partial \boldsymbol{U}_k}{\partial \boldsymbol{q}}\right)_{\boldsymbol{q}=\boldsymbol{q}_{eq}}} \tag{2.45}$$

Linearized equations of motion In the neighborhood of an equilibrium configuration, the linearized equations of motion take the form

$$\boxed{\boldsymbol{M}\ddot{\boldsymbol{q}} + \boldsymbol{G}\dot{\boldsymbol{q}} + \boldsymbol{K}^* \boldsymbol{q} = \mathbf{o}} \tag{2.46}$$

where $\boldsymbol{G}$ is the skew-symmetric matrix of gyroscopic coupling.

Example 1: a rotating mass

Let us once more consider the rotating mass problem depicted in Fig. 2.1 and for which the equilibrium position was found on page 38. The linearized equations of motion are obtained by noting that $\mathcal{T}_1 = 0$ here, that the inertia coefficient is simply m in this example and that

$$\left.\frac{\partial^2 \mathcal{V}^*}{\partial \tilde{x}^2}\right|_{\tilde{x}=0} = k - \Omega^2 m$$

The linearized equation of motion is then

$$m\ddot{\tilde{x}} + (k - \Omega^2 m)\tilde{x} = 0$$

Example 2: a two-dimensional rotating spring-mass system

Let us derive the equations of motion for the system of figure (2.3) made of a rotating wheel of radius R inside which a mass m is attached through a system of springs of natural length equal to the radius of the wheel and through a viscous damper. The rotation speed of the wheel is prescribed to be constant and equal to Ω. Considering a coordinate system (x, y) rotating with the wheel and aligned with the undeformed springs, we choose the displacements x and y in the rotating frame as degrees of freedom. In an inertial frame coinciding with (x, y) at time $t = 0$, the mass m has the following absolute position

$$\begin{aligned} \xi_1 &= x\cos(\Omega t) - y\sin(\Omega t) \\ \xi_2 &= x\sin(\Omega t) + y\cos(\Omega t) \end{aligned}$$

Absolute velocities are then

$$\begin{aligned} \dot{u}_1 &= \dot{x}\cos(\Omega t) - x\Omega\sin(\Omega t) - \dot{y}\sin(\Omega t) - y\Omega\cos(\Omega t) \\ \dot{u}_2 &= \dot{x}\sin(\Omega t) + x\Omega\cos(\Omega t) + \dot{y}\cos(\Omega t) - y\Omega\sin(\Omega t) \end{aligned}$$

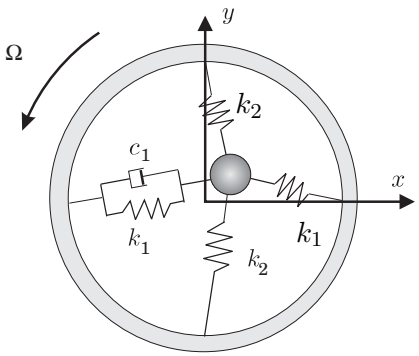

Figure 2.3: Rotating system with two degrees of freedom

Hence the kinetic energy is given by [2]

$$\mathcal{T} = \frac{1}{2}m\Big[\big(\dot{x} - \Omega y\big)^2 + \big(\dot{y} + \Omega x\big)^2\Big]$$

Clearly we have

$$\begin{aligned}
\mathcal{T}_0 &= \frac{1}{2}m\Omega^2(y^2 + x^2) \\
\mathcal{T}_1 &= m\Omega(-\dot{x}y + \dot{y}x) \\
\mathcal{T}_2 &= \frac{1}{2}m(\dot{x}^2 + \dot{y}^2)
\end{aligned}$$

The potential energy is obtained as

$$\mathcal{V} = \frac{1}{2}k_1\left((a_{1,left} - R)^2 + (a_{1,right} - R)^2\right) + \frac{1}{2}k_2\left((a_{2,left} - R)^2 + (a_{2,right} - R)^2\right)$$

where the current spring length are defined by

$$\begin{aligned}
a_{1,left} &= \sqrt{(R + x)^2 + y^2} \\
a_{1,right} &= \sqrt{(R - x)^2 + y^2} \\
a_{2,left} &= \sqrt{(R - y)^2 + x^2} \\
a_{2,right} &= \sqrt{(R + y)^2 + x^2}
\end{aligned}$$

The damper creates a force proportional to speed and is thus null in an equilibrium position.

[2] One can also express the absolute velocities in the rotating coordinate system so that

$$\begin{aligned}
v_1 &= \dot{u}_1 \cos\Omega t + \dot{u}_2 \sin\Omega t = \dot{x} - y\Omega \\
v_2 &= -\dot{u}_1 \sin\Omega t + \dot{u}_2 \cos\Omega t = \dot{y} + x\Omega
\end{aligned}$$

and, since the norm of a vector does not depend on the reference frame, one computes $\mathcal{T} = \frac{1}{2}m(v_1^2 + v_2^2)$ which yields the same result.

Explicitly writing the equilibrium condition (2.38) is lengthy in this case. However it is readily observed that one of the equilibrium configuration corresponds to $x = y = 0$. The linearized stiffness coefficients can then be found by applying the definition (2.40), which is very intricate given the complex expression of $\mathcal{V}$. Therefore, it is easier to directly write the quadratic approximation of $\mathcal{V}$ around $x = y = 0$ as

$$\mathcal{V} \simeq \frac{1}{2}k_1\left(2x^2\right) + \frac{1}{2}k_2\left(2y^2\right)$$

indicating that the the stiffness coefficients are

$$\begin{aligned} k_{11}^* &= \left.\frac{\partial^2(\mathcal{V}-\mathcal{T}_0)}{\partial x^2}\right|_{x=y=0} = 2k_1 - m\Omega^2 \\ k_{12}^* = k_{21}^* &= \left.\frac{\partial^2(\mathcal{V}-\mathcal{T}_0)}{\partial x\partial y}\right|_{x=y=0} = 0 \\ k_{22}^* &= \left.\frac{\partial^2(\mathcal{V}-\mathcal{T}_0)}{\partial y^2}\right|_{x=y=0} = 2k_2 - m\Omega^2 \end{aligned}$$

The inertia coefficients m_{sr} are easily obtained from $\mathcal{T}_2$ and the gyroscopic terms are computed by (2.43):

$$g_{12} = -g_{21} = \left.\frac{\partial^2\mathcal{T}_1}{\partial y\partial\dot{x}}\right|_{x=y=0} - \left.\frac{\partial^2\mathcal{T}_1}{\partial\dot{y}\partial x}\right|_{x=y=0} = -2m\Omega$$

Finally, observing that the damper yields a linearized force $-c_1\dot{x}$ in the direction of x, we find the linearized equations of motion according to (2.46)

$$\begin{cases} m\ddot{x} - 2m\Omega\dot{y} - m\Omega^2 x + c_1\dot{x} + 2k_1 x = 0 \\ m\ddot{y} + 2m\Omega\dot{x} - m\Omega^2 y + 2k_2 y = 0 \end{cases}$$

They can also be put in the matrix form

$$\boldsymbol{M}\ddot{\boldsymbol{q}} + \big(\boldsymbol{C} + \boldsymbol{G}\big)\dot{\boldsymbol{q}} + \boldsymbol{K}^*\boldsymbol{q} = 0$$

where the vector of generalized displacements $\boldsymbol{q}^T = \begin{bmatrix} x & y \end{bmatrix}$ and the mass, damping, effective stiffness and gyroscopic coupling matrices are defined below:

$$\boldsymbol{M} = \begin{bmatrix} m & 0 \\ 0 & m \end{bmatrix} \qquad \boldsymbol{C} = \begin{bmatrix} c_1 & 0 \\ 0 & 0 \end{bmatrix}$$

$$\boldsymbol{G} = \begin{bmatrix} 0 & -2m\Omega \\ 2m\Omega & 0 \end{bmatrix} \qquad \boldsymbol{K}^* = \begin{bmatrix} 2k_1 - \Omega^2 m & 0 \\ 0 & 2k_2 - \Omega^2 m \end{bmatrix}$$

Chapter 3

Linearized stability of systems around equilibrium positions

3.1 The concept of stability

In the previous chapter we have described how the dynamic forces and the kinetic and potential energies can be approximated so that the Lagrange's equations yield linear equations of motion around equilibrium positions.

So far however, nothing has been said about the stability of the equilibrium, namely about the manner in which the system can leave its equilibrium position. In general, we might say that a system is stable around an equilibrium configuration if the possible dynamic motion of the system results in generalized displacement q_s that remain small. Hence, for stable equilibrium positions, the deviations from equilibrium remain small. More specifically, one can state that *a system is linearly stable around an equilibrium position when a perturbation δq_s results in dynamic displacements that remain small and thus bounded in time.*

To analyze the stability of a system in the vicinity of an equilibrium configuration, we can consider the linearized equations of motion and investigate if dynamic behavior modes of the free system exist (i.e. without forces external to the system) that exhibit non-bounded amplitudes. Typically, linearized equations of free motion take the form of a second order time-differential set of equations

$$\boldsymbol{M}\ddot{\boldsymbol{q}} + (\boldsymbol{C} + \boldsymbol{G})\dot{\boldsymbol{q}} + \boldsymbol{K}\boldsymbol{q} = \boldsymbol{0} \tag{3.1}$$

where $\boldsymbol{C}$ and $\boldsymbol{G}$ are damping and gyroscopic matrices. Note that, whereas $\boldsymbol{G}$ is a skew symmetric matrix such that $\boldsymbol{G}\dot{\boldsymbol{q}}$ are forces resulting from inertia force coupling (see section 2.3.2), $\boldsymbol{C}$ is a symmetric matrix such that $\boldsymbol{C}\dot{\boldsymbol{q}}$ are the linearized forces due to damping.

Any free motion behavior solution of (3.1) can be expressed as a combination of free responses having as general expression

$$\boldsymbol{q} = \boldsymbol{x}e^{\lambda t} \tag{3.2}$$

where $\boldsymbol{x}$ is a free linear mode of displacement, generally complex, and λ is in general a complex number.[1]

Substituting the general form (3.2) into the free vibration equation (3.1), we find that $\boldsymbol{x}$ and λ must satisfy

$$\left(\lambda^2 \boldsymbol{M} + \lambda(\boldsymbol{C} + \boldsymbol{G}) + \boldsymbol{K}\right) \boldsymbol{x} = 0 \tag{3.3}$$

Hence a free motion of the form (3.2) with $\boldsymbol{x} \neq \boldsymbol{0}$ exists only if the system of equation (3.3) is redundant, namely for values of λ that make the determinant of (3.3) zero. Free motion solutions thus exist for λ solution of the eigenvalue problem

$$\det\left(\lambda^2 \boldsymbol{M} + \lambda(\boldsymbol{C} + \boldsymbol{G}) + \boldsymbol{K}\right) = 0 \tag{3.4}$$

The stability of the system is then dependent on the sign of the real part of the solutions of (3.4):

> *if there exists a λ solution of (3.4) with a strictly positive real part, then there exist free motion displacements that are not bounded in time and the system is thus unstable*

In the analysis of equilibrium configurations and linearized equations of the previous chapter, we have seen that in the case where rheonomic constraints impose overall motion, the system is submitted to additional stiffness-like and gyroscopic forces. Therefore, we will discuss separately the stability of system with or without overall motion.

3.2 Stability of systems with no overall motion

When no rheonomic constraints are applied to the system, the linear equations describing the dynamics around an equilibrium configuration takes the form

$$\boldsymbol{M}\ddot{\boldsymbol{q}} + \boldsymbol{C}\dot{\boldsymbol{q}} + \boldsymbol{K}\boldsymbol{q} = \boldsymbol{0} \tag{3.5}$$

We will first consider the case when there are no damping terms and show that such systems exhibit conservation of energy. In that case, the stability can be traced back to the properties of the stiffness matrix. We will then discuss the general case of damped systems in the absence of overall motion.

[1] Let us note that the fact that the displacement modes $\boldsymbol{x}$ can be complex means that during the free motion described by (3.2), the degrees of freedom do not move in a synchronous way, but can have phase shifts with respect to one another. Indeed, we can write

$$\boldsymbol{q} = \boldsymbol{x} e^{\lambda t} = \left[\Re(\boldsymbol{x}) + i\Im(\boldsymbol{x})\right] e^{(\Re(\lambda) + i\Im(\lambda))t}$$

clearly showing that, if one considers the real part of $\boldsymbol{q}$, there can be different phase shifts between degrees of freedom depending on the corresponding real and imaginary parts in $\boldsymbol{q}$. It is also observed that when λ is complex, the response is oscillating harmonically with a exponentially increasing or decreasing amplitude.

3.2.1 Conservation of energy

Let us first consider the case where no damping forces are present and where all forces in the system derive from a potential $\mathcal{V}$. Assuming all constraints to be scleronomic, the kinetic energy is quadratic in the generalized velocities as in (2.18) and therefore

$$2\mathcal{T} = \sum_{s=1}^{n} \dot{q}_s \frac{\partial \mathcal{T}}{\partial \dot{q}_s} \tag{3.6}$$

and after differentiation

$$2\frac{d\mathcal{T}}{dt} = \sum_{s=1}^{n} \ddot{q}_s \frac{\partial \mathcal{T}}{\partial \dot{q}_s} + \sum_{s=1}^{n} \dot{q}_s \frac{d}{dt}\Big(\frac{\partial \mathcal{T}}{\partial \dot{q}_s}\Big) \tag{3.7}$$

On the other hand, since $\mathcal{T}$ is a function of $\boldsymbol{q}$ and $\dot{\boldsymbol{q}}$, we also have

$$\frac{d\mathcal{T}}{dt} = \sum_{s=1}^{n} \ddot{q}_s \frac{\partial \mathcal{T}}{\partial \dot{q}_s} + \sum_{s=1}^{n} \dot{q}_s \frac{\partial \mathcal{T}}{\partial q_s} \tag{3.8}$$

Subtracting (3.8) from (3.7) and using Lagrange's equation in the case all forces derive from a potential $\mathcal{V}$, we find

$$\frac{d\mathcal{T}}{dt} = \sum_{s=1}^{n} \dot{q}_s \Big[\frac{d}{dt}\Big(\frac{\partial \mathcal{T}}{\partial \dot{q}_s}\Big) - \frac{\partial \mathcal{T}}{\partial q_s}\Big] = \sum_{s=1}^{n} \dot{q}_s \left(-\frac{\partial \mathcal{V}}{\partial q_s}\right)$$

and thus

$$\boxed{\frac{d}{dt}(\mathcal{T} + \mathcal{V}) = 0} \tag{3.9}$$

showing that the system is conservative and thus

$$\mathcal{T} + \mathcal{V} = \mathcal{E} \tag{3.10}$$

where $\mathcal{E}$ is the energy level given to the system.

Note that the energy conservation in sceleronomic systems as shown above is valid even for large displacements. However, considering the displacements to be small and in the vicinity of an equilibrium position, the energy conservation allows to easily analyze the stability of a system as discussed next.

3.2.2 Stability of conservative systems

In the case of a conservative system, $\mathcal{T} + \mathcal{V}$ remains constant. Choosing the origin of $\mathcal{V}$ such that $\mathcal{V} = 0$ at equilibrium and assuming that an initial energy $\mathcal{E}$ is given to the system at $t = 0$, energy conservation at any later instant implies

$$\mathcal{T} + \mathcal{V} = \mathcal{E} \tag{3.10}$$

Furthermore let us assume as before that the origin of the generalized coordinates is set at an equilibrium position so that the equilibrium satifies (2.19), namely

$$\left(\frac{\partial \mathcal{V}}{\partial q_s}\right)_{\boldsymbol{q}=0} = 0 \qquad s = 1, \cdots n \tag{2.19}$$

It may then be stated that

> *The equilibrium position (2.19) is stable when an energy bound $\mathcal{E}^*$ exists such that, for any energy $\mathcal{E} < \mathcal{E}^*$ given to the system, one has $\mathcal{T} \leq \mathcal{E}$ at any later instant, equality occurring only at equilibrium.*

This is illustrated in Figure 3.1. As a consequence, in the vicinity of a stable equilibrium

$$\mathcal{V} \geq 0 \tag{3.11}$$

showing that a stable equilibrium position corresponds to a *relative minimum* of the potential energy.

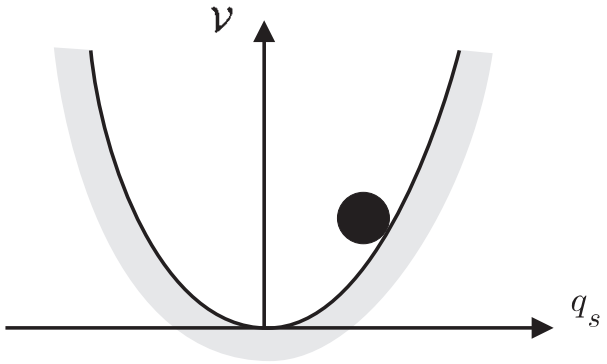

Figure 3.1: Potential of a stable system

Recalling the quadratic approximation (2.22) of $\mathcal{V}$ in the neighborhood of equilibrium, the stability condition (3.11) writes

$$\mathcal{V}(\boldsymbol{q}) \simeq \frac{1}{2}\sum_{s=1}^{n}\sum_{r=1}^{n} k_{sr} q_s q_r = \frac{1}{2}\boldsymbol{q}^T \boldsymbol{K} \boldsymbol{q} > 0 \qquad \text{for } \boldsymbol{q} \neq 0 \tag{2.22}$$

Hence *a conservative system is stable if and only if $\boldsymbol{K}$ is positive definite.*

3.2.3 Modes and frequencies of stable conservative systems

The linearized equations of motion for conservative systems write

$$\boldsymbol{M}\ddot{\boldsymbol{q}} + \boldsymbol{K}\boldsymbol{q} = \boldsymbol{0} \tag{3.12}$$

and free motion modes (3.2) satisfy

$$(\lambda^2\boldsymbol{M} + \boldsymbol{K})\boldsymbol{x} = \boldsymbol{0} \tag{3.13}$$

Let us pre-multiply (3.13) by the complex conjugate of $\boldsymbol{x}$ so that

$$\begin{aligned} \lambda^2 &= -\frac{(\Re(\boldsymbol{x}) - i\Im(\boldsymbol{x}))^T\boldsymbol{K}(\Re(\boldsymbol{x}) + i\Im(\boldsymbol{x}))}{(\Re(\boldsymbol{x}) - i\Im(\boldsymbol{x}))^T\boldsymbol{M}(\Re(\boldsymbol{x}) + i\Im(\boldsymbol{x}))} \\ &= -\frac{\Re(\boldsymbol{x})^T\boldsymbol{K}\Re(\boldsymbol{x}) + \Im(\boldsymbol{x})^T\boldsymbol{K}\Im(\boldsymbol{x})}{\Re(\boldsymbol{x})^T\boldsymbol{M}\Re(\boldsymbol{x}) + \Im(\boldsymbol{x})^T\boldsymbol{M}\Im(\boldsymbol{x})} \end{aligned} \tag{3.14}$$

where we used the fact that $\boldsymbol{M}$ is symmetric positive definite and $\boldsymbol{K}$ is symmetric. Hence, in conservative systems, λ^2 is always real and therefore, recalling the free motion equations (3.13), we can state that

> *for conservative systems, the free vibration modes $\boldsymbol{x}$ are real and thus (3.2) represents a synchronous motion.*

Furthermore, from (3.14),

$$\lambda^2 < 0 \qquad \text{if } \boldsymbol{K} \text{ is positive definite} \tag{3.15}$$

Thus in the case where $\boldsymbol{K}$ is positive definite, we can define a real ω such that

$$\lambda = \pm i\omega$$

showing that the free motion described by the general form (3.2) corresponds to an oscillation motion and is thus stable (as already discovered using the energy conservation here above).

3.2.4 Free motion and stability of non-conservative systems

In general, when no overall motion is imposed to the system, and when non-conservative forces are present, the linearized equations of motion around an equilibrium position write like (3.5). To analyze the stability, one must find the solutions λ roots of

$$\det\left(\lambda^2\boldsymbol{M} + \lambda\boldsymbol{C} + \boldsymbol{K}\right) = 0 \tag{3.16}$$

which can be put in a standard symmetric eigenvalue problem using the state space formulation:

$$\boldsymbol{A}\dot{\boldsymbol{z}} + \boldsymbol{B}\boldsymbol{z} = \boldsymbol{0} \tag{3.17}$$

where

$$\boldsymbol{z} = \begin{bmatrix} \dot{\boldsymbol{q}} \\ \boldsymbol{q} \end{bmatrix} \tag{3.18}$$

and with the symmetric matrices

$$\boldsymbol{A} = \begin{bmatrix} \boldsymbol{0} & \boldsymbol{M} \\ \boldsymbol{M} & \boldsymbol{C} \end{bmatrix} \qquad \boldsymbol{B} = \begin{bmatrix} -\boldsymbol{M} & \boldsymbol{0} \\ \boldsymbol{0} & \boldsymbol{K} \end{bmatrix} \tag{3.19}$$

Looking for free motion in the general form of

$$\boldsymbol{z} = \begin{bmatrix} \lambda \boldsymbol{x} \\ \boldsymbol{x} \end{bmatrix} e^{\lambda t} \tag{3.20}$$

the stability is analyzed by monitoring the sign of the real part of λ solutions of

$$\det(\lambda \boldsymbol{A} + \boldsymbol{B}) = 0 \tag{3.21}$$

It can be shown that, if the system is stable without damping, it remains stable if $\boldsymbol{C}$ is not negative definite, which is always true in case of passive damping. In that case, the free modes $\boldsymbol{x}$ are generally complex and the eigenvalues λ are either complex conjugate with negative real parts (small damping) or pure real negative in case of high (super-critical) damping. If $\boldsymbol{C}$ is negative definite (due for instance to active control), the presence of damping might destabilize the system.

Example 1: the double pendulum

Consider the double pendulum described in Figure 1.7 where the relative angles are used as degrees of freedom. The linearized equations around the equilibrium position $\theta_1 = \theta_2 = 0$ where derived on page 32. Since the system is conservative and does not undergo overall motion, the stability of the system can be determined either by computing the eigenvalues λ of (3.13) or by verifying the positiveness of the stiffness matrix. Let us compute the eigenvalues ν of the stiffness matrix:

$$\det\left(\begin{bmatrix} (m_1+m_2)g\ell_1 + m_2 g\ell_2 & m_2 g\ell_2 \\ m_2 g\ell_2 & m_2 g\ell_2 \end{bmatrix} - \nu \boldsymbol{I}\right) = 0$$

yielding the characteristic polynomial

$$\left((m_1+m_2)g\ell_1 + m_2 g\ell_2 - \nu\right)\left(m_2 g\ell_2 - \nu\right) - \left(m_2 g\ell_2\right)^2 = 0$$

or

$$\nu^2 - \left((m_1+m_2)g\ell_1 + 2m_2 g\ell_2\right)\nu + (m_1+m_2)m_2 g^2 \ell_1 \ell_2 = 0$$

Calling $\alpha = (m_1+m_2)g\ell_1 + 2m_2 g\ell_2$, the roots are

$$\nu = \frac{\alpha \pm \sqrt{\alpha^2 - 4(m_1+m_2)m_2 g^2 \ell_1 \ell_2}}{2}$$

which are clearly positive. Hence the system is stable around the equilibrium position.

If we now consider the equilibrium position corresponding to $\theta_1 = \pi$, $\theta_2 = 0$, we see from the linearized equations obtained around that position on page 32 that the stiffness matrix is exactly equal to minus the stiffness matrix obtained for the equilibrium position $\theta_1 = \theta_2 = 0$ treated here above. Hence, we can conclude that both eigenvalues of the stiffness matrix associated with the position $\theta_1 = \pi$, $\theta_2 = 0$ are negative and the equilibrium is thus unstable. The system is said to have a degree of instability equal to 2.

Finally, let us consider the equilibrium position $\theta_1 = \theta_2 = \pi$ for which the linearized equations were developed on page 32. The eigenvalues ν of the stiffness matrix are found as follows:

$$\det\left(\begin{bmatrix} -(m_1+m_2)g\ell_1 + m_2 g\ell_2 & m_2 g\ell_2 \\ m_2 g\ell_2 & m_2 g\ell_2 \end{bmatrix} - \nu \boldsymbol{I}\right) = 0$$

yielding the characteristic polynomial

$$\left(-(m_1+m_2)g\ell_1 + m_2 g\ell_2 - \nu\right)\left(m_2 g\ell_2 - \nu\right) - \left(m_2 g\ell_2\right)^2 = 0$$

or

$$\nu^2 + \left((m_1+m_2)g\ell_1 - 2m_2 g\ell_2\right)\nu - (m_1+m_2)m_2 g^2 \ell_1 \ell_2 = 0$$

Calling $\beta = (m_1+m_2)g\ell_1 - 2m_2 g\ell_2$, the roots are

$$\nu = \frac{-\beta \pm \sqrt{\beta^2 + 4(m_1+m_2)m_2 g^2 \ell_1 \ell_2}}{2}$$

showing then one root is positive whereas the other is negative. Hence the stiffness matrix is not positive definite and the system is unstable around the equilibrium position $\theta_1 = \theta_2 = \pi$ (degree of instability equal to 1).

Example 2: the coupled pendulums

Let us consider once more the coupled pendulum described in Figure 2.2 and for which the linearized mass and stiffness matrices around $\theta_1 = \theta_2 = 0$ are given on page 34. Again, one can either verify that the stiffness matrix is positive definite or compute the eigenvalues λ of the free motion. Let us in this example compute the actual values of λ solution of the eigenproblem (3.13), namely

$$\det\left(\lambda^2 \begin{bmatrix} m\ell^2 & 0 \\ 0 & m\ell^2 \end{bmatrix} + \begin{bmatrix} mg\ell + ka^2 & -ka^2 \\ -ka^2 & mg\ell + ka^2 \end{bmatrix}\right) = 0$$

yielding the characteristic polynomial

$$\left(\lambda^2 + \frac{g}{\ell} + \alpha^2\right)^2 - \alpha^4 = 0$$

where we defined $\alpha^2 = \frac{ka^2}{m\ell^2}$. Noting that the characteristic equation can be written as

$$\left((\lambda^2 + \frac{g}{\ell} + \alpha^2) - \alpha^2\right)\left((\lambda^2 + \frac{g}{\ell} + \alpha^2) + \alpha^2\right) = 0$$

the roots are directly found as

$$\lambda = \pm i\sqrt{\frac{g}{\ell}} \qquad \text{and} \qquad \lambda = \pm i\sqrt{\frac{g}{\ell} + 2\alpha^2}$$

Hence the free motions are oscillations of frequencies equal to the frequency of the single uncoupled pendulum or of frequency equal to $\sqrt{\frac{g}{\ell} + 2\alpha^2}$.

Example 3: the guided pendulum

Consider the guided double pendulum described in Figure 1.9. Its linearized equations of motion around the equilibrium configuration $\theta_1 = \theta_2 = 0$ are given where derived on page 36 when assuming

$$\ell = R \qquad e = R/2 \qquad L = R \qquad m_1 = m_2 = m \qquad mg = \frac{kR}{16}$$

Since in this example the absolute angles of the guided double pendulum are taken as generalized degrees of freedom, the stiffness matrix is diagonal (no stiffness coupling). Determining the stability of the system is thus easily performed by analyzing the eigenvalues of the stiffness matrix:

$$\det\left(\begin{bmatrix} -\frac{kR^2}{24} & 0 \\ 0 & mgR \end{bmatrix} - \nu \boldsymbol{I}\right) = 0$$

yielding the eigenvalues

$$\nu = -\frac{kR^2}{24} \qquad \text{and} \qquad \nu = mgR$$

Hence the system is unstable around the equilibrium configuration $\theta_1 = \theta_2 = 0$ (instability of degree 1).

3.3 Stability of systems undergoing overall motion

When rheonomic constraints are applied on the system, the linearized equations of motion have the general form (3.1). The reaction forces corresponding to rheonomic constraints often introduce energy in the system and the total energy of the system is no longer conserved. Hence, analyzing the stability of an equilibrium position requires finding the roots λ of (3.4). If there exist solutions λ of (3.4) having a positive real part, the system is unstable since the free motion amplitude can increase in an unbounded way.

Let us note that (3.4) is not a standard eigenvalue problem. A standard eigenvalue problem is found by setting the linear free motion equations (3.1) in the state space form as follows:

$$\tilde{\boldsymbol{A}}\dot{\boldsymbol{z}} + \tilde{\boldsymbol{B}}\boldsymbol{z} = \boldsymbol{0} \tag{3.22}$$

where, as before,

$$\boldsymbol{z} = \begin{bmatrix} \dot{\boldsymbol{q}} \\ \boldsymbol{q} \end{bmatrix}$$

and where the corresponding matrices are defined as

$$\tilde{\boldsymbol{A}} = \begin{bmatrix} \boldsymbol{M} & \boldsymbol{0} \\ \boldsymbol{0} & \boldsymbol{K}^* \end{bmatrix} \qquad \tilde{\boldsymbol{B}} = \begin{bmatrix} \boldsymbol{G}+\boldsymbol{C} & \boldsymbol{K}^* \\ -\boldsymbol{K}^* & \boldsymbol{0} \end{bmatrix} \tag{3.23}$$

where the notation $\boldsymbol{K}^*$ is used to remind that the stiffness matrix derives from a modified potential that includes also the transport energy (see section 2.3.2). Note that $\tilde{\boldsymbol{A}}$ is symmetric whereas $\tilde{\boldsymbol{B}}$ is skew symmetric if $\boldsymbol{C} = 0$. Again, assuming free motion in the form of (3.20), the system is stable if all eigenvalues of

$$\det(\lambda\tilde{\boldsymbol{A}} + \tilde{\boldsymbol{B}}) = 0 \tag{3.24}$$

have non-positive real parts.

One should be aware of the fact that, due to the presence of the gyroscopic terms $\boldsymbol{G}\dot{\boldsymbol{x}}$, the system can be stable even if $\boldsymbol{K}^*$ is not positive definite. This is a major difference with the case of conservative systems studied in the previous section. In the absence of damping (i.e. when $\boldsymbol{C} = 0$), it can be shown that [14, chap.III-6]:

- *If $\boldsymbol{K}^*$ has no zero eigenvalue and has an **odd** number of strictly negative eigenvalues, then there exists at least one λ with a positive real part and thus the system is unstable.*
- *If $\boldsymbol{K}^*$ possesses an **even** number of strictly negative eigenvalues, all the other eigenvalues being strictly positive, then there exists a skew-symmetric matrix $\boldsymbol{G}$ such that every root λ is pure imaginary and non-zero, and thus for which the system is stable.*

Furthermore let us note that, unlike in conservative systems, the presence of damping (even passive) can either stabilize or destabilize the system (see for instance the effect of damping on rotors in [5]).

Example 1: the rotating rod

The mass sliding on a rotating bar (Figure 2.1) has a single degree of freedom. The equilibrium is achieved at a position where the restoring force from the spring exactly compensates the centrifugal force. The linearized equation of motion around the equilibrium is given on page 41. Let us note that since there is only one degree of freedom for the system, no gyroscopic forces are present. The stability of the equilibrium is then easily studied by computing the eigenvalue λ corresponding to the linear free motion, namely

$$\lambda^2 m + (k - \Omega^2 m) = 0$$

thus

$$\lambda^2 = -\frac{k - \Omega^2 m}{m}$$

The system is thus stable when $\Omega < \sqrt{k/m}$, namely when the rotation speed imposed to the bar is lower then the eigenfrequency of the spring-mass system. If $\Omega > \sqrt{k/m}$ the equilibrium position is unstable since one of the roots λ is then real positive. Physically the instability for high rotation speeds can be explained by the fact that when the displacement on the bar increases, the centrifugal force increases faster then the restoring force applied by the spring.

Example 2: mass in an inertia wheel

Consider now the system of Figure 2.3 where a mass is linked through springs and a damper to an inertia wheel rotating at a constant and imposed speed. The linearized mass, gyroscopic, damping and stiffness matrices are given on page 43 for the motion around the equilibrium position at the center of the wheel.

In order to investigate the stability of the system, we have to solve the eigenvalue problem (3.4) or (3.24) for λ, considering the linearized matrices of page 43

$$\boldsymbol{M} = \begin{bmatrix} m & 0 \\ 0 & m \end{bmatrix} \qquad \boldsymbol{C} = \begin{bmatrix} c_1 & 0 \\ 0 & 0 \end{bmatrix}$$

$$\boldsymbol{G} = \begin{bmatrix} 0 & -2m\Omega \\ 2m\Omega & 0 \end{bmatrix} \qquad \boldsymbol{K}^* = \begin{bmatrix} 2k_1 - \Omega^2 m & 0 \\ 0 & 2k_2 - \Omega^2 m \end{bmatrix}$$

Let us assume that $m = 1$, $k_1 = 50$ and $k_2 = 98$. Damping is consider as zero (i.e. $c_1 = 0$). The natural frequencies of the non-rotating system are

$$\begin{aligned} \omega_1 &= \sqrt{2k_1/m} = 10 \qquad \text{in the } x \text{ direction} \\ \omega_2 &= \sqrt{2k_2/m} = 14 \qquad \text{in the } y \text{ direction.} \end{aligned}$$

We observe that

- when $\Omega < \omega_1$, $\boldsymbol{K}^*$ is positive definite;
- when $\omega_1 < \Omega < \omega_2$, $\boldsymbol{K}^*$ has one strictly negative eigenvalue;
- when $\omega_2 < \Omega$, $\boldsymbol{K}^*$ has two strictly negative eigenvalue (it is negative definite),

Setting up the state space form (3.22), one can solve the standard eigenvalue problem for λ (e.g. using Matlab®). In Figure 3.2.a we plot the real and imaginary part of all eigenvalues λ when the rotation speed is varied from 0 to 25. It is seen that

- for $\Omega < \omega_1$, all λ are purely imaginary. One of the conjugate pair tends towards zero (oscillation with decreasing frequency) while the other conjugate pair corresponds to an increasing frequency. The system is stable.
- for $\omega_1 < \Omega < \omega_2$, two eigenvalues λ become purely real, one positive, one negative. The system is unstable. The two other λ are the purely imaginary ones corresponding to an increasing frequency.
- for $\omega_2 < \Omega$, all eigenvalues λ are again purely imaginary. The system is stable.

These results are in agreement with the theory. The re-stabilization of the system for $\Omega > \omega_2$ (negative definite $\boldsymbol{K}^*$) is clearly due to the presence of the gyroscopic forces.

If we now take $k_1 = k_2$, $\omega_1 = \omega_2$, the stiffness matrix is always definite (positive or negative). The values of λ are plotted in Figure 3.2.b. Clearly the equilibrium position is now stable for any rotation speed Ω.

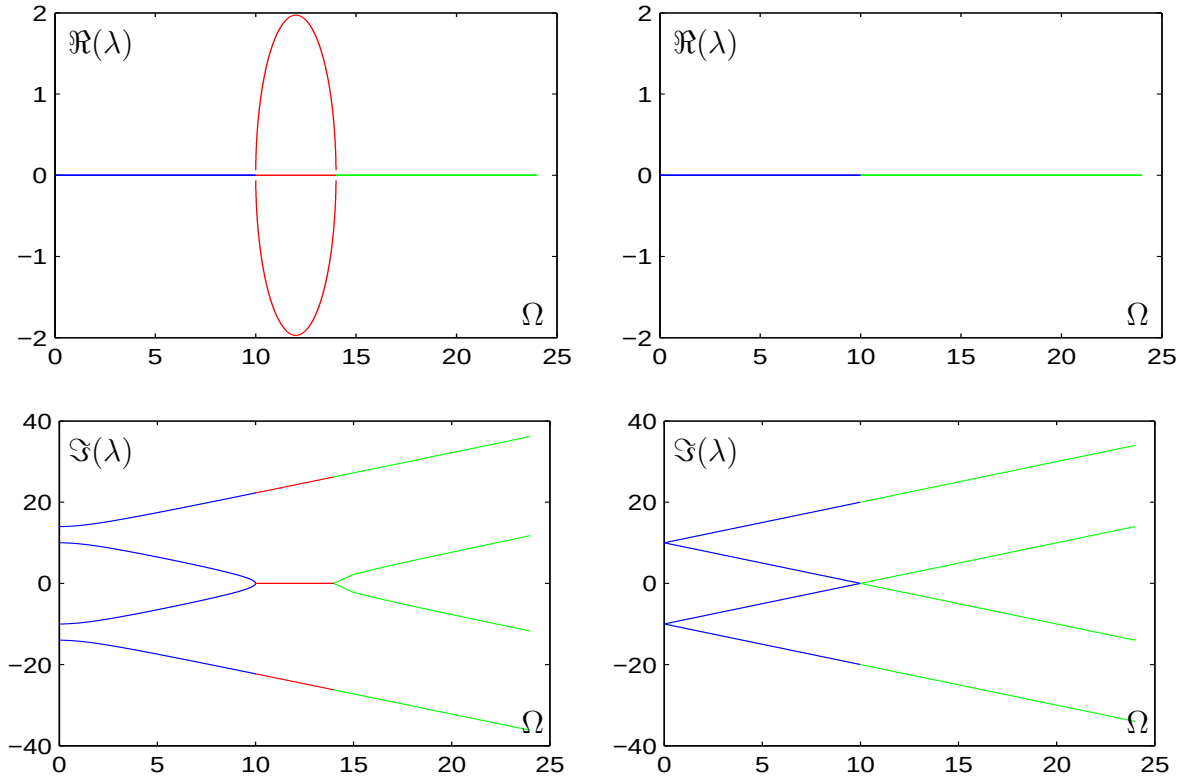

a. $k_1 \neq k_2$ b. $k_1 = k_2$

Figure 3.2: Real and imaginary parts of λ for the inertia wheel problem

Remark 1 - Resonance instabilities Let us note that the stability we investigate here corresponds to the stability of the equilibrium when the system is in free motion (no external force). However, in practice, rotating system are very often submitted to external forces due for instance to bearing contact, out-of-balance masses or fluctuating forces such as aerodynamic forces on the blades of turbines. Hence, in nearly every practical application, rotation systems are submitted to external excitations that have a frequency equal to n times the rotation speed (n is sometimes called the *engine order*). For instance,

- gravity will introduce an harmonic excitation in the rotating frame with a frequency equal to the rotation speed;
- if M bearing elements are placed around the rotating system, the corresponding excitation support forces will generate harmonic forces in the rotating frame with frequency $M\Omega$ and possibly secondary contents in multiples of $M\Omega$. The same can be said when M blades are placed on a turbine, the aerodynamic being generated by a non-uniform flow.

Hence, in rotating systems, one should check if the relevant engine orders coincide with system eigenvalues since, in the case, instabilities related to *resonance* will

appear.

To that purpose, let us consider the graph of the imaginary part of λ (i.e. frequencies) in Figure 3.2.a. (known as *Campbell diagrams*). In dynamic analysis of rotating systems it is then customary to plot lines $\omega = n\Omega$ corresponding to relevant engine orders (see Figure 3.3): the intersection between the engine order lines and the eigenfrequency curves indicate resonance points and therefore rotation speeds that must be avoided when operating the system.

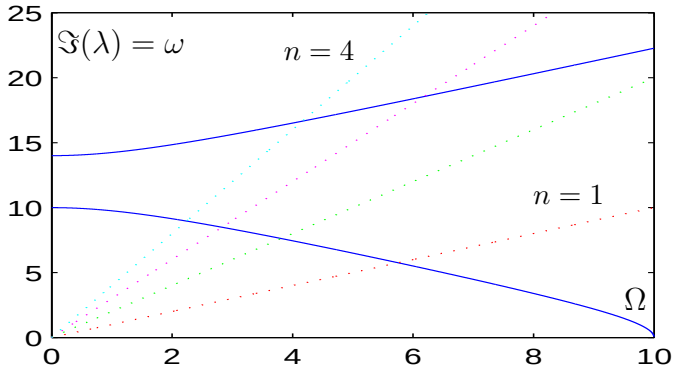

Figure 3.3: Engine orders and resonance of rotating systems

The study of these phenomena is beyond this text, but one should be aware that, in rotating systems, the stability of the equilibrium in free motion is not always the most dangerous phenomenon since resonance with engine orders can happen for much lower Ω.

Remark 2 - Gyroscopic effects physical interpretation Gyroscopic forces and centrifugal forces are in fact fictitious forces in the sense that they appear in the equation of motion of the system when they are expressed with respect to a moving (i.e. rotating) frame (similarly to deceleration forces experienced in a lift). Although centrifugal forces can usually be easily interpreted, gyroscopic forces are more difficult to explain. In order to have a physical insight, let us assume that in the inertia wheel system, the mass m remains on the rotating x axis and moves with a varying velocity $\dot{x}$ as described in Figure 3.4. We will graphically show that such a motion in fact corresponds to absolute accelerations given to m which will prove the presence of centrifugal and gyroscopic forces.

In Figure 3.4.a, we show the configuration and absolute velocities of the system at a given time and at a small time interval Δt later. In the time interval the axis have rotated be an amount $\Delta\varphi = \Omega\Delta t$. The velocity along the x axis has changed because of the relative acceleration $\ddot{x}$ along x and the velocity along y has changed because its position on the x axis has changed by $\Delta x = \dot{x}\Delta t$. Also, observe that in that time interval the direction of the axes x and y has changed.

If we now analyze the variation of the absolute velocity (Figure 3.4.b), we observe that:

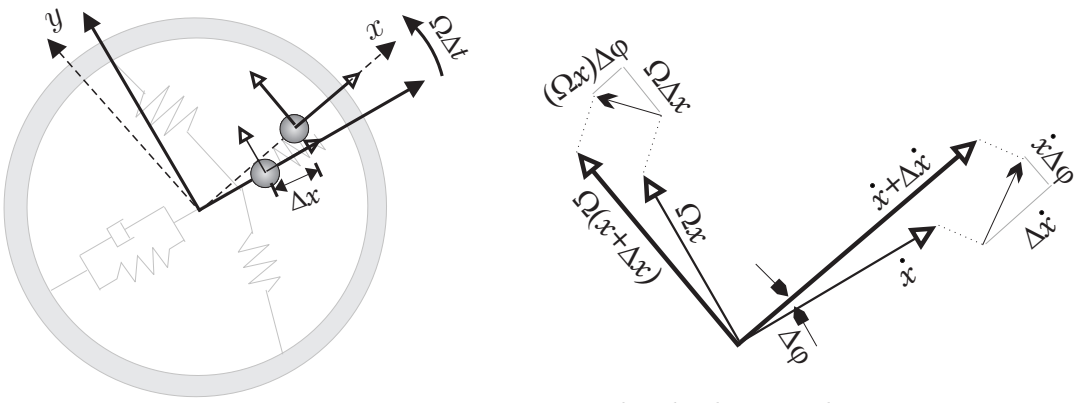

a. constant speed along x

b. absolute accelerations measured in rotating frame

Figure 3.4: Physical interpretation of the gyroscopic coupling

- the velocity change along x results in the absolute acceleration components
  a. $\frac{\Delta \dot{x}}{\Delta t} = \ddot{x}$ along x due to the relative velocity variation,
  b. $\frac{\dot{\boldsymbol{x}}\Delta\varphi}{\Delta t} = \dot{x}\Omega$ along y due to the change of direction of the x axis,
- the velocity change along y results in the absolute acceleration components,
  c. $\frac{-(x\Omega)\Delta\varphi}{\Delta t} = -x\Omega^2$ along x due to the change of direction of the y axis,
  d. $\frac{\Delta x\Omega}{\Delta t} = \dot{x}\Omega$ along y due to the change of position of the mass along x in the time interval.

Clearly, [a.] is the relative acceleration, [b.]+[d.] are the Coriolis accelerations and [c.] is the centripetal acceleration. As said before, if the mass m has the motion assumed here, namely an accelerated motion along the relative axis x, gyroscopic forces must be applied in the y direction to create the Coriolis accelerations. Also, a centrifugal force must be applied along x to create the centripetal acceleration additional to the relative acceleration.

From this discussion it is clear that the gyroscopic effect arises only if the degrees of freedom are expressed in a moving reference frame (typically when rheonomic constraints are present) and when relative speeds exist.

Chapter 4

Vibration modes and mode superposition

In the previous chapter, we have discussed the existence of free motion modes around an equilibrium position. In particular, for conservative systems, we have shown that the free motion modes correspond to a synchronous vibration modes. Here we will show that these modes play a central role in describing the dynamical response of a system.

4.1 Free vibration of undamped discrete systems

Linear systems arise when studying the mechanics of structure under small deformation and small rotations/displacements. The behavior of any non-linear problem around an equilibrium position can also be modeled by a linear system. Hence, studying the linear dynamics of a system is at the very heart of most structural studies and are therefore considered in more details hereafter.

Free vibration behavior plays a central role in the dynamical analysis of linear systems. Indeed, the free vibration modes entirely characterize the dynamical properties of a structure because they represent the characteristic behavior of a structure when inertia and internal forces exactly compensate.

To compute vibration modes and frequencies, general eigensolvers (such as implemented in Matlab) can be used. However, due to the specific properties of the matrices describing the dynamics of systems, particular techniques should be used to solve large practical problems. These numerical aspects are the topic of another course.

4.1.1 Eigenmodes and eigenfrequencies of non-damped structures

Let us consider the linear dynamics equations of a stable discrete (or discretized) system when no external forces are applied :

$$\boldsymbol{M}\ddot{\boldsymbol{q}} + \boldsymbol{K}\boldsymbol{q} = \boldsymbol{0} \tag{4.1}$$

where $\boldsymbol{M}$ and $\boldsymbol{K}$ are respectively the linear mass and stiffness matrices. Remember that $\boldsymbol{M}$ is symmetric positive definite by construction. $\boldsymbol{K}$ is symmetric. Moreover it is positive definite for stable systems (see section 3.2.2). Let us seek a particular solution such that the generalized coordinates are governed to a common factor by the same temporal law, that is to say that the solution is a *synchronous response* of the form, namely of response where a unique time function governs all degree of freedom:

$$\boldsymbol{q} = \boldsymbol{x}\phi(t) \tag{4.2}$$

$\boldsymbol{x}$ is a vector of constants *known to a common scale factor* and gives *the eigenshape* of the motion in the sense that the ratio of two degrees of freedom remains independent of time and is always equal to the ratio of the corresponding components of $\boldsymbol{x}$. Substituting a solution of this type yields

$$\ddot{\phi}(t)\boldsymbol{M}\boldsymbol{x} + \phi(t)\boldsymbol{K}\boldsymbol{x} = \boldsymbol{0} \tag{4.3}$$

Let us assume that matrices $\boldsymbol{M}$ and $\boldsymbol{K}$ are non-singular. Equation (4.3) can be put in the form

$$\boldsymbol{K}\boldsymbol{x} = -\frac{\ddot{\phi}(t)}{\phi(t)}\boldsymbol{M}\boldsymbol{x} \tag{4.4}$$

where $\boldsymbol{M}\boldsymbol{x}$ and $\boldsymbol{K}\boldsymbol{x}$ do not vanish if one excepts the trivial solution $\boldsymbol{x} = \boldsymbol{0}$. Therefore, the time-dependent and space-dependent variables can be separated as

$$\left\{ \begin{array}{rcl} \dfrac{\ddot{\phi}(t)}{\phi(t)} & = & \lambda^2 \\ \boldsymbol{K}\boldsymbol{x} & = & -\lambda^2\boldsymbol{M}\boldsymbol{x} \end{array} \right. \tag{4.5}$$

where λ is a constant with respect to time. In section 3.1 we showed that, due to the symmetric positiveness of $\boldsymbol{M}$ and $\boldsymbol{K}$,

λ^2 is a real and negative quantity

The constant λ may thus be renamed $i\omega$ with ω real and equations (4.5) become

$$\left\{ \begin{array}{rcl} \dfrac{\ddot{\phi}(t)}{\phi(t)} & = & -\omega^2 \\ \big(\boldsymbol{K} - \omega^2\boldsymbol{M}\big)\boldsymbol{x} & = & \boldsymbol{0} \end{array} \right. \tag{4.6}$$

This last system of n linear and homogeneous equations admits a non-trivial solution $\boldsymbol{x}_{(r)}$ such that

$$\big(\boldsymbol{K} - \omega_r^2\boldsymbol{M}\big)\boldsymbol{x}_{(r)} = \boldsymbol{0} \tag{4.7}$$

if ω_r^2 is a root of the algebraic equation

$$\det\big(\boldsymbol{K} - \omega^2\boldsymbol{M}\big) = 0 \tag{4.8}$$

The eigenvalue equation (4.8) is of degree n in ω^2 and possesses thus n roots ω_r^2 which have been shown to be real and positive. To each root ω_r^2 there corresponds a real solution $\boldsymbol{x}_{(r)}$ solution of (4.7)—the *eigenmode* associated with the eigenvalue ω_r^2.

A special kind of eigenmode are displacement modes which do not generate internal forces: *the rigid body modes* $\boldsymbol{u}$. They satisfy the fundamental relation

$$\boldsymbol{K}\boldsymbol{u} = \boldsymbol{0} \tag{4.9}$$

Comparing with (4.7), rigid-body modes can be interpreted as eigenmodes of zero eigenfrequencies. Hence, since a system has n eigenmodes in total, *a structure having m rigid-body modes $\boldsymbol{u}$ has $n - m$ elastic modes $\boldsymbol{x}_{(r)}$ for which the eigenfrequency is non-zero.*

4.1.2 Oscillation of free vibration modes

Owing to the relationship (4.6), the temporal solution ϕ_r associated with the mode $\boldsymbol{x}_{(r)}$ is governed by the equation

$$\ddot{\phi}_r(t) + \omega_r^2 \phi_r(t) = 0 \tag{4.10}$$

If the eigenfrequency is non-zero,

$$\phi_r(t) = \alpha_r \cos \omega_r t + \beta_r \sin \omega_r t \tag{4.11}$$

The eigenvalue ω_r can thus be interpreted as the *circular frequency* of mode r. We will also call it *frequency* although strictly speaking frequency ν (in *hertz*) and circular frequency ω (in *radians per second*) are related by $\nu = \omega/2\pi$.

It is to be stressed that the stability property of solution (4.11) is an immediate consequence of the positive definite character of $\boldsymbol{M}$ and $\boldsymbol{K}$.

If the eigenfrequency is zero in (4.10), the related mode is a rigid-body mode. Thus (4.10) yields

$$\ddot{\phi}(t) = 0 \tag{4.12}$$

The time-dependent part of the solution corresponds to a transport motion of the type

$$\phi(t) = \gamma + \delta t \tag{4.13}$$

Hence it may be said that the linearized vibration analysis provides two types of solutions:

- Rigid-body modes $\boldsymbol{u}_{(i)}$, in number equal to the degree of singularity of the stiffness matrix, which may be regarded as eigenmodes with zero eigenfrequency. Their time function (4.13) describes an overall transport motion.
- Eigenmodes $\boldsymbol{x}_{(r)}$ associated with non-zero eigenfrequencies ω_r. For each of them there is a corresponding modal solution (4.11) representing a vibration about the overall motion.

Finally, let us note that any linear combination of these modes satisfies the free vibration equation (4.1). The amplitude coefficients α_r, β_r, γ and δ in (4.11, 4.13) are defined by the initial conditions as discussed later.

Example: the double pendulum

Let us reconsider the double pendulum problem (Figure 1.7) and the linear matrices obtained in section 2.2.2 around the equilibrium $\theta_1 = \theta_2 = 0$. On page 50, we have shown that this equilibrium position is stable. Let us then compute the free vibration modes around that equilibrium position. Let us assume that $m_1 = 4m$ and $m_2 = m$, and $\ell_1 = 2\ell$, $\ell_2 = \ell$. Considering the linear matrices for the absolute angles (see matrices page 33), the vibration modes are solution of the eigenproblem

$$\left(\begin{bmatrix} 10mg\ell & 0 \\ 0 & mg\ell \end{bmatrix} - \omega^2 \begin{bmatrix} 20m\ell^2 & 2m\ell^2 \\ 2m\ell^2 & m\ell^2 \end{bmatrix} \right) \begin{bmatrix} \theta_1 \\ \theta_2 \end{bmatrix} = \boldsymbol{0}$$

Let us introduced the notation $\nu^2 = \omega^2 \ell / g$ for the non-dimensional frequencies and the length ratio, so that the eigenproblem writes

$$\left(\begin{bmatrix} 10 & 0 \\ 0 & 1 \end{bmatrix} - \nu^2 \begin{bmatrix} 20 & 2 \\ 2 & 1 \end{bmatrix} \right) \begin{bmatrix} \theta_1 \\ \theta_2 \end{bmatrix} = \boldsymbol{0}$$

The characteristic polynomial of the equation is

$$(10 - 20\nu^2)(1 - \nu^2) - 4\nu^4 = 0$$

Hence the eigenfrequencies are

$$\nu_1^2 = \frac{\omega_1^2 \ell}{g} = 0.4336$$

$$\nu_2^2 = \frac{\omega_2^2 \ell}{g} = 1.4414$$

The eigenmodes are then found by assuming they have the form (remember that they are defined at a constant!)

$$\boldsymbol{x}_{(1)} = \begin{bmatrix} 1 \\ X_1 \end{bmatrix} \qquad \boldsymbol{x}_{(2)} = \begin{bmatrix} 1 \\ X_2 \end{bmatrix}$$

Using the first equation in the eigenvalue problem, one finds

$$\boldsymbol{X}_1 = \frac{10 - 20\nu_1^2}{2\nu_1^2} = 1.5311$$

$$\boldsymbol{X}_2 = \frac{10 - 20\nu_2^2}{2\nu_2^2} = -6.5311$$

It is always a good idea to verify the result by checking if the eigenmodes satisfy also the second equation of the eigenproblem, namely

$$\boldsymbol{X}_1 = \frac{2\nu_1^2}{1 - \nu_1^2} = 1.5311$$

$$\boldsymbol{X}_2 = \frac{2\nu_2^2}{1 - \nu_2^2} = -6.5311$$

The eigensolutions are thus

$$\omega_1^2 = 0.4336\frac{g}{\ell} \qquad \boldsymbol{x}_{(1)} = \begin{bmatrix} 1 \\ 1.5311 \end{bmatrix}$$

$$\omega_2^2 = 1.4414\frac{g}{\ell} \qquad \boldsymbol{x}_{(2)} = \begin{bmatrix} 1 \\ -6.5311 \end{bmatrix}$$

At this point one should visualize the modes on a small graphic.

4.1.3 Orthogonality of eigenmodes

Let us examine the case of two eigenmodes denoted $\boldsymbol{x}_{(r)}$ and $\boldsymbol{x}_{(s)}$ associated with distinct frequencies ω_r and ω_s such that $\omega_r \neq \omega_s$. Premultiplying by $\boldsymbol{x}_{(s)}^T$ the eigenproblem (4.7) satisfied by $\boldsymbol{x}_{(r)}$ yields

$$\boldsymbol{x}_{(s)}^T \boldsymbol{K} \boldsymbol{x}_{(r)} = \omega_r^2 \boldsymbol{x}_{(s)}^T \boldsymbol{M} \boldsymbol{x}_{(r)} \tag{4.14}$$

Similarly, starting from the equation verified by eigenmode $\boldsymbol{x}_{(s)}$ and premultiplying by $\boldsymbol{x}_{(r)}^T$, we obtain

$$\boldsymbol{x}_{(r)}^T \boldsymbol{K} \boldsymbol{x}_{(s)} = \omega_s^2 \boldsymbol{x}_{(r)}^T \boldsymbol{M} \boldsymbol{x}_{(s)} \tag{4.15}$$

Subtracting (4.15) from (4.14) while taking into account the symmetry of the mass and stiffness matrices provides the result

$$\left(\omega_r^2 - \omega_s^2\right) \boldsymbol{x}_{(s)}^T \boldsymbol{M} \boldsymbol{x}_{(r)} = 0$$

and thus, for distinct eigenfrequencies,

$$\boldsymbol{x}_{(s)}^T \boldsymbol{M} \boldsymbol{x}_{(r)} = 0 \tag{4.16}$$

Moreover, the substitution of this result into (4.14) also yields

$$\boldsymbol{x}_{(s)}^T \boldsymbol{K} \boldsymbol{x}_{(r)} = 0 \tag{4.17}$$

Equations (4.16) and (4.17) are the *orthogonality relationships* between eigenmodes of distinct eigenfrequencies with respect to the mass and stiffness matrices. They play an essential role when expressing the general solution of the equations of motion for an n-degree-of-freedom vibrating system.

In order to obtain the physical interpretation of these relationships, let us view (4.16) as the product of the inertia forces $\boldsymbol{M}\boldsymbol{x}_{(r)}$ of eigenmode r by the eigenmode $\boldsymbol{x}_{(s)}$. Equation (4.16) thus expresses that

> *The work produced by the inertia forces of mode r on a displacement described by mode s is zero.*

Similarly, equation (4.17) expresses that

The work produced by the elastic forces of mode r on a displacement described by mode s is zero.

The quadratic forms

$$\boldsymbol{x}_{(r)}^T \boldsymbol{K} \boldsymbol{x}_{(r)} = \gamma_r \tag{4.18}$$

$$\boldsymbol{x}_{(r)}^T \boldsymbol{M} \boldsymbol{x}_{(r)} = \mu_r \tag{4.19}$$

measure respectively the contribution of mode r to the deformation energy and to the kinetic energy. They are respectively called the *generalized stiffness* and the *generalized mass* of mode r. Both quantities are known only to a constant factor since the amplitude of eigenmode $\boldsymbol{x}_{(r)}$ is undetermined. This indeterminacy may be removed by calculating their ratio: setting $r = s$ into equation (4.14) one obtains[1]

$$\frac{\boldsymbol{x}_{(r)}^T \boldsymbol{K} \boldsymbol{x}_{(r)}}{\boldsymbol{x}_{(r)}^T \boldsymbol{M} \boldsymbol{x}_{(r)}} = \frac{\gamma_r}{\mu_r} = \omega_r^2 \tag{4.20}$$

The indeterminacy in the norm of eigenmode $\boldsymbol{x}_{(r)}$ allows us, when necessary, to choose it appropriately, the most common choices being

- setting the largest component to unity or
- setting the generalized mass to unity.

When the latter choice is adopted, the orthogonality relationships may be rewritten in the simpler form

$$\boxed{\begin{aligned} \boldsymbol{x}_{(s)}^T \boldsymbol{K} \boldsymbol{x}_{(r)} &= \omega_r^2 \delta_{rs} \\ \boldsymbol{x}_{(s)}^T \boldsymbol{M} \boldsymbol{x}_{(r)} &= \delta_{rs} \end{aligned}} \tag{4.19}$$

where δ is Kronecker's symbol defined as

$$\delta_{rs} = \begin{cases} 1 & \text{if } r = s \\ 0 & \text{if } r \neq s \end{cases}$$

Example: The double pendulum

Let us consider the modes found for the double pendulum on page 63.

$$\boldsymbol{x}_{(1)} = \begin{bmatrix} 1 \\ 1.5311 \end{bmatrix}$$

$$\boldsymbol{x}_{(2)} = \begin{bmatrix} 1 \\ -6.5311 \end{bmatrix}$$

[1] The quotient $\frac{\boldsymbol{x}^T \boldsymbol{K} \boldsymbol{x}}{\boldsymbol{x}^T \boldsymbol{M} \boldsymbol{x}} = \omega^2$ for any vector $\boldsymbol{x}$ is called the *Rayleigh quotient*.

The modal masses can be computed as

$$\mu_1 = \boldsymbol{x}_{(1)}^T \begin{bmatrix} 20 & 2 \\ 2 & 1 \end{bmatrix} \boldsymbol{x}_{(1)} = 28.4689$$

$$\mu_2 = \boldsymbol{x}_{(2)}^T \begin{bmatrix} 20 & 2 \\ 2 & 1 \end{bmatrix} \boldsymbol{x}_{(2)} = 36.5311$$

One verifies that

$$\boldsymbol{x}_{(2)}^T \begin{bmatrix} 20 & 2 \\ 2 & 1 \end{bmatrix} \boldsymbol{x}_{(1)} = 0$$

Further, let us compute the modal stiffnesses as

$$\gamma_1 = \boldsymbol{x}_{(1)}^T \begin{bmatrix} 10 & 0 \\ 0 & 1 \end{bmatrix} \boldsymbol{x}_{(1)} = 12.3444$$

$$\gamma_2 = \boldsymbol{x}_{(2)}^T \begin{bmatrix} 10 & 0 \\ 0 & 1 \end{bmatrix} \boldsymbol{x}_{(2)} = 52.6556$$

and verify that

$$\boldsymbol{x}_{(2)}^T \begin{bmatrix} 10 & 0 \\ 0 & 1 \end{bmatrix} \boldsymbol{x}_{(1)} = 0$$

One also verifies that

$$\omega_1^2 \frac{\ell}{g} = \frac{\gamma_1}{\mu_1} = 0.4336$$

$$\omega_2^2 \frac{\ell}{g} = \frac{\gamma_2}{\mu_2} = 1.4414$$

which correspond to the frequencies found on page 63.

Finally the mass-normalized modes are obtained as

$$\tilde{\boldsymbol{x}}_{(1)} = \frac{\boldsymbol{x}_{(1)}}{\sqrt{\mu_1}} = \begin{bmatrix} 0.1874 \\ 0.2870 \end{bmatrix}$$

$$\tilde{\boldsymbol{x}}_{(2)} = \frac{\boldsymbol{x}_{(2)}}{\sqrt{\mu_2}} = \begin{bmatrix} 0.1655 \\ -1.0806 \end{bmatrix}$$

4.1.4 Degeneracy theorem and generalized orthogonality relationships

When a structure exhibits some form of symmetry, different modes can exist for a same eigenfrequency. In that case, some eigenvalues are multiple roots of the characteristic polynomial (4.8) and we will call m that multiplicity. The purpose of the degeneracy theorem is to generalize the orthogonality concept between eigenmodes to the case where several eigensolutions degenerate and give rise to a multiple eigenvalue.

The degeneracy theorem states that

To a multiple root ω_p^2 of system

$$\boldsymbol{K}\boldsymbol{x} - \omega^2 \boldsymbol{M}\boldsymbol{x} = \boldsymbol{0}$$

corresponds a number of linearly independent eigenvectors equal to the root multiplicity.

In other words, the m eigenvectors corresponding to an eigenvalue with multiplicity m are linearly independent and may be combined in order to give an orthogonal basis spanning a subspace of dimension m.

Example: a mass suspended in two directions

Let us consider a mass m suspended to a wall in the horizontal and vertical direction with springs of equal stiffness k (fig. 4.1). The vibration of the system is described by the eigenvalue problem

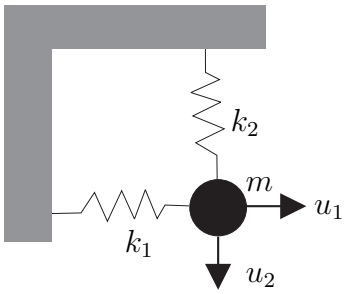

Figure 4.1: Example of a system with a multiple frequency

$$\left(\begin{bmatrix} k & 0 \\ 0 & k \end{bmatrix} - \omega^2 \begin{bmatrix} m & 0 \\ 0 & m \end{bmatrix} \right) \begin{bmatrix} x \\ y \end{bmatrix} = 0$$

where x and y are the horizontal and vertical displacements of the mass. The characteristic polynomial of the eigenvalue problem is

$$(k - \omega^2 m)^2 = 0$$

and thus

$$\omega^2 = \frac{k}{m}$$

is an eigenvalue of multiplicity 2. We note that any choice

$$\boldsymbol{x}_{(s)} = \begin{bmatrix} X \\ Y \end{bmatrix}$$

is an eigenmode. We can *choose*

$$\boldsymbol{x}_{(1)} = \begin{bmatrix} 1 \\ 0 \end{bmatrix} \qquad \boldsymbol{x}_{(2)} = \begin{bmatrix} 0 \\ 1 \end{bmatrix}$$

as eigenmodes satisfying the $\boldsymbol{K}$ and $\boldsymbol{M}$ orthogonality.

4.2 Mode Superposition

4.2.1 Modal decoupling and normal equations

Let us for now assume that no damping is present in the system. When an n-degree-of-freedom system is submitted to external forces $\boldsymbol{p}(t)$ known as a function of time, its transient response is governed by equation

$$\boxed{\begin{array}{c}\boldsymbol{M}\ddot{\boldsymbol{q}} + \boldsymbol{K}\boldsymbol{q} = \boldsymbol{p}(t) \\ \text{given} \;\; \boldsymbol{q}(0) = \boldsymbol{q}_0, \;\; \dot{\boldsymbol{q}}(0) = \dot{\boldsymbol{q}}_0\end{array}} \tag{4.20}$$

Since the normal vibration modes represent an orthogonal set of n vectors, any arbitrary vector can be expanded in the basis of the modes, i.e. any vector of dimension n can be exactly represented by linear combination of the modes $\boldsymbol{x}_{(r)}$ satisfying the free vibration problem (4.7). Hence, the system response may be expressed through modal expansion as

$$\boldsymbol{q}(t) = \sum_{s=1}^{n} \eta_s(t) \boldsymbol{x}_{(s)} \tag{4.21}$$

where $\eta_s(t)$ are the time-dependent amplitudes of the modal components, that is the coordinates of $\boldsymbol{q}(t)$ in the basis of the eigenmodes.

Substituting (4.21) into (4.20) and premultiplying by each eigenmode $\boldsymbol{x}_{(r)}$ successively in order to project the dynamic equilibrium equations onto the modal directions, we find

$$\boldsymbol{x}_{(r)}^T \left(\boldsymbol{M} \sum_{s=1}^{n} \boldsymbol{x}_{(s)} \ddot{\eta}_s(t) + \boldsymbol{K} \sum_{s=1}^{n} \boldsymbol{x}_{(s)} \eta_s(t) \right) = \boldsymbol{x}_{(r)}^T \boldsymbol{p}(t)$$

Owing to orthogonality (4.21) between eigenmodes, we find the uncoupled equations for the modal amplitudes called the *normal equations*

$$\ddot{\eta}_r(t) + \omega_r^2 \eta_r(t) = \phi_r(t) \qquad\qquad r = 1, \ldots, n \tag{4.22}$$

with the *modal participation factor* of mode r to the loading

$$\phi_r(t) = \frac{\boldsymbol{x}_{(r)}^T \boldsymbol{p}(t)}{\mu_r} \tag{4.23}$$

The normal equations (4.22) show that,

> *in the absence of damping, calculating the response of an n-degree-of-freedom system reduces to the solution of n uncoupled single-degree-of-freedom systems excited by the external forces (4.23).*

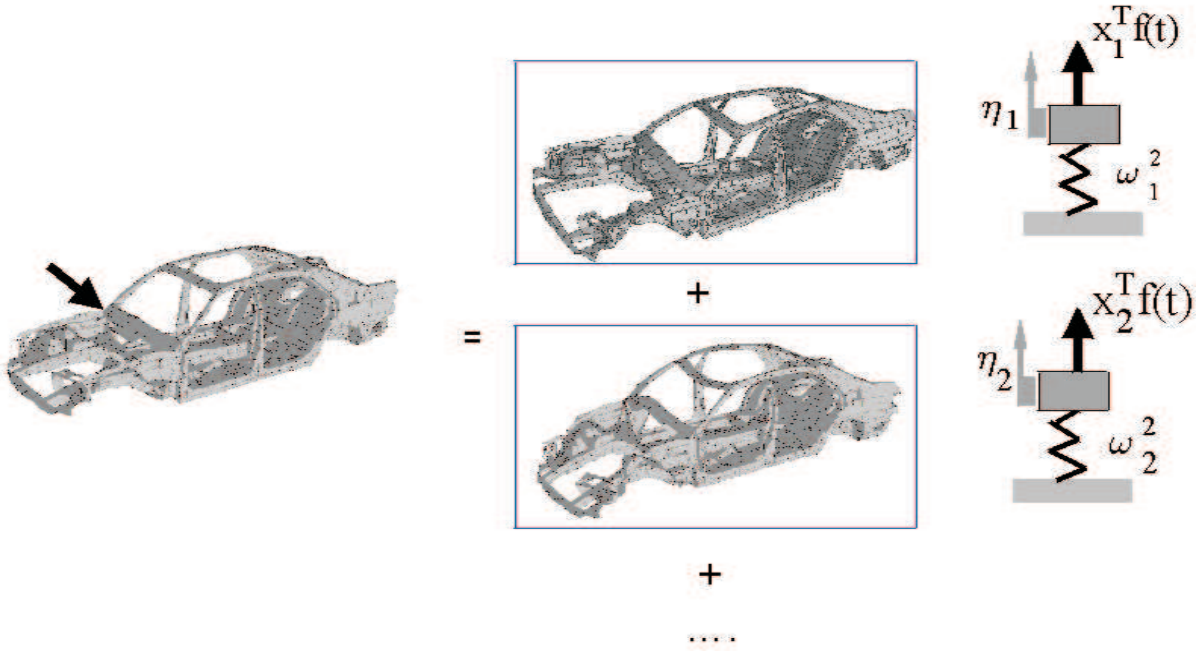

Figure 4.2: Schematic representation of mode superposition

A schematic representation of mode superposition is given in Figure 4.2. This result is fundamental in treating the dynamics of structures since it transforms the fully coupled dynamical equation into a set of scalar differential equations. Note that if the first modes are rigid body modes, then the normal equations are still like in (4.22) except that the corresponding frequency is zero, showing that there is no associated elastic term.

The initial conditions for $\eta_s(t=0)$ in the normal equations (4.22) are found by projecting the initial condition for $\boldsymbol{q}$ on the model basis:

$$\boldsymbol{q}_0 = \sum_{s=1}^{n} \boldsymbol{x}_{(s)} \eta_s(0) \qquad \text{and} \qquad \dot{\boldsymbol{q}}_0 = \sum_{s=1}^{n} \boldsymbol{x}_{(s)} \dot{\eta}_s(0)$$

The initial conditions are then found by premultiplication by $\boldsymbol{x}_{(r)}^T \boldsymbol{M}$:

$$\begin{aligned} \eta_r(0) &= \frac{\boldsymbol{x}_{(r)}^T \boldsymbol{M} \boldsymbol{q}_0}{\mu_r} \\ \dot{\eta}_r(0) &= \frac{\boldsymbol{x}_{(r)}^T \boldsymbol{M} \dot{\boldsymbol{q}}_0}{\mu_r} \qquad r = 1, \ldots n \end{aligned} \tag{4.24}$$

4.2.2 Time integration of the normal equations

General solution of normal equations Each of the normal equations may be integrated in the form of a convolution product. To that purpose, let us define the Laplace

transform $\bar{\eta}_r$ and $\bar{\phi}_r$

$$\bar{\eta}_r(s) = \mathcal{L}\left(\eta_r(t)\right) = \int_0^{+\infty} \mathrm{e}^{-st}\eta_r(t)dt \tag{4.25}$$

$$\bar{\phi}_r(s) = \mathcal{L}\left(\phi_r(t)\right) = \int_0^{+\infty} \mathrm{e}^{-st}\phi_r(t)dt \tag{4.26}$$

The Laplace transform of a normal equation (4.22) is then

$$s^2\bar{\eta}_r(s) - s\eta_r(0) - \dot{\eta}_r(0) + \omega_r^2\bar{\eta}_r(s) = \bar{\phi}_r(s) \qquad r = 1, \ldots n$$

Hence,

$$\bar{\eta}_r(s) = \frac{s\eta_r(0) + \dot{\eta}_r(0) + \bar{\phi}_r(s)}{s^2 + \omega_r^2} \qquad r = 1, \ldots n \tag{4.27}$$

Let us assume that no rigid body modes are present. The inverse Laplace transform of (4.27) is found by defining $h_r(t)$ as

$$\begin{aligned} h_r(t) &= \mathcal{L}^{-1}\left(\frac{1}{s^2 + \omega_r^2}\right) \\ &= \frac{\sin\omega_r t}{\omega_r} \end{aligned} \tag{4.28}$$

and recalling that

$$\mathcal{L}^{-1}\left(\frac{s}{s^2 + \omega_r^2}\right) = \cos\omega_r t$$

The solution $\eta_r(t)$ is then found from (4.27) as

$$\eta_r(t) = \eta_r(0)\cos(\omega_r t) + \dot{\eta}_r(0)h_r(t) + \int_0^t \phi_r(\tau)\ h_r(t-\tau)\, d\tau \tag{4.29}$$

The first two terms of this solution represent the response to the initial conditions. The last term is a convolution product known as *Duhamel's integral* and represents the forced response to the external loads $\boldsymbol{p}(t)$. The coefficients $\eta_r(0)$ and $\dot{\eta}_r(0)$ are the modal components of the given initial conditions $\boldsymbol{q}_0$ and $\dot{\boldsymbol{q}}_0$ (see equation 4.24).

Impulse response interpretation Physically, solution (4.29) can be interpreted with the concept of the impulse response: when an impulse $\phi(\tau)d\tau$ is applied at time τ to a one-degree-of-freedom system described by the normal equations (4.22), the response is a jump in the velocity such that

$$\Delta\dot{\eta}(\tau) = \phi(\tau)d\tau$$

Observing then from the second term in the response (4.29) that $h_r(t)$ is the time response to an initial velocity, it is understood that $h_r(t-\tau)$ is the dynamic response of the system to a change of velocity at time τ. Therefore, if we now assume that any force can be decomposed in a series of impulses such as described in Figure 4.3, the convolution product in (4.29) is understood as the sum of the responses to impulses at times τ between $t = 0$ and t.

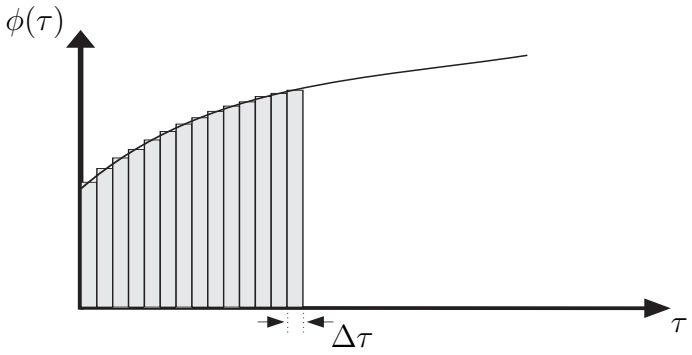

Figure 4.3: Forcing function as a series of impulses

4.3 Mode Superposition for forced harmonic response

The case of the forced harmonic response of an n-degree-of-freedom oscillator is important mainly for two reasons:

- On one hand, the system response in the frequency domain is the easiest one to identify experimentally.
- On the other hand, the harmonic regime is representative of many excitation cases encountered in engineering practice, such as vibration induced by unbalance, and torsional vibration in engines.

Forced vibration of an n-degree-of-freedom oscillator is defined as the motion resulting from the application of a harmonic force with constant amplitude

$$\boxed{\boldsymbol{M}\ddot{\boldsymbol{q}} + \boldsymbol{K}\boldsymbol{q} = \boldsymbol{s}\cos\omega t} \tag{4.30}$$

where ω is *the excitation frequency*. The forced response is then the part of the response synchronous to the excitation

$$\boldsymbol{q} = \boldsymbol{x}\cos\omega t \tag{4.31}$$

Substituting the solution form (4.31) into the equations of motion (4.30) yields the algebraic system governing the amplitude of the response

$$\big(\boldsymbol{K} - \omega^2\boldsymbol{M}\big)\boldsymbol{x} = \boldsymbol{s} \tag{4.32}$$

Let us solve this algebraic problem by an eigenmode series expansion including the possible presence of m rigid-body modes

$$\boldsymbol{x} = \sum_{i=1}^{m} \xi_i \boldsymbol{u}_{(i)} + \sum_{s=m+1}^{n} \eta_s \boldsymbol{x}_{(s)}$$

Substituting in equation (4.32) the amplitude development above and taking account of eigenmode orthogonality provides the n spectral coordinates

$$\xi_i = -\frac{\boldsymbol{u}_{(i)}^T\boldsymbol{s}}{\omega^2\mu_i} \qquad\qquad \eta_s = \frac{\boldsymbol{x}_{(s)}^T\boldsymbol{s}}{\big(\omega_s^2 - \omega^2\big)\mu_s}$$

A factorization to the right gives the forced response amplitude expression

$$\boldsymbol{x} = \Big\{ -\frac{1}{\omega^2} \sum_{i=1}^{m} \frac{\boldsymbol{u}_{(i)} \boldsymbol{u}_{(i)}^T}{\mu_i} + \sum_{s=m+1}^{n} \frac{\boldsymbol{x}_{(s)} \boldsymbol{x}_{(s)}^T}{\big(\omega_s^2 - \omega^2\big)\mu_s} \Big\} \boldsymbol{s} \tag{4.33}$$

This solution clearly indicates that when the excitation frequency ω is close to an eigenfrequency ω_r, the amplitude of the response goes to infinity and the response shape corresponds to mode $\boldsymbol{x}_{(r)}$.

Remark Let us note that the solution $\boldsymbol{x}$ to (4.32) can also be computed directly by factorizing $\boldsymbol{K} - \omega^2 \boldsymbol{M}$. Obviously, using a direct solver for $\boldsymbol{x}$ is faster then computing the eigensolutions and applying (4.33). However, when analyzing the dynamic behavior in a frequency range, the forced response amplitude must be computed for several excitation frequencies ω^2. In that case the mode superposition approach is much more efficient since a direct solution requires a new factorization of $\boldsymbol{K} - \omega^2 \boldsymbol{M}$ to be performed every time ω is changed.

4.3.1 Frequency response function

Let us analyze the forced harmonic response x_k of a degree of freedom k to a harmonic excitation s_k on that same degree-of-freedom. From (4.33) we find

$$\frac{x_k}{s_k}(\omega^2) = a_{kk}(\omega^2) = -\frac{1}{\omega^2} \sum_{i=1}^{m} \frac{u_{k(i)}^2}{\mu_i} + \sum_{s=m+1}^{n} \frac{x_{k(s)}^2}{\big(\omega_s^2 - \omega^2\big)\mu_s} \tag{4.34}$$

This *frequency response function* $a_{kk}(\omega^2)$ possesses the fundamental property

$$\frac{da_{kk}}{d\omega^2} = \frac{1}{(\omega^2)^2} \sum_{i=1}^{m} \frac{u_{k(i)}^2}{\mu_i} + \sum_{s=1}^{n-m} \frac{x_{k(s)}^2}{\big(\omega_s^2 - \omega^2\big)^2 \mu_s} > 0$$

i.e. that amplitude response is always increasing with excitation frequency.

When no rigid body modes are present, the frequency response function $a_{kk}(\omega^2)$ is as plotted in Figure 4.4. It clearly shows the resonance when the excitation frequency ω is close to an eigenfrequency. Also, it is observed that two resonance eigenfrequencies ω_r and ω_{r+1} are separated by an *antiresonance frequency* noted ω_r^k. By contrast with the resonance eigenfrequencies, the antiresonance frequencies are specific to the degree of freedom k associated with a_{kk}. From a physical point of view, they may be regarded as the resonance eigenfrequencies of the modified system obtained by fixing degree of freedom q_k. Let us recall that the principle of the undamped dynamic absorber is a direct application of the antiresonance concept, since it consists of adding a one-degree-of-freedom system to the existing system in order to impose the condition that one of the antiresonance frequencies ω_r^k of degree of freedom number k coincides with the excitation frequency.

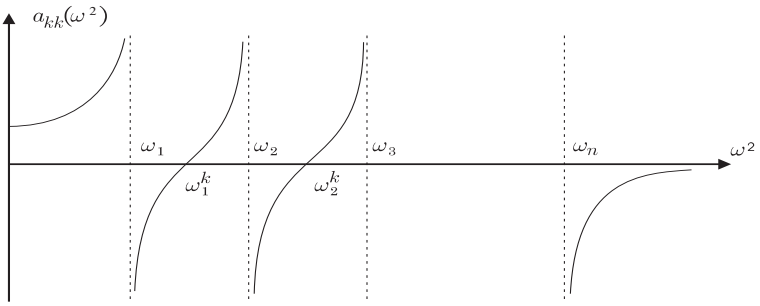

Figure 4.4: Frequency response function

4.4 Approximation by truncated modal series

When expressing the system response to external loading through mode superposition, it generally occurs that the number of degrees of freedom is so large that the modal expansion has to be restricted to a subset of k modes. Indeed, computing eigensolutions is a very expensive procedure and therefore, in practice, only a small number of modes can be obtained. An approximate solution can then be built by truncating the modal superposition. The accuracy of the truncated representation will be discussed.

4.4.1 Mode displacement method

When only k eigensolutions are computed, a simple way to get an approximation to the dynamic response is to neglect the higher modes. Therefore, in the *modal displacement method*, the transient dynamic response to (4.20) is approximated by

$$\boldsymbol{q}(t) \simeq \sum_{s=1}^{k} \eta_s(t)\boldsymbol{x}_{(s)} \qquad\qquad k < n \tag{4.35}$$

where $\eta_s(t)$ are solution of the normal equations (4.22), and can be expressed as in (4.29).

The forced harmonic response is approximates by truncating the expansion (4.33):

$$\boldsymbol{x} = \Big\{ -\frac{1}{\omega^2} \sum_{i=1}^{m} \frac{\boldsymbol{u}_{(i)}\boldsymbol{u}_{(i)}^T}{\mu_i} + \sum_{s=m+1}^{k} \frac{\boldsymbol{x}_{(s)}\boldsymbol{x}_{(s)}^T}{\big(\omega_s^2 - \omega^2\big)\mu_s} \Big\} \boldsymbol{s} \tag{4.36}$$

Clearly, this is a good approximation of (4.33) as long as the excitation frequency ω^2 is much smaller then the highest eigenfrequency ω_k^2 in the truncated series. Let us further discuss the convergence of the mode displacement method.

4.4.2 Accuracy of the approximation

In order to analyze the accuracy of such an approximation, let us assume that the external load is of type

$$\boldsymbol{p}(t) = \boldsymbol{g}\varphi(t)$$

where $\boldsymbol{g}$ designates a static load distribution applied with the time-variation law $\varphi(t)$. For a system initially at rest, (4.29) yields the transient response by the truncated series

$$\boldsymbol{q}(t) = \sum_{s=1}^{k} \frac{\boldsymbol{x}_{(s)}\boldsymbol{x}_{(s)}^T\boldsymbol{g}}{\mu_s} \frac{1}{\omega_s} \int_0^t \sin\big(\omega_s(t-\tau)\big)\varphi(\tau)\,d\tau \tag{4.37}$$

the convergence of which determines the quality of the displacement solution. One notes that each term of the series is expressed as the product of two factors:

- A spatial factor whose amplitude

$$\frac{\boldsymbol{x}_{(s)}\boldsymbol{x}_{(s)}^T\boldsymbol{g}}{\mu_s}$$

  depends only on the projection of the load on the mode under consideration.

- A temporal factor

$$\theta_s(t) = \frac{1}{\omega_s} \int_0^t \sin\big(\omega_s(t-\tau)\big)\varphi(\tau)\,d\tau$$

  which depends simultaneously on the system eigenspectrum and on the time variation of the system excitation.

The convergence of the modal expansion (4.37) is thus governed by two types of convergence:

- A *convergence of quasi-static type* occurring if the applied load $\boldsymbol{g}$ admits a sufficiently accurate spatial representation in the basis of the $k < n$ retained eigenmodes. This is equivalent to assuming that $\boldsymbol{p}$ must be nearly orthogonal to the $(n-k)$ omitted eigenmodes which therefore will not be excited or will be only slightly excited.

- A *convergence of spectral type* conditioned by the convergence to zero of the convolution products (4.37) when progressing in the eigenspectrum of the system. It thus depends both on the frequency content of the excitation and on the system eigenspectrum. For example:

  – in the indicial case, $\varphi(t) = 1$ for $t > 0$ and

$$\theta_s(t) = \frac{1 - \cos\omega_s t}{\omega_s^2}$$

  – in the harmonic case, $\varphi(t) = \cos(\omega t)$ and

$$\theta_s(t) = \frac{\omega_s \sin\omega t - \omega \sin\omega_s t}{\omega_s\big(\omega_s^2 - \omega^2\big)}$$

The global convergence of development (4.37) results from the combination of both convergence types described, and it thus remains difficult to measure quantitatively since it depends on the vibration modes which have not been computed during the eigenvalue analysis and hence have been neglected.

4.5 Modal analysis of damped systems

When taking into account a dissipation mechanism described by a viscous dissipation, the damped vibration problem is then governed by equation

$$\boldsymbol{M}\ddot{\boldsymbol{q}} + \boldsymbol{C}\dot{\boldsymbol{q}} + \boldsymbol{K}\boldsymbol{q} = \boldsymbol{p}(t) \tag{4.38}$$

with $\boldsymbol{C}$, a symmetric and non-negative damping matrix.

The presence of the damping term complicates considerably the solution of the problem and makes it more difficult to understand the behavior of dynamic systems. Taking it into account is, however, most essential in the elaboration of methods allowing the experimental determination of modal characteristics such as eigenmodes, eigenfrequencies and generalized masses. We are thus considering the behavior of the damped system to a certain extent for computational reasons but also for experimental purposes.

Let us consider the *conservative system* associated with the real system: it is governed by equations $\boldsymbol{M}\ddot{\boldsymbol{q}} + \boldsymbol{K}\boldsymbol{q} = \boldsymbol{0}$ and its eigenmodes and eigenfrequencies will be noted respectively $\boldsymbol{x}_{(r)}$ and ω_{0r}^2. Let us try, as in the undamped case, to solve the system of equations (4.38) through a modal expansion in terms of eigenmodes $\boldsymbol{x}_{(r)}$ of the associated conservative system

$$\boldsymbol{q} = \sum_{s=1}^{n} \eta_s(t)\boldsymbol{x}_{(s)} \tag{4.39}$$

The presence of the damping term causes a coupling of the resulting equations. Indeed, by substituting (4.39) into (4.38) and making use of the eigenmode orthogonality relationships with respect to $\boldsymbol{M}$ and $\boldsymbol{K}$, one obtains

$$\ddot{\eta}_r + \sum_{s=1}^{n} \frac{\beta_{rs}}{\mu_r}\dot{\eta}_s + \omega_{0r}^2\eta_r = \phi_r(t) \qquad\qquad r = 1, \ldots, n \tag{4.40}$$

with the *damping coefficients*

$$\beta_{rs} = \boldsymbol{x}_{(r)}^T \boldsymbol{C}\boldsymbol{x}_{(s)} \tag{4.41}$$

which do not vanish in general, even for $r \neq s$. The modal participation factors $\phi_r(t)$ in the excitation are still defined by equation (4.23). The form (4.40) of the resulting equations shows that, unless restrictive assumptions are made with respect to the damping distribution, the modal approach is not interesting for obtaining a numerical solution to the equations of motion. Indeed, the normal equations remain coupled by the damping coefficients β_{rs}.

Nevertheless, even when the relative importance of the damping terms prevents any simplifying assumptions, the modal approach is of interest when the displacement representation is limited to a small number of modes, since the system size to be integrated is then reduced to the number of modes retained in the spectral expansion of the solution.

A more general mode superposition scheme can be devised in terms of vibration modes of the damped system. Looking for a free vibration in the form of $\boldsymbol{q} = \boldsymbol{z}\mathrm{e}^{\lambda t}$, the complex

eigenmodes are defined as the solution of the damped eigenvalue problem

$$\left(\lambda_s^2 \boldsymbol{M} + \lambda_s \boldsymbol{C} + \boldsymbol{K}\right) \boldsymbol{z}_{(s)} = 0 \tag{4.42}$$

which can be put in a standard eigenvalue problem by considering the state space form (see section 3.2.4)

$$(\lambda_s \boldsymbol{A} + \boldsymbol{B}) \begin{bmatrix} \lambda_s \boldsymbol{z}_{(s)} \\ \boldsymbol{z}_{(s)} \end{bmatrix} = \boldsymbol{0} \tag{4.43}$$

where

$$\boldsymbol{A} = \begin{bmatrix} \boldsymbol{0} & \boldsymbol{M} \\ \boldsymbol{M} & \boldsymbol{C} \end{bmatrix} \qquad \boldsymbol{B} = \begin{bmatrix} -\boldsymbol{M} & \boldsymbol{0} \\ \boldsymbol{0} & \boldsymbol{K} \end{bmatrix} \tag{4.44}$$

Note that in this case the eigenmodes and eigenvalues are complex indicating that the free vibration solutions are non-synchronous (see section 3.1) and represent damped oscillations (if positive and non-critical damping). The complex modes $\boldsymbol{z}_{(s)}$ also satisfy orthogonality relationships with respect to the matrices $\boldsymbol{A}$ and $\boldsymbol{B}$ and can therefore be used to define a mode superposition in the state-space similarly to the superposition of mode superposition for conservative systems. We will not detail this technique here (see e.g. [3]).

In many practical cases, the damping in the structure is small and in that particular case, modal superposition using the free vibration modes $\boldsymbol{x}_{(r)}$ of the associated conservative system still leads to a uncoupled set of normal equations as explained next.

4.5.1 Modal damping assumption for lightly damped structures

Equation (4.40) shows that the computation of the damped response would be considerably simplified if the coupling through damping did not exist ($\beta_{kl} = 0, k \neq l$). In order for this to be the case, the dissipation forces should have the same distribution forces as inertia and elastic forces, but there is no reason for this to be so.

However, the damping distribution is almost always ill-defined and thus it is generally necessary to make an assumption regarding its repartition. The simplest assumption consists then in assuming that the matrix $[\beta_{rs}]$ is diagonal. This assumption has no real physical background but it will be shown to be consistent with the assumption that the structure is *lightly damped*.

To show it, let us analyze the free vibrations of the damped system starting from the homogeneous system of equations

$$\boldsymbol{M}\ddot{\boldsymbol{q}} + \boldsymbol{C}\dot{\boldsymbol{q}} + \boldsymbol{K}\boldsymbol{q} = \boldsymbol{0} \tag{4.45}$$

and let us introduce the assumption that the damping terms are of an order of magnitude lower than the stiffness and mass terms.

Equation (4.45) admits solutions of general form

$$\boldsymbol{q} = \boldsymbol{z}\, e^{\lambda t}$$

with roots λ_k and vibration eigenmodes $\boldsymbol{z}_{(k)}$ solutions of

$$\big(\lambda_k^2\boldsymbol{M}+\lambda_k\boldsymbol{C}+\boldsymbol{K}\big)\boldsymbol{z}_{(k)}=\boldsymbol{0} \tag{4.46}$$

Without damping one would have $\lambda_k=\pm i\omega_{0k}$ and $\boldsymbol{z}_{(k)}=\boldsymbol{x}_{(k)}$, ω_{0k} and $\boldsymbol{x}_{(k)}$ being the eigenmodes and eigenfrequencies of the associated conservative system

$$\big(\boldsymbol{K}-\omega_{0k}^2\boldsymbol{M}\big)\boldsymbol{x}_{(k)}=\boldsymbol{0} \tag{4.47}$$

If the system is assumed to be lightly damped, it can be supposed that λ_k and $\boldsymbol{z}_{(k)}$ differ only slightly from $i\omega_{0k}$ and $\boldsymbol{x}_{(k)}$ respectively

$$\boxed{\begin{array}{rcl}\lambda & = & i\omega_{0k}+\Delta\lambda\\ \boldsymbol{z}_{(k)} & = & \boldsymbol{x}_{(k)}+\Delta\boldsymbol{z}\end{array}} \tag{4.48}$$

Substituting (4.48) into equation (4.46) yields

$$\big\{\big(-\omega_{0k}^2+2i\omega_{0k}\Delta\lambda+(\Delta\lambda)^2\big)\boldsymbol{M}+\big(i\omega_{0k}+\Delta\lambda\big)\boldsymbol{C}+\boldsymbol{K}\big\}\,\big(\boldsymbol{x}_{(k)}+\Delta\boldsymbol{z}\big)=\boldsymbol{0}$$

Neglecting next the second-order terms and taking account of the fundamental relationship (4.47) verified by eigenmode $\boldsymbol{x}_{(k)}$, one obtains

$$\Big(\boldsymbol{K}-\omega_{0k}^2\boldsymbol{M}\Big)\Delta\boldsymbol{z}+\Big(2i\omega_{0k}\boldsymbol{M}+\boldsymbol{C}\Big)\boldsymbol{x}_{(k)}\Delta\lambda+i\omega_{0k}\boldsymbol{C}\big(\boldsymbol{x}_{(k)}+\Delta\boldsymbol{z}\big)\simeq\boldsymbol{0} \tag{4.49}$$

The light-damping assumption allows one to neglect the terms in $\boldsymbol{C}\Delta\lambda$ and $\boldsymbol{C}\Delta\boldsymbol{z}$. One then obtains the first-order relationship

$$\Big(\boldsymbol{K}-\omega_{0k}^2\boldsymbol{M}\Big)\Delta\boldsymbol{z}+i\omega_{0k}\Big(\boldsymbol{C}+2\Delta\lambda\boldsymbol{M}\Big)\boldsymbol{x}_{(k)}\simeq\boldsymbol{0} \tag{4.50}$$

from which, after multiplication by $\boldsymbol{x}_{(k)}^T$, the correction to the eigenvalue may be extracted

$$\boldsymbol{x}_{(k)}^T\Big(\boldsymbol{C}+2\Delta\lambda\boldsymbol{M}\Big)\boldsymbol{x}_{(k)}\simeq 0$$

and

$$\Delta\lambda\simeq-\frac{\beta_{kk}}{2\mu_k}$$

providing the approximate expression

$$\boxed{\lambda_k\simeq-\frac{\beta_{kk}}{2\mu_k}+i\omega_{0k}} \tag{4.51}$$

Result (4.51) has two important consequences:

- *Each eigenvalue correction takes the form of a real negative part and thus transforms each term of the fundamental solution into a damped oscillatory motion.* This is a direct consequence of the positiveness of $\boldsymbol{C}$.

- *This first-order correction involves only the diagonal damping terms*

$$\beta_{kk} = \boldsymbol{x}_{(k)}^T \boldsymbol{C} \boldsymbol{x}_{(k)} \tag{4.52}$$

and thus the influence of the non-diagonal terms is only of second order.

Therefore one is authorized to neglect the non-diagonal damping terms without significant alteration of the eigenspectrum of the lightly damped system.

It is also possible to obtain from equation (4.50) the eigenmode correction through a modal expansion in terms of the undamped system eigenmodes

$$\Delta \boldsymbol{z} = \sum_{\substack{s=1 \\ s \neq k}}^{n} \alpha_s \boldsymbol{x}_{(s)}$$

After substitution and premultiplication by $\boldsymbol{x}_{(l)}^T$ for $l \neq k$ one obtains

$$\boldsymbol{x}_{(l)}^T \Big(\boldsymbol{K} - \omega_{0k}^2 \boldsymbol{M} \Big) \sum_{\substack{s=1 \\ s \neq k}}^{n} \alpha_s \boldsymbol{x}_{(s)} + i\omega_{0k} \boldsymbol{x}_{(l)}^T \Big(\boldsymbol{C} + 2\Delta\lambda \boldsymbol{M} \Big) \boldsymbol{x}_{(k)} \simeq \boldsymbol{0}$$

and, taking account of the orthogonality relationships,

$$\alpha_l = \frac{i\omega_{0k} \beta_{kl}}{\mu_l \big(\omega_{0k}^2 - \omega_{0l}^2 \big)}$$

and the resulting eigenmode expression

$$\boxed{\boldsymbol{z}_{(k)} = \boldsymbol{x}_{(k)} + \sum_{\substack{s=1 \\ s \neq k}}^{n} i\omega_{0k} \frac{\beta_{ks}}{\mu_s (\omega_{0k}^2 - \omega_{0s}^2)} \boldsymbol{x}_{(s)}} \tag{4.53}$$

Formula (4.53) is valid only if the β_{kl} are first-order quantities and if $(\omega_{0k}^2 - \omega_{0s}^2)$ remains finite. It shows that, *as long as the eigenfrequencies of the associated conservative system are well separated, it may be considered that the influence on the eigenmodes of the coupling through damping is of the same order of magnitude as the damping coefficients* β_{ks}.

It also shows that the eigenmode correction is an imaginary term, having as its consequence the fact that *a free vibration of the damped system is no longer a synchronous motion of the whole system.* Indeed,

$$\boldsymbol{q} = \boldsymbol{z}\, e^{\lambda t} = \big[\boldsymbol{x}_{(k)} + i\, \Im m(\Delta \boldsymbol{z}) \big] e^{(i\omega_{0k} + \Delta\lambda)t}$$

and degree of freedom q_i is no longer in phase with another degree of freedom q_j.

In summary, we showed that

for lightly damped systems with well separated eigenvalues, the eigenmode expression (3.1.12) can be approximated by $\boldsymbol{z}_{(k)} \simeq \boldsymbol{x}_{(k)}$ *and the general solution of the free vibration system takes the form*

$$\boldsymbol{q} \simeq \boldsymbol{x}_{(k)} e^{(i\omega_{0k}+\Delta\lambda)t}$$

which is consistent with the approximation

$$\boldsymbol{x}_{(k)}^T \boldsymbol{C} \boldsymbol{x}_{(s)} = \beta_{kk}\delta_{ks}$$

The discussion above shows that the modal damping assumption is in most cases physically consistent with the low-damping assumption: when a system is weakly damped and when its eigenfrequencies are well separated, the effect of the cross-damping terms $\beta_{ks}, k \neq s$, on the eigenspectrum can be neglected. This assumption, known as the *diagonal* or *modal damping* assumption, is often attributed to *Basile*, although previously proposed by *Lord Rayleigh*. It allows one to simplify the normal equations (4.40) in the form

$$\ddot{\eta}_r + \frac{\beta_r}{\mu_r}\dot{\eta}_r + \omega_r^2 \eta_r = \phi_r(t) \qquad\qquad r = 1, \ldots, n$$

where β_r now represents the diagonal damping term (4.52). By analogy with the single-degree-of-freedom system, one may define a *modal damping coefficient*

$$\varepsilon_r = \frac{\beta_r}{2\omega_{0r}\mu_r} \tag{4.54}$$

such that the contribution of eigenmode r to the solution becomes aperiodic when $\varepsilon_r \geq 1$. The normal equations are then rewritten in the form

$$\ddot{\eta}_r + 2\varepsilon_r\omega_{0r}\dot{\eta}_r + \omega_{0r}^2\eta_r = \phi_r(t) \qquad r = 1, \ldots, n \tag{4.55}$$

When computing the dynamic response of a damped structure by mode superposition, one can thus directly specify the modal damping coefficients (4.54). But one can also construct a diagonal damping matrix by taking a weighted sum of the mass and stiffness matrices, namely

$$\boldsymbol{C} = a\boldsymbol{K} + b\boldsymbol{M} \tag{4.56}$$

This gives

$$\beta_r = a\gamma_r + b\mu_r$$

and one obtains the modal damping coefficients

$$\varepsilon_r = \frac{1}{2}\left(a\omega_{0r} + \frac{b}{\omega_{0r}}\right) \tag{4.57}$$

Nevertheless, as shown in Figure 4.5, matrix (4.56) will generate a higher damping in the lower and higher frequency ranges, and a lower one in the intermediate range. Therefore, whenever possible, the modal damping coefficients ε_r will be determined from experimental vibration testing.

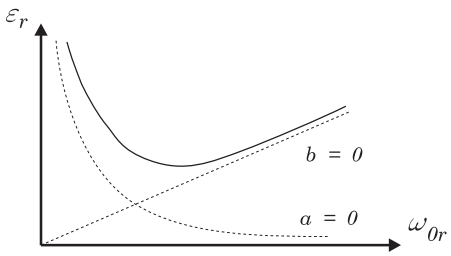

Figure 4.5: Modal damping matrix: weighted sum of mass and stiffness matrices

Example 1

Let us consider the one-dimensional problem with two degrees of freedom depicted in figure 4.6.a. The system matrices can easily be found to be

$$\boldsymbol{M} = \begin{bmatrix} m & 0 \\ 0 & 2m \end{bmatrix} \qquad \boldsymbol{C} = \begin{bmatrix} 2c & -c \\ -c & c \end{bmatrix} \qquad \boldsymbol{K} = \begin{bmatrix} 2k & -k \\ -k & 3k \end{bmatrix}$$

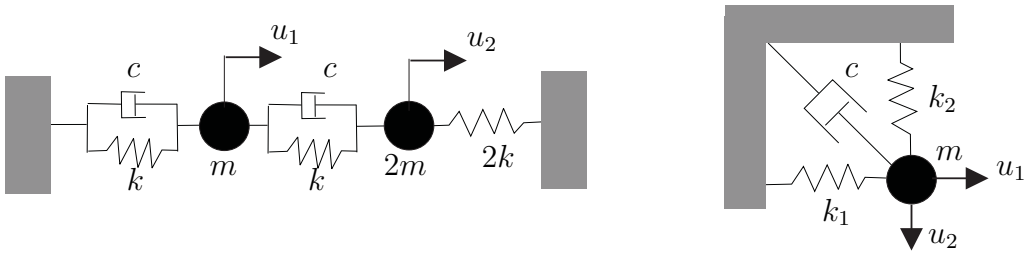

a. One dimensional problem *b. Two-dimensional problem*

Figure 4.6: Example of damped systems

The eigensolutions of the associated conservative system are found by solving

$$\det\left(\begin{bmatrix} 2 & -1 \\ -1 & 3 \end{bmatrix} - \omega^2 \frac{m}{k} \begin{bmatrix} 1 & 0 \\ 0 & 2 \end{bmatrix}\right) = 0$$

Defining $\nu^2 = \omega^2 \frac{m}{k}$ the non-dimensional frequency, the characteristic polynomial writes

$$(2 - \nu^2)(3 - 2\nu^2) - 1 = 0$$

which roots yield

$$\nu_1^2 = 1 \qquad \text{and} \qquad \omega_{01}^2 = \frac{k}{m}$$
$$\nu_2^2 = \frac{5}{2} \qquad \text{and} \qquad \omega_{02}^2 = \frac{5k}{2m}$$

and the eigenmodes are found to be

$$\boldsymbol{x}_{(1)} = \begin{bmatrix} 1 \\ 1 \end{bmatrix} \qquad \text{and} \qquad \boldsymbol{x}_{(2)} = \begin{bmatrix} 1 \\ -1/2 \end{bmatrix}$$

with modal masses of $\mu_1 = 3m$ and $\mu_2 = 1.5m$. The modal damping matrix is

$$\boldsymbol{\beta} = \begin{bmatrix} \boldsymbol{x}_{(1)}^T \\ \boldsymbol{x}_{(2)}^T \end{bmatrix} \begin{bmatrix} 2c & -c \\ -c & c \end{bmatrix} \begin{bmatrix} \boldsymbol{x}_{(1)} & \boldsymbol{x}_{(2)} \end{bmatrix} = c \begin{bmatrix} 1 & 1 \\ 1 & 13/4 \end{bmatrix}$$

Let us assume that $c = 0.06\sqrt{km}$ so that the diagonal modal damping ratios are

$$\begin{aligned} \varepsilon_1 &= \frac{\beta_{11}}{2\omega_{01}\mu_1} = 0.0100 \\ \varepsilon_1 &= \frac{\beta_{22}}{2\omega_{02}\mu_2} = 0.0411 \end{aligned}$$

Note that the second modal damping is higher since, in the first mode, the damper between the two masses is not active.

Let us now compute the complex modes and eigenvalues of the system by computing the eigensolutions of the state space form (3.21), namely solving the eigenproblem

$$\left(\lambda \begin{bmatrix} \boldsymbol{0} & \boldsymbol{M} \\ \boldsymbol{M} & \boldsymbol{C} \end{bmatrix} + \begin{bmatrix} -\boldsymbol{M} & \boldsymbol{0} \\ \boldsymbol{0} & \boldsymbol{K} \end{bmatrix} \right) \begin{bmatrix} \lambda \boldsymbol{z} \\ \boldsymbol{z} \end{bmatrix} = 0$$

This can be found using for instance Matlab:

$$\begin{aligned} \lambda_1 &= (-0.009986 + i1.0002)\sqrt{\frac{k}{m}} \qquad \boldsymbol{z}_{(1)} = \begin{bmatrix} 0.5246 + i0.4715 \\ 0.5065 + i0.4932 \end{bmatrix} \\ \lambda_2 &= (-0.065014 + i1.5794)\sqrt{\frac{k}{m}} \qquad \boldsymbol{z}_{(2)} = \begin{bmatrix} 0.2482 - i0.3796 \\ -0.1114 + i0.1964 \end{bmatrix} \end{aligned}$$

Applying the approximation derived in (4.51) for small damping, one finds

$$\begin{aligned} \lambda_1 &= -\frac{\beta_{11}}{2\mu_1} \pm i\omega_{01} = (-0.01 + i)\sqrt{\frac{k}{m}} \\ \lambda_2 &= -\frac{\beta_{22}}{2\mu_2} + i\omega_{02} = (-0.065 + i1.5811)\sqrt{\frac{k}{m}} \end{aligned}$$

which is clearly a good approximation of the complex eigenvalue. Hence the small damping assumption is valid in this case. Let us also note that the complex eigenmodes of the damped system as found by Matlab (see above) are defined at a complex constant. So, in order to compare them to the non-damped eigenmodes $\boldsymbol{x}_{(s)}$, we can also write

$$\begin{aligned} \boldsymbol{z}_{(1)} &= \begin{bmatrix} 0.5246 + i0.4715 \\ 0.5065 + i0.4932 \end{bmatrix} / (0.5246 + i0.4715) = \begin{bmatrix} 1 \\ 1.0015 + i0.03997 \end{bmatrix} \\ \boldsymbol{z}_{(2)} &= \begin{bmatrix} 0.2482 - i0.3796 \\ -0.1114 + i0.1964 \end{bmatrix} / (0.2482 - i0.3796) = \begin{bmatrix} 1 \\ -0.4970 + i0.03138 \end{bmatrix} \end{aligned}$$

showing that the complex mode are very close to the modes of the associated conservative system, thanks to the fact that the damping is small and that the eigenfrequencies are well separate.

Example 2

Let us consider now the mass suspended in the horizontal and vertical direction by springs of stiffness k_1 and k_2 respectively (figure figure 4.6.b). A damper is attached to the mass at an angle of 45 degrees. As discussed in the example page 66, the eigenfrequencies of the system are very close if $k_1 \simeq k_2$ and therefore, in the present case, the complex modes will be complex combinations of the undamped modes due to the presence of coupling through the damper.

4.5.2 Forced harmonic response of lightly damped systems

Let us assume harmonic motion with excitation frequency ω

$$\boldsymbol{K}\boldsymbol{q} + \boldsymbol{C}\dot{\boldsymbol{q}} + \boldsymbol{M}\ddot{\boldsymbol{q}} = \boldsymbol{s}e^{i\omega t} \tag{4.58}$$

and assume that the response is limited to the forced term $\boldsymbol{q} = \boldsymbol{z}e^{i\omega t}$, so that the excitation and response amplitudes verify the complex equation[2]

$$\Big(\boldsymbol{K} - \omega^2\boldsymbol{M} + i\omega\boldsymbol{C}\Big)\boldsymbol{z} = \boldsymbol{s} \tag{4.59}$$

The modal damping assumption allows us to construct the modal expansion of the dynamic influence coefficient matrix in terms of undamped eigenmodes. Indeed, assuming for simplicity's sake that no rigid-body modes are present, the response amplitude is developed in terms of eigenmodes

$$\boldsymbol{z} = \sum_{s=1}^{n} \alpha_s \boldsymbol{x}_{(s)}$$

The orthogonality relationships together with the modal damping assumption provide the coefficients

$$\alpha_r = \frac{\boldsymbol{x}_{(r)}^T \boldsymbol{s}}{\mu_r\Big(\omega_{0r}^2 - \omega^2 + 2i\varepsilon_r\omega\omega_{0r}\Big)}$$

Hence the modal expansion of the forced harmonic response

$$\boldsymbol{z} = \sum_{s=1}^{n} \frac{1}{\big(\omega_{0s}^2 - \omega^2 + 2i\varepsilon_s\omega\omega_{0s}\big)} \frac{\boldsymbol{x}_{(s)}\boldsymbol{x}_{(s)}^T}{\mu_s}\boldsymbol{s} \tag{4.60}$$

As for the non-damped case (4.34), we can define a frequency response function between the forced harmonic response amplitude at x_k and the excitation amplitude on k, namely

$$\frac{z_k}{s_k}(\omega^2) = a_{kk}(\omega^2) = \sum_{s=1}^{n} \frac{1}{\big(\omega_{0s}^2 - \omega^2 + 2i\varepsilon_s\omega\omega_{0s}\big)} \frac{x_{k(s)}^2}{\mu_s} \tag{4.61}$$

[2]Note that the damping matrix $\boldsymbol{C}$ is constant with respect to ω in the viscous case and has the form $\frac{1}{\omega}\boldsymbol{C}'$ in the hysteretic case.

As an example, we consider a lightly damped system with three degrees of freedom and with no rigid-body mode. The coefficients $a_{kk}(\omega^2)$ are represented on a Nyquist diagram in figure 4.7. It is observed that, if the system eigenfrequencies are sufficiently separated from each other, only one term at a time can contribute significantly to the development (4.61) for a given ω. This produces a Nyquist diagram formed by concentric circles, the "circle" being characteristic of the harmonic response of a damped single-degree-of-freedom system.

In the opposite case of clustered eigenfrequencies and of stronger damping, the Nyquist diagram is more complex, since several modes contribute simultaneously in a significant manner to the influence coefficients (4.61) for a given excitation frequency ω (figure 4.8). The Nyquist diagram is then characterized by loops. Note that in that case, the assumption of light damping might not be valid anymore. Since the expression of the frequency function (4.61) was obtained by neglecting the coupling between modes due to damping, it might be a crude approximation of the true frequency response function in this case.

4.6 Experimental identification of eigen-parameters

> *"In theory, theory and practice are the same ... In practice they're not!"*
> – Yogi Berra

Computing natural frequencies and vibration modes of a structure always implies using assumptions in the model due to discretization, definition of boundary conditions, ... Hence it is essential to validate a model against actual measurements in order to gain confidence in the model and, if necessary, to modify it.

In this section, we will shortly outline the principles underlying experimental procedures to measure the eigen-parameters (frequencies and modes) of structures. We will restrict our discussion by assuming that the structure is lightly damped. In case the light-damping assumption is not valid, identification of the complex modes should be considered (see e.g. [3, 7, 2]).

Modal testing techniques can be divided in two class of procedures. The first tries to excite the structure according to one of its non-damped eigenmode by applying excitations using shakers that exactly compensate for the damping forces. These techniques called *mode appropriation* will be discussed in the next section. A second class of modal identification uses the frequency response function measured on a structure and searches the modal parameters so that the theoretical expression (4.61) fits the measured harmonic response. These *non-appropriation methods* will be briefly illustrated in section 4.6.2.

4.6.1 Force appropriation testing

The most frequent objective of a vibration test is to determine the modal characteristics (eigenmodes and eigenfrequencies) of the associated conservative system. A natural procedure consists of forcing the vibration of the structure in each of the eigenmodes successively

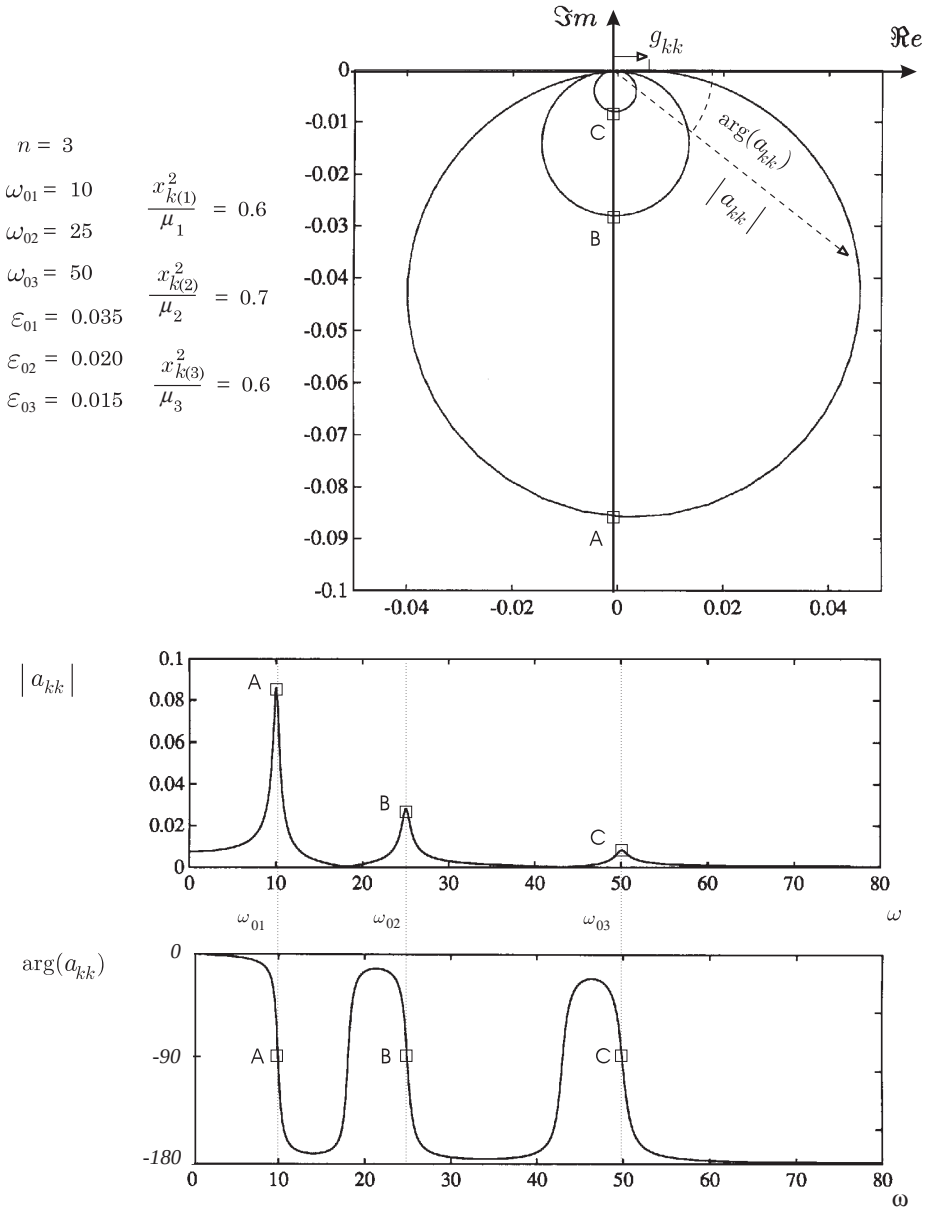

Figure 4.7: Nyquist diagram, amplitude and phase lag (small damping and well separate eigenfrequencies

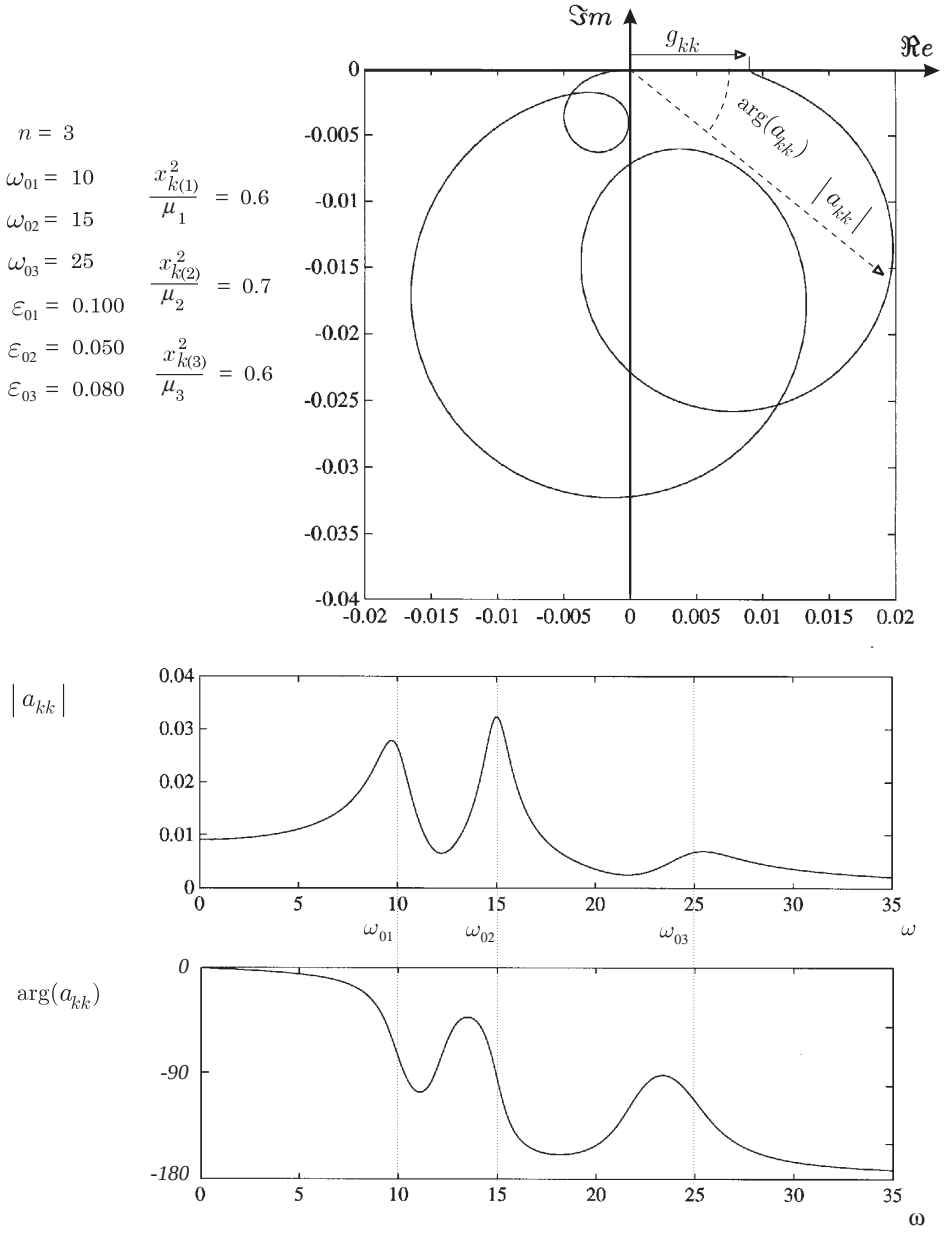

Figure 4.8: Nyquist diagram, amplitude and phase lag (high damping and close eigenfrequencies

through appropriate excitation by proper tuning of the frequency and force amplitudes of the excitation.

There is no direct method to determine the appropriate excitation of a given vibration mode. It must be obtained through successive approximations. In order to evaluate if a structure is indeed excited in one of its eigenmodes, one can use the *phase lag quadrature criterion* discussed next.

When a harmonic vibration test is performed on a damped system, the amplitudes of applied forces and the response amplitudes at the different points verify the complex relationship (4.59)

$$\Big(\boldsymbol{K} - \omega^2 \boldsymbol{M} + i\omega \boldsymbol{C}\Big)\boldsymbol{z} = \boldsymbol{s} \tag{4.59}$$

Extracting a given eigenmode of the associated conservative system through appropriate excitation is equivalent to assuming that

$$\boldsymbol{z} = \boldsymbol{x}_{(k)} \qquad \text{and} \qquad \omega = \omega_{0k}$$

Equation (4.59) then becomes

$$\Big(\boldsymbol{K} - \omega_{0k}^2 \boldsymbol{M} + i\omega_{0k} \boldsymbol{C}\Big)\boldsymbol{x}_{(k)} = \boldsymbol{s}_{(k)} \tag{4.62}$$

where $\boldsymbol{s}_{(k)}$ is the excitation mode which allows one to achieve the appropriate excitation. Because ω_{0k}^2 and $\boldsymbol{x}_{(k)}$ are eigensolutions of the associated conservative system, one has

$$\Big(\boldsymbol{K} - \omega_{0k}^2 \boldsymbol{M}\Big)\boldsymbol{x}_{(k)} = \boldsymbol{0}$$

and the expression of the excitation which makes it possible to excite eigenmode $\boldsymbol{x}_{(k)}$ at its resonance frequency results from equation (4.62)

$$\boldsymbol{s}_{(k)} = i\omega_{0k} \boldsymbol{C} \boldsymbol{x}_{(k)} \tag{4.63}$$

This shows that the excitation is then in phase with the dissipation forces and thus has a phase lag of 90° with respect to the response.

The reciprocal is always true: if it is supposed that all excitation forces are synchronous and that the response at every point of the structure is in phase quadrature with the excitation, the phase relationship between response and excitation may be expressed by assuming that $\boldsymbol{z}$ is a real vector and $\boldsymbol{s}$ an imaginary one. The real and imaginary parts may then be separated in equation (4.59)

$$\big(\boldsymbol{K} - \omega^2 \boldsymbol{M}\big)\boldsymbol{z} = \boldsymbol{0}$$

$$\boldsymbol{s} = i\omega \boldsymbol{C} \boldsymbol{z}$$

showing that the only admissible solutions for ω and $\boldsymbol{z}$ are the eigensolutions of the associated conservative system.

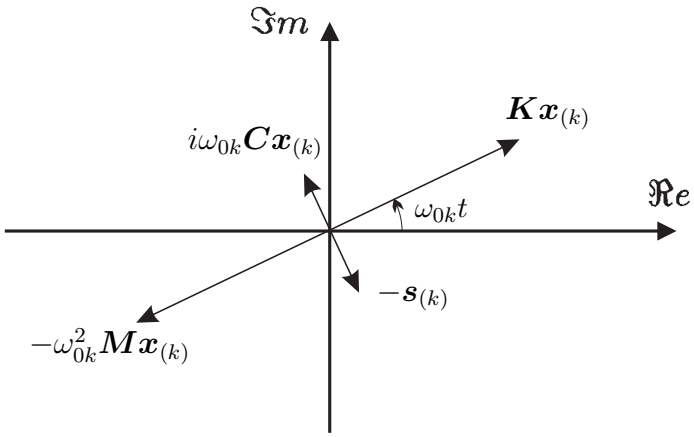

Figure 4.9: Representation of phase quadrature in the complex plane under appropriate excitation

In order to understand the concept of phase quadrature, let us consider the representation of the equation of motion in the complex plane. When the excitation is appropriate, all degrees of freedom are in phase and dynamic equilibrium is expressed in the form

$$\left(\boldsymbol{K} - \omega_{0k}^2\boldsymbol{M} + i\omega_{0k}\boldsymbol{C}\right)\boldsymbol{x}_{(k)} - \boldsymbol{s}_{(k)} = \boldsymbol{0} \tag{4.64}$$

the complex plane representation of which is given by figure 4.9.

Figure 4.9 shows that, when the excitation is appropriate, the elastic forces $\boldsymbol{K}\boldsymbol{x}_{(k)}$ and the inertia forces $\omega_{0k}^2\boldsymbol{M}\boldsymbol{x}_{(k)}$ cancel each other as if the system were vibrating in an undamped fashion, while the excitation force $\boldsymbol{s}_{(k)}$ equilibrates the damping forces which are proportional to velocity and thus have a phase advance of $\pi/2$.

The *phase quadrature criterion* may thus be formulated as follows:

> *The structure vibrates according to one of the eigenmodes of the associated conservative system* if and only if *all degrees of freedom vibrate synchronously and have a phase lag of $\pi/2$ with respect to the excitation.*

Once the phase quadrature criterion is verified during the experimental test, one may take note of ω_{0k} and measure the corresponding eigenshape $\boldsymbol{x}_{(k)}$.

Indicators such as active and reactive power dissipated in the shakers can be used in order to guide the operator when tuning the amplitude and frequency of the shakers to reach an appropriate excitation [3]. This issue will not be discussed here.

The methods based on excitation appropriation are by far the most reliable ones to determine the modal characteristics of structures (eigenfrequencies and mode shapes, generalized masses, modal damping coefficients). They allow visualization of the real modes of the structure. Moreover, in the case of appropriate excitation, the eigenmodes and the

frequencies of the structure are measured directly, which also allows observation of the non-linear behaviors.

These methods are, however, long and delicate to implement, since they require a simultaneous excitation of several degrees of freedom and lead to trial-and-error procedures to reach the appropriate excitation conditions (phase quadrature between excitation and response at all shakers, or reactive power stationarity). Moreover, this experimental technique requires a lot of equipment, as suggested by the sketch of the testing setup in figure 4.10.

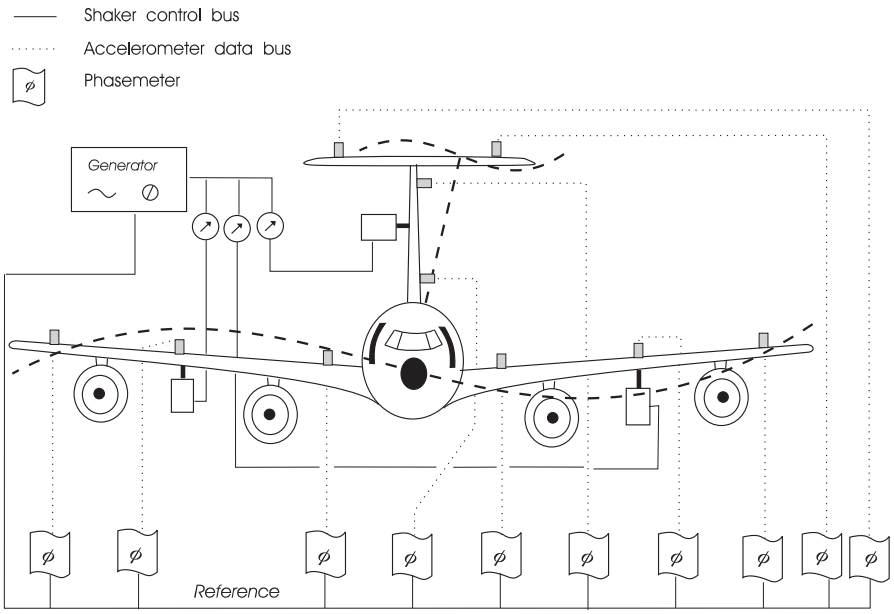

Figure 4.10: Experimental setup for modal analysis of a large structure using appropriate excitation [16].

The appropriation technique is also called *phase resonance method*. Use of these methods is therefore limited to the testing of structures for which it is necessary to have very accurate knowledge of modal properties—airplanes and spacecraft in particular—and for which testing techniques based on the measurement of transfer functions (see next section) are often less precise because they assume linearity and require substantial signal processing and/or numerical processing. [3]

[3]The dynamic of aircrafts needs to be well identified in order to predict dynamic interaction with the aerodynamics. Those tests are commonly known as Ground Vibration Tests or GVT. In particular GVT results are used to estimate *flutter* speeds, namely flying speeds where the wings of the aircraft exhibits negatively damped vibration due to the dynamic interaction between the flow around the wings and the structural vibration. The Airbus A380 aircraft was tested in 2006 in Toulouse. The GVT of the A380 required measuring 896 outputs (structural accelerations) and applying excitations with 21 shakers. About 300 modes where measured and the entire test campaign lasted for 23 days ... The test mainly was performed using non-appropriation techniques (see section 4.6.2) but the characteristics of the most important modes were checked and refined using the appropriation strategy.

4.6.2 Non-appropriation testing

The force appropriation techniques as described above are reliable but very time-consuming and expensive. Another class of modal identification techniques consists in measuring frequency response functions, namely the forced harmonic response of the structure when excited harmonically (see section 4.3). The modal parameters are then found by comparing the measured frequency response function (FRF) to its theoretical expression in terms of mode superposition (4.33). Identification procedures based on this idea use forces that are not explicitly related to forces of a single mode and are therefore called non-appropriation techniques.

Figure 4.11.a depicts a schematic setup to measure FRFs between an input point j and two so-called output points. A shaker (hydraulic or electromagnetic) is placed on the structure to excite a certain degree of freedom on j with a harmonic force of amplitude s_j (component j of $\boldsymbol{s}$) and an excitation frequency ω. Sensors (accelerometers, displacement sensors or a laser beam) are then placed is well-chosen locations to measure the forced harmonic response $z_1, z_2 \ \ldots$ corresponding to degrees of freedom $1, 2 \ \ldots$. The excitation frequency is then varied slowly in a specified frequency range of interest (so-called sine-sweep). Comparing the response amplitudes to the amplitude of the input excitation the magnitude of the FRFs are found. Measuring also the phase of the responses compared to the input phase yields the phase of the FRFs.

Applying a sine-sweep to measure the FRFs is a lengthy procedure especially if the damping is small. Indeed in that case, when modifying the excitation frequency, one must wait till the transient dynamical effects are damped out before actually measuring the forced harmonic response. Therefore, a faster way to obtain the FRFs is to excite the structure simultaneously in the entire frequency range of interest by applying a random excitation through a shaker or simply by applying an impact with a hammer (figure 4.11.b). The excitation and responses are then looked at as being a superposition of harmonic contributions: the FRFs are computed by first applying a fast Fourier transform (FFT) to the measurement and then comparing the Fourier components of the responses and excitation.

Once the FRFs (magnitudes and phase) between points of a structure are known, one can identify the modal parameters (i.e. frequencies, modal dampings and mode shapes) by fitting the theoretical FRF expression (4.33) to the measurements, namely by computing the values of ω_s, ε_s, μ_s and $\boldsymbol{x}_{(s)}$ so that the measurements can be approximated by the theoretical expression (4.33). This is illustrated in figure 4.12. Note that during dynamic testing, only a certain number of points are measured and/or excited. Hence the FRFs are measured only for a limited number of degree of freedom and only the mode shapes at those locations can be deduced. The wire-frame graphics in figure 4.12 indicate the actual result of the modal identification of a car using a certain number of measurement points. Comparing the identified modes with modes computed from a finite element model must then be done by the analyst.

Remarks

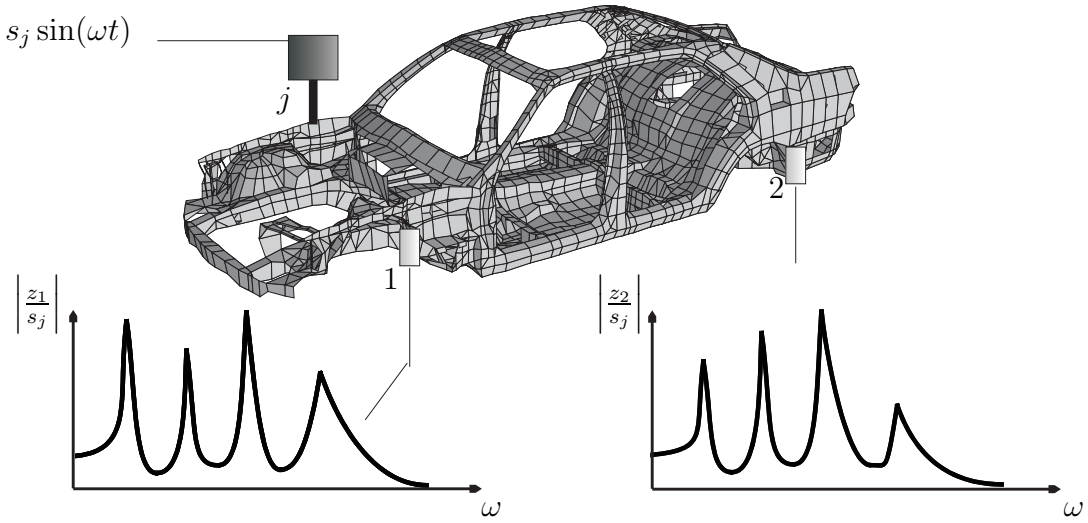

a. applying a sine sweep

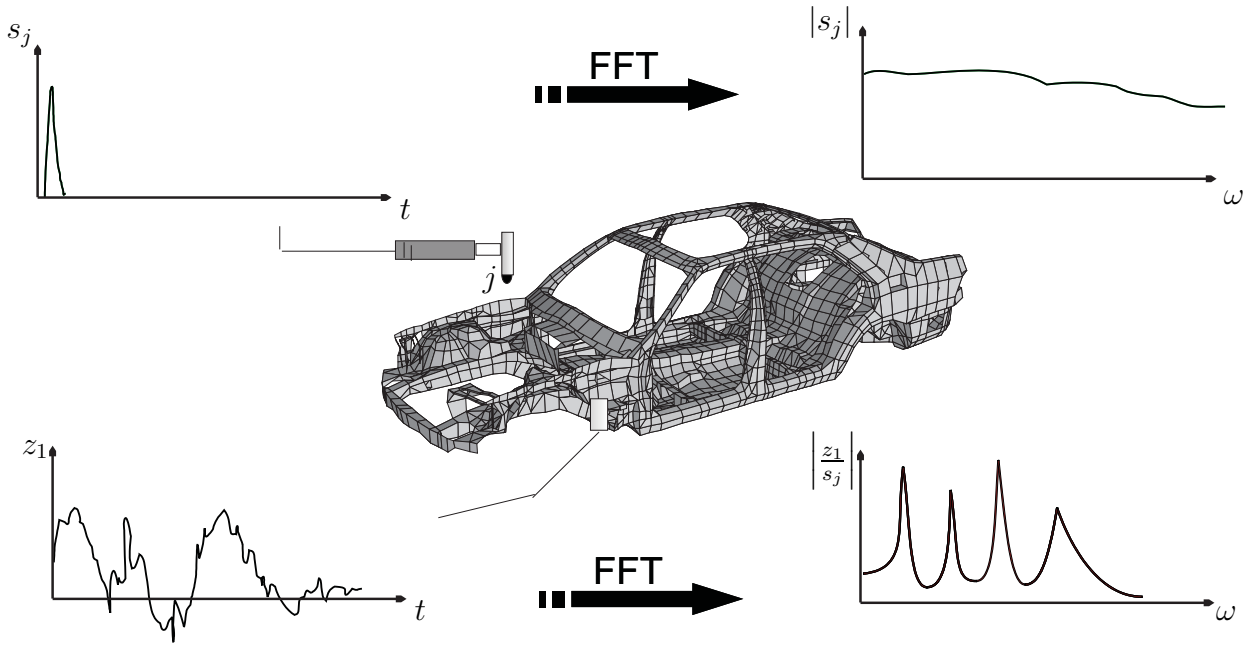

b. using an impact hammer

Figure 4.11: Measurement of frequency response functions

- Real structures are continuous and thus have an infinite number of degrees of freedom. For the experimentation one must choose the *order of the model* to be fitted in the identification, namely the number of degrees of freedom n that are assumed in the model. The identification process will then try to find the best fit to the measurements based on n modes in the superposition (4.33). In practice, the number of modes in the analyzed frequency range is not known and one does not know how many modes are required to properly fit the FRFs. Therefore, the identification is typically performed for an increasing order number until the identified modal parameters for the specified frequency range do not change anymore when the order is increased further.

- It is clear that non-appropriation techniques heavily rely on the assumption that the system behaves linearly. Indeed, the harmonic response is assumed to obey to the theoretical response (4.33) of a linear model. Also, when performing random excitation and impact hammer tests, deducing the harmonic response from a Fourier transform implicitly assumes that the responses depend linearly on the inputs. For that reason and because non-appropriation techniques involve significant numerical treatment of the measurements for signal processing and model fitting, these techniques are less accurate then appropriation techniques described in section 4.6.1. Nevertheless, non-appropriation techniques are fast and do not require extensive hardware equipment. Non-appropriation techniques are thus most often used in practice, appropriation techniques being used only if the modes and damping need to be measured with high accuracy (such as for the wings of aircrafts).

- The field of dynamical testing is a topic by itself. Issues such as identification techniques, sensor placement, signal processing or model updating will not be treated here (see for instance lecture wb1406 or [7, 2, 8])

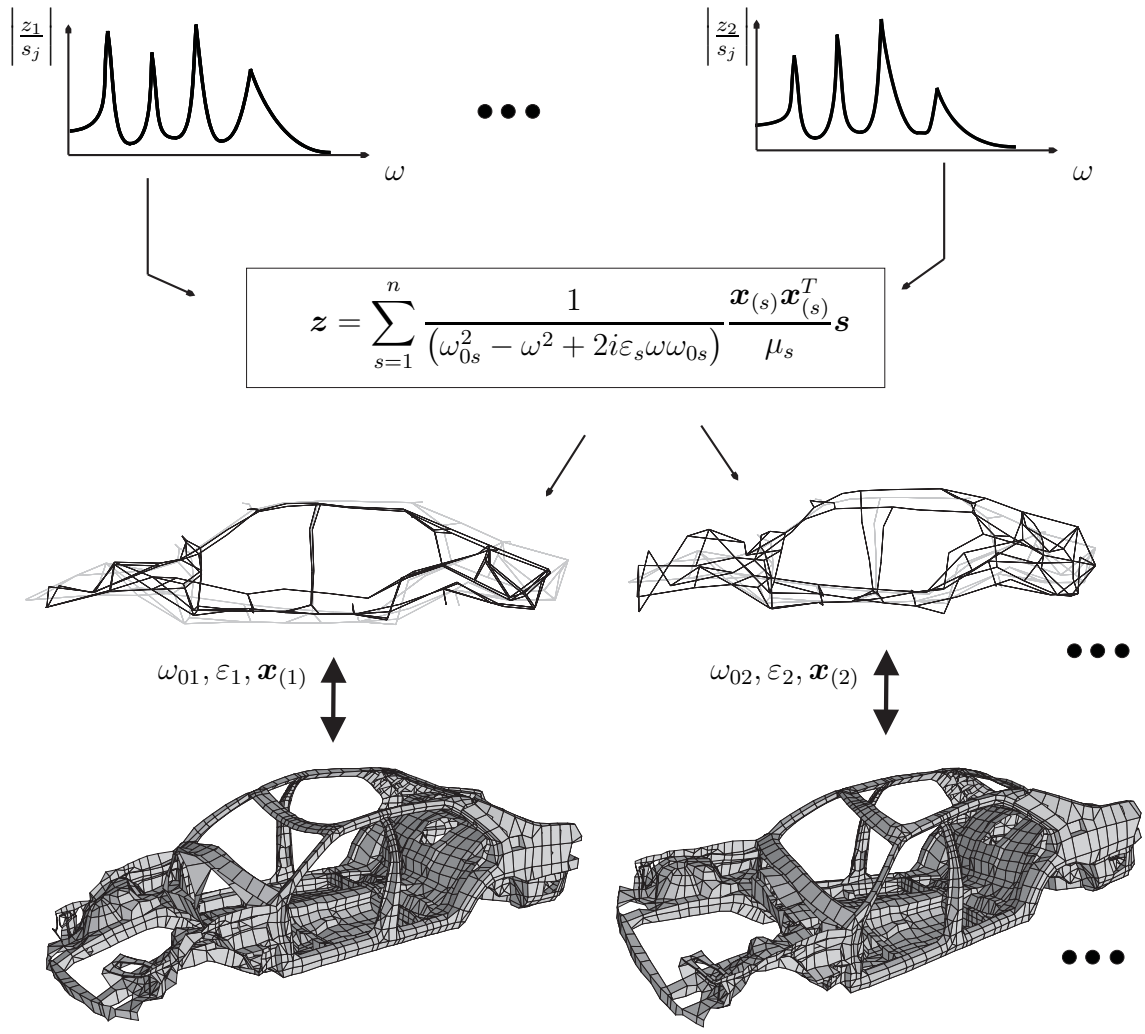

Figure 4.12: Modal identification from frequency response functions

Chapter 5

Continuous systems: linear dynamics and discretization

The number of degrees of freedom of a discrete system is fixed by its number of masses N, and its mathematical model consists of a set of n coupled ordinary differential equations.

In practice, the representation of a physical system by a discrete model is usually an idealized view. In most cases, the main bodies which compose a mechanical system are deformable, and the elastic elements (springs) which connect the main bodies also have their own inertia. Therefore, each constituent of a system possesses simultaneously inertia, stiffness and damping properties: the mathematical model of a continuous system undergoing time-dependent deformation used in *elastodynamics* is then relevant.

In order to formulate the governing equations of a continuous system, we will resort to the theory of continuum mechanics where the equations of motion are expressed in terms of the displacement field

$$u(x, y, z, t)$$
$$v(x, y, z, t)$$
$$w(x, y, z, t)$$

together with the boundary conditions to be satisfied. The space variables x, y and z being continuous, the system so described possesses an infinity of degrees of freedom.

Unfortunately, very few practical continuous problems have a closed form solution and therefore discretization techniques need to be used in order to approximate the system and to compute its dynamic behavior using the techniques for discrete systems.

In section 5.1, we shortly recall the basic dynamic equations in a continuous media and for the specific case of a bar and a beam. The energy expression for a continuous system will also be recalled. In section 5.2, the Rayleigh-Ritz approximation method will be discussed. The finite Element method for linear dynamics is then presented in section 5.3.

5.1 Elastodynamics of continuous systems

5.1.1 Definitions

Let us consider an elastic body undergoing in time a certain motion measured from the undeformed configuration. The latter is supposed to be time-invariant, and corresponds to the equilibrium position of the system in the absence of external forces (figure 5.1).

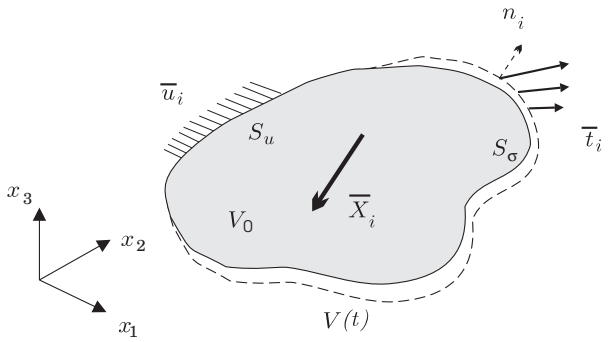

Figure 5.1: Continuous systems: definitions

Let us define the following variables:

- $V(t)$ – the volume occupied by the elastic body in the deformed configuration and its associated mass density ρ
- V_0 – the volume in the undeformed configuration and its associated mass density ρ_0; V_0 is supposed to be time-invariant and is adopted as a reference configuration (*Lagrangian* description of motion)
- $x_i = [x_1, x_2, x_3]$ – the Cartesian coordinates of a given point of the undeformed body; we will also use the more explicit notation (x, y, z) whenever possible
- $u_i(x_j, t) = [u_1, u_2, u_3]$ – the displacement field observed at any point resulting from the dynamic deformation of the body; we will also use the more explicit notation (u, v, w) associated with (x, y, z)
- $S = S_u + S_\sigma$ – the total surface of the body in undeformed configuration can be split into

  S_u the portion of surface on which the displacements are imposed:

  $$u_i = \overline{u}_i$$

S_σ the complementary part of the surface on which surface tractions are imposed:

$$t_i = \overline{t}_i$$

- $\overline{X}_i$ – the applied body forces
- $\overline{t}_i$ – the surface tractions imposed on S_σ
- n_i – the direction cosines of the outward normal to the surface S
- $\overline{u}_i$ – the displacements imposed on S_u

Assuming small deformations and small displacements, the linear expression for the deformation (strains) tensor ε_{ij} inside the body is

$$\varepsilon_{ij} = \frac{1}{2}\left(\frac{\partial u_j}{\partial x_i} + \frac{\partial u_i}{\partial x_j}\right) \tag{5.1}$$

We further assume that the material is *linear* and *elastic*, so that stresses inside the body are related to strains by

$$\sigma_{ij} \;=\; C_{ijkl}\,\varepsilon_{kl} \tag{5.2}$$

where Einstein's summation convention is assumed and where C_{ijkl} are the elastic coefficients of the material.

5.1.2 Dynamic linear equilibrium in a continuous media

Let us consider an infinitesimal volume inside the body. Figure 5.2 shows such a small undeformed volume and the stress components acting on it in the x_1 direction. Observe that the usual convention is used:

- a stress component σ_{ij} corresponds to a force per unit area in the direction i applied on a face with normal in the direction j.
- σ_{ij} is positive in the direction of x_i on a face with outer normal in the direction of x_i.

First let us investigate the rotational equilibrium of the infinitesimal volume around the axis x_2 in figure 5.2. Taking as rotating axis a line parallel to x_2 and passing through the center of the infinitesimal volume, the equilibrium writes

$$-\left(\sigma_{31}(x_1,x_2,x_3) + \sigma_{31}(x_1+dx_1,x_2,x_3)\right) a_1 \frac{dx_1}{2} \tag{5.3}$$

$$+\left(\sigma_{13}(x_1,x_2,x_3) + \sigma_{13}(x_1,x_2,x_3+dx_3)\right) a_3 \frac{dx_3}{2} = 0 \tag{5.4}$$

where a_i are the surface area of the faces with normal in the direction x_i:

$$a_1 = dx_2 dx_3 \qquad a_2 = dx_1 dx_3 \qquad a_3 = dx_1 dx_2$$

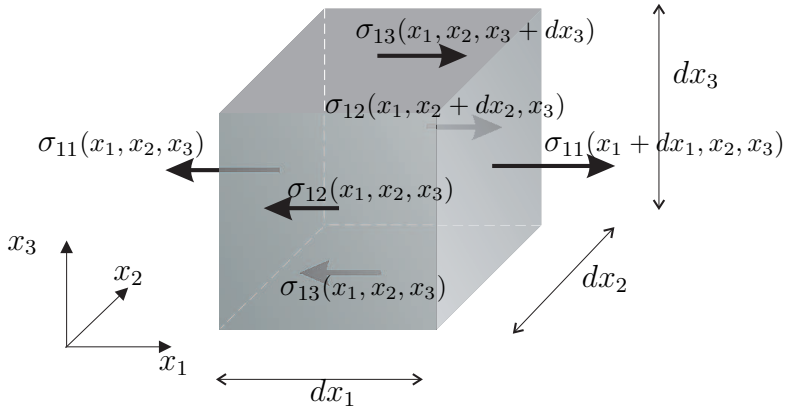

Figure 5.2: Equilibrium in a continuous systems

Noting that

$$\begin{aligned}\sigma_{31}(x_1, x_2, x_3 + dx_3) &= \sigma_{31}(x_1, x_2, x_3) + \frac{\partial \sigma_{31}}{\partial x_3} dx_3 + O(dx_3^2) \\ \sigma_{13}(x_1 + dx_1, x_2, x_3) &= \sigma_{13}(x_1, x_2, x_3) + \frac{\partial \sigma_{13}}{\partial x_1} dx_1 + O(dx_1^2)\end{aligned}$$

and calling $dV = dx_1 dx_2 dx_3$ the infinitesimal volume, the rotational equilibrium (5.4) yields

$$-2\sigma_{31}(x_1, x_2, x_3)dV + 2\sigma_{13}(x_1, x_2, x_3)dV = 0 \tag{5.5}$$

and thus

$$\sigma_{31}(x_1, x_2, x_3) = \sigma_{13}(x_1, x_2, x_3) \tag{5.6}$$

The same reasoning can be developed for the rotation equilibrium about the other axis so that we can write

$$\sigma_{ij} = \sigma_{ji} \tag{5.7}$$

which proves the symmetry of the stress tensor, exactly as in statics.[1]

Let us now consider the translational equilibrium of the small volume in figure 5.2. In the x_1 direction we find

$$\begin{aligned}&(\sigma_{11}(x_1 + dx_1, x_2, x_3) - \sigma_{11}(x_1, x_2, x_3))\, a_1 && (5.8)\\ &+ (\sigma_{12}(x_1, x_2 + dx_2, x_3) - \sigma_{12}(x_1, x_2, x_3))\, a_2 \\ &+ (\sigma_{13}(x_1, x_2, x_3 + dx_3) - \sigma_{13}(x_1, x_2, x_3))\, a_2 \\ &\qquad + \left(\overline{X}_1 - \rho \ddot{x}_1\right) dV \quad = 0 && (5.9)\end{aligned}$$

[1]Note that this is no longer true if one also considers externally applied volume moments

Recalling that

$$\begin{aligned}
\sigma_{11}(x_1+dx_1,x_2,x_3)-\sigma_{11}(x_1,x_2,x_3) &= \frac{\partial\sigma_{11}}{\partial x_1}dx_1+O(dx_1^2)\\
\sigma_{12}(x_1,x_2+dx_2,x_3)-\sigma_{12}(x_1,x_2,x_3) &= \frac{\partial\sigma_{12}}{\partial x_2}dx_2+O(dx_2^2)\\
\sigma_{13}(x_1,x_2,x_3+dx_3)-\sigma_{11}(x_1,x_2,x_3) &= \frac{\partial\sigma_{13}}{\partial x_3}dx_3+O(dx_3^2)
\end{aligned}$$

the equilibrium (5.9) yields

$$\frac{\partial\sigma_{1i}}{\partial x_i}+\overline{X}_1-\rho\ddot{x}_1=0 \tag{5.10}$$

where Einstein's summation convention is assumed. In a similar way, the translational equilibrium can be written in the directions x_2 and x_3 so that the linear equilibrium in the volume of a continuum is expressed by

$$\frac{\partial}{\partial x_i}\sigma_{ji}+\overline{X}_j-\rho_0\ddot{u}_j=0 \qquad \text{in } V_0 \qquad j=1,2,3 \tag{5.11}$$

Finally, on the surface of a continuous body, one can write as for the static case the following relations between applied surface traction and body stresses:

$$t_j=n_i\sigma_{ij}=\overline{t}_j \qquad \text{on } S_\sigma \qquad j=1,2,3 \tag{5.12}$$

which result from the infinitesimal equilibrium in the vicinity of the surface.

Let us stress that the linear equilibrium equations have been derived here based on the stresses as if there existed in the non-deformed body. Obviously, in reality, when stresses are present, the body deforms and the equilibrium should be written for the stress as existing in the deformed configuration (as illustrated in figure 5.3), and the measure of the deformation would be non-linear in terms of spatial derivatives of displacements. The true equilibrium equations are thus non-linear, but, assuming small deformations and small rotations of every infinitesimal volume into the continuum, the linear equilibrium (5.11) can be taken as an accurate approximation.

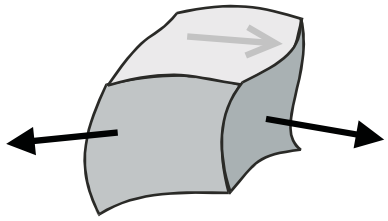

Figure 5.3: Equilibrium in the deformed continuous systems

To summarize, the linear elastodynamic behavior of a continuum body is fully described by the following equilibrium, constitutive and compatibility conditions:

$$\boxed{\begin{array}{ll} \dfrac{\partial}{\partial x_i}\sigma_{ji} + \overline{X}_j - \rho_0 \ddot{u}_j = 0 & \text{in } V_0 \\ t_j = n_i \sigma_{ij} = \overline{t}_j & \text{on } S_\sigma \\ \sigma_{ij} = \sigma_{ji} & \\ & \\ \sigma_{ij} = C_{ijkl}\,\varepsilon_{kl} & \\ & \\ \varepsilon_{ij} = \dfrac{1}{2}\left(\dfrac{\partial u_j}{\partial x_i} + \dfrac{\partial u_i}{\partial x_j}\right) & \\ u_j = \overline{u}_j & \text{on } S_u \end{array}} \tag{5.13}$$

5.1.3 Matrix notations

Let us now define the following matrix quantities:

- the arrays $\boldsymbol{u}$, $\boldsymbol{\sigma}$ and $\boldsymbol{\varepsilon}$ collecting the displacement, stress and strain components

$$\boldsymbol{u} = \left[\begin{array}{ccc} u_1 & u_2 & u_3 \end{array}\right]^T \tag{5.14}$$

$$\boldsymbol{\sigma} = \left[\begin{array}{cccccc} \sigma_{11} & \sigma_{22} & \sigma_{33} & \sigma_{12} & \sigma_{23} & \sigma_{13} \end{array}\right]^T \tag{5.15}$$

$$\boldsymbol{\varepsilon} = \left[\begin{array}{cccccc} \varepsilon_{11} & \varepsilon_{22} & \varepsilon_{33} & \gamma_{12} & \gamma_{23} & \gamma_{13} \end{array}\right]^T \tag{5.16}$$

with $\gamma_{ij} = 2\varepsilon_{ij}$

- the spatial differentiation operator

$$\boldsymbol{D}^T = \begin{bmatrix} \dfrac{\partial}{\partial x_1} & 0 & 0 & \dfrac{\partial}{\partial x_2} & 0 & \dfrac{\partial}{\partial x_3} \\ 0 & \dfrac{\partial}{\partial x_2} & 0 & \dfrac{\partial}{\partial x_1} & \dfrac{\partial}{\partial x_3} & 0 \\ 0 & 0 & \dfrac{\partial}{\partial x_3} & 0 & \dfrac{\partial}{\partial x_2} & \dfrac{\partial}{\partial x_1} \end{bmatrix} \tag{5.17}$$

- the associated matrix of the direction cosines of the outward normal

$$\boldsymbol{N}^T = \begin{bmatrix} n_1 & 0 & 0 & n_2 & 0 & n_3 \\ 0 & n_2 & 0 & n_1 & n_3 & 0 \\ 0 & 0 & n_3 & 0 & n_2 & n_1 \end{bmatrix} \tag{5.18}$$

- the matrix of Hooke's law elastic coefficients $\boldsymbol{H}$ such that

$$\boldsymbol{\sigma} \;=\; \boldsymbol{H}\boldsymbol{\varepsilon} \tag{5.19}$$

For isotropic elastic material in three dimension, Hookes matrix is

$$\boldsymbol{H}^{-1} = \frac{1}{E}\begin{bmatrix} 1 & -\nu & -\nu & 0 & 0 & 0 \\ -\nu & 1 & -\nu & 0 & 0 & 0 \\ -\nu & -\nu & 1 & 0 & 0 & \\ 0 & 0 & 0 & 1/G & 0 & 0 \\ 0 & 0 & 0 & 0 & 1/G & 0 \\ 0 & 0 & 0 & 0 & 0 & 1/G \end{bmatrix} \tag{5.20}$$

where E, ν and $G = E/2(1+\nu)$ are respectivly Young's modulus, Poisson's ratio and the shear modulus of the material. One can also write

$$\boldsymbol{H} = \begin{bmatrix} \lambda+2G & \lambda & \lambda & 0 & 0 & 0 \\ \lambda & \lambda+2G & \lambda & 0 & 0 & 0 \\ \lambda & \lambda & \lambda+2G & 0 & 0 & 0 \\ 0 & 0 & 0 & G & 0 & 0 \\ 0 & 0 & 0 & 0 & G & 0 \\ 0 & 0 & 0 & 0 & 0 & G \end{bmatrix} \tag{5.21}$$

where $\lambda = \frac{E\nu}{(1+\nu)(1-2\nu)}$ and G are known as Lamé's coefficients.

The equations expressing linear dynamic equilibrium may then be written in the matrix form

$$\boxed{\begin{array}{ll} \boldsymbol{D}^T\boldsymbol{\sigma} + \bar{\boldsymbol{X}} - \rho\ddot{\boldsymbol{u}} = \boldsymbol{0} & \text{in } V \\ \boldsymbol{N}^T\boldsymbol{\sigma} = \bar{\boldsymbol{t}} & \text{on } S_\sigma \\ \\ \boldsymbol{\sigma} = \boldsymbol{H}\boldsymbol{\varepsilon} & \\ \\ \boldsymbol{\varepsilon} = \boldsymbol{D}\boldsymbol{u} & \\ \boldsymbol{u} = \bar{\boldsymbol{u}} & \text{on } S_u \end{array}} \tag{5.22}$$

5.1.4 Kinetic and Potential energy of a continuous system

The kinetic energy of the continuous system of figure 5.1 may be evaluated from an integration over the reference volume: by making use of Einstein's notation it takes the form

$$\mathcal{T}(u) = \frac{1}{2}\int_{V_0} \rho_0 \dot{u}_i \dot{u}_i \, dV \tag{5.23}$$

where the subscript $_0$ stresses the fact that the integration volume and the mass density are taken in the non-deformed reference configuration. Note that, in the linear analysis, we assume that the equilibrium is written for the non-deformed configuration and thus that $V \simeq V_0$ and $\rho \simeq \rho_0$.

The total potential energy $\mathcal{V}$ results from the summation of the strain energy of the body and the potential energy of the external forces, supposed conservative

$$\mathcal{V} = \mathcal{V}_{int} + \mathcal{V}_{ext} \tag{5.24}$$

The strain energy can be expressed by

$$\mathcal{V}_{int} = \int_{V_0} W(\varepsilon_{ij}) \, dV \tag{5.25}$$

where $W(\varepsilon_{ij})$ is the internal energy density defined as

$$W(\varepsilon_{ij}) = \int_0^{\varepsilon_{ij}} \sigma_{ij} \, d\varepsilon_{ij} \tag{5.26}$$

such that

$$\sigma_{ij} = \frac{\partial W}{\partial \varepsilon_{ij}} \tag{5.27}$$

Assuming that the material is *linear* and *elastic* and that the deformations and displacements are small, Hookes law (5.2) and the linear expression (5.1) for the strains can be used and therefore

$$W = \frac{1}{2} C_{ijkl}\varepsilon_{ij}\varepsilon_{kl} \tag{5.28}$$

or using the matrix notations,

$$\begin{aligned} W &= \frac{1}{2}\boldsymbol{\varepsilon}^T \boldsymbol{H} \boldsymbol{\varepsilon} \\ &= \frac{1}{2}(\boldsymbol{D}\boldsymbol{u})^T \boldsymbol{H} (\boldsymbol{D}\boldsymbol{u}) \end{aligned} \tag{5.29}$$

The external potential energy is computed by assuming the existence of body forces $\overline{X}_i$ and external surface tractions $\overline{t}_i$ on the portion S_σ of the surface

$$\mathcal{V}_{ext} = -\int_{V_0} \overline{X}_i(t) u_i \, dV - \int_{S_\sigma} \overline{t}_i(t) u_i \, dS \tag{5.30}$$

5.1.5 The bar

Let us consider a bar of section $A(x)$ (figure 5.4) for which displacements and stresses are supposed constant over the cross section—a valid assumption for thin cross sections.

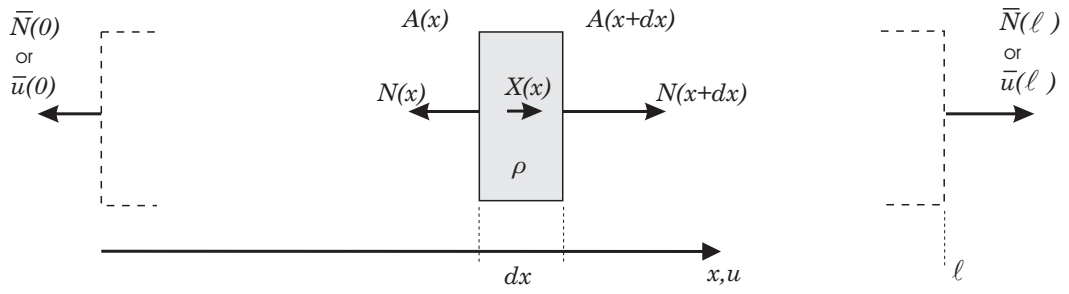

Figure 5.4: Bar element in extension

An external load per unit length $\overline{X}$ is applied to the bar along direction x, and either an axial force $\overline{N}$ or a displacement $\overline{u}$ is imposed at the ends. In linear elasticity, the axial load $N(x)$ is expressed by

$$N(x) = A(x)\sigma_x(x) = EA\varepsilon_x \tag{5.31}$$

with, under the small displacement assumption,

$$\varepsilon_x = \frac{\partial u}{\partial x} \tag{5.32}$$

It is easily verified that the equilibrium equation of the bar element of figure 5.5 writes

$$\boxed{\frac{\partial}{\partial x}\left(EA\frac{\partial u}{\partial x}\right) - m\ddot{u} + \overline{X} = 0 \qquad \text{for} \quad 0 < x < \ell} \tag{5.33}$$

with the end conditions in $x = 0$ and $x = \ell$

$$EA\frac{\partial u}{\partial x} = \overline{N} \quad \text{or} \quad u = \overline{u} \tag{5.34}$$

$m = \rho A$ is the mass per unit length.

The system energies are given by

$$\begin{aligned} \mathcal{V}_{int} &= \frac{1}{2}\int_0^\ell EA\left(\frac{\partial u}{\partial x}\right)^2 dx \\ \mathcal{T} &= \frac{1}{2}\int_0^\ell m\dot{u}^2\, dx \end{aligned}$$

The potential energy of external forces is given by

$$\mathcal{V}_{ext} = -\int_0^\ell \overline{X}u\, dx + \overline{N}(0)u(0) - \overline{N}(\ell)u(\ell)$$

Note that free vibration modes exist for the continuous system. They will not be discussed here (see for instance lecture wb1308 or [3]).

5.1.6 The beam with no shear deformation

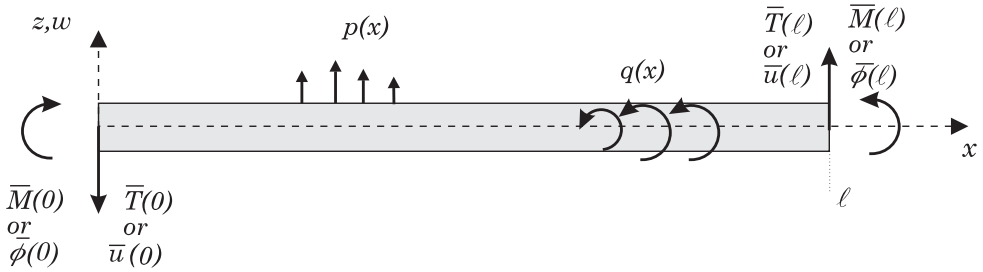

Figure 5.5: Transverse vibration of beams

Let us consider a beam of length ℓ, of mass density ρ_0 and of cross section A. We will suppose that the beam is subjected to a distributed vertical load $p(x,t)$ and to distributed moments $q(x,t)$ per unit length. At the beam ends, either the shear loads $\overline{T}$ or the bending moments $\overline{M}$ are applied or the displacements $\overline{w}$ or rotations $\overline{\phi}$ are imposed (figure 5.5).

Kinematic assumptions The axis system Oxyz is such that Oz and Oy correspond to the principal inertia axes. To analyze the transverse vibrations of the beam in bending, let us introduce the following kinematic assumptions:

1. The beam cross section is not deformable;
2. The transverse displacement on it is uniform and, for simplicity's sake, is limited to the displacement in the Oxz plane

$$w = w(x) \qquad\qquad v = 0 \tag{5.35}$$

3. The axial displacement component results from the rotation of the cross section. The rotation is such that the cross sections remain orthogonal to the neutral axis

$$u(x,z) = -z\frac{\partial w}{\partial x} \tag{5.36}$$

With the assumption of geometric linearity, we write the strain expressions

$$\varepsilon_x = \frac{\partial u}{\partial x} = -z\frac{\partial^2 w}{\partial x^2} \tag{5.37}$$

$$\varepsilon_z = \frac{\partial w}{\partial z} = 0 \tag{5.38}$$

$$\varepsilon_{xz} = \frac{1}{2}\left(\frac{\partial w}{\partial x} + \frac{\partial u}{\partial z}\right) = 0 \tag{5.39}$$

The last equation (5.39) shows that assumption (5.36) is equivalent to neglecting the shear deformation of the material. This assumption, called the *Bernoulli* assumption, is illustrated by figure 5.6.

Rotational equilibrium It is easily verified that in a first-order approximation the rotational equilibrium of a beam segment can be expressed by (see figure 5.7)

$$M(x) - M(x+dx) - T(x)dx + (p - \rho A\ddot{w})dx\frac{dx}{2} = \left(q - \rho I(x)\frac{\partial \ddot{w}}{\partial x}\right)dx$$

where $I(x) = \displaystyle\int_A z^2\ dA$ is the geometric moment of inertia of the cross section. We will define

- $m = A\rho$ the mass per unit of beam length
- $r^2 = \frac{I}{A}$ where r is the gyration radius of the cross section

Making dx tend to 0,

$$T(x) = -\frac{\partial M}{\partial x} + mr^2\frac{\partial \ddot{w}}{\partial x} - q \tag{5.40}$$

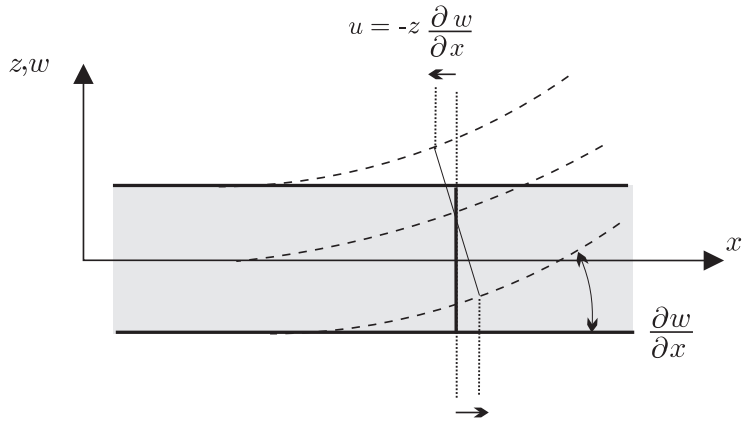

Figure 5.6: Bernoulli's kinematic assumption

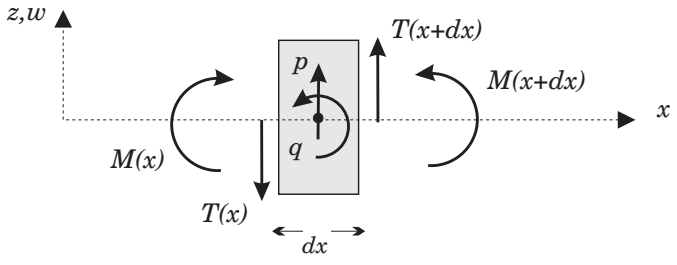

Figure 5.7: Equilibrium of a beam segment

Transverse translational equilibrium Let us now write the translational equilibrium in the transverse direction of the beam segment (figure fig449):

$$p\,dx - T(x) + T(x+dx) = m\ddot{w}\,dx$$

and thus

$$p + \frac{\partial T}{\partial x} = m\ddot{w} \tag{5.41}$$

Substituting (5.41) into (5.40),

$$\frac{\partial^2 M}{\partial x^2} - \frac{\partial}{\partial x}\left(mr^2\frac{\partial \ddot{w}}{\partial x}\right) + m\ddot{w} = p - \frac{\partial q}{\partial x} \tag{5.42}$$

The moment on a cross-section is related to the curvature by (see figure 5.8)

$$\begin{aligned} M(x) &= -\int_{A(x)} z\sigma_{xx}dA \\ &= -\int_{A(x)} z\varepsilon_{xx}EdA \\ &= \int_{A(x)} z^2\frac{\partial^2 w}{\partial x^2}EdA \\ &= E\frac{\partial^2 w}{\partial x^2}\int_{A(x)} z^2 dA = EI\frac{\partial^2 w}{\partial x^2} \end{aligned} \tag{5.43}$$

where EI is the bending stiffness of the cross section and $\dfrac{\partial^2 w}{\partial x^2}$ is the beam curvature.

Substituting (5.43) into (5.42) finally yields the equilibrium equation

$$\boxed{m\ddot{w} - \frac{\partial}{\partial x}\left(mr^2\frac{\partial \ddot{w}}{\partial x}\right) + \frac{\partial^2}{\partial x^2}\left(EI\frac{\partial^2 w}{\partial x^2}\right) = p - \frac{\partial q}{\partial x}} \tag{5.44}$$

with the boundary conditions at $x = 0$ and at $x = \ell$

- on the transverse displacement

$$w = \overline{w} \qquad \text{or} \qquad T = mr^2\frac{\partial \ddot{w}}{\partial x} - \frac{\partial}{\partial x}\left(EI\frac{\partial^2 w}{\partial x^2}\right) - q = \overline{T} \tag{5.45}$$

- on the rotation

$$\frac{\partial w}{\partial x} = \overline{\phi} \qquad \text{or} \qquad M = EI\frac{\partial^2 w}{\partial x^2} = \overline{M} \tag{5.46}$$

where M and T are, respectively, the bending moments and shear loads.

Let us observe that this equation is a fourth order differential equation in space. The kinematic assumption of no shear deformation remains valid provided that the ratio $\frac{I}{A} = r^2$ remains small. It is thus consistent in this case to neglect the rotatory inertia of the cross sections and thus the term $mr^2\frac{\partial \ddot{w}}{\partial x}$ is often neglected in the equation (5.44) of the Bernoulli beam.

Energy expressions The strain energy of the system is written

$$\begin{aligned}\mathcal{V}_{int} &= \frac{1}{2}\int_A\int_0^\ell Ez^2\left(\frac{\partial^2 w}{\partial x^2}\right)^2 dx\,dA \\ &= \frac{1}{2}\int_0^\ell EI\left(\frac{\partial^2 w}{\partial x^2}\right)^2 dx \end{aligned} \tag{5.47}$$

The kinetic energy is given by

$$\begin{aligned}\mathcal{T} &= \frac{1}{2}\int_0^\ell\int_{A(x)}\rho\left(\dot{u}^2+\dot{w}^2\right)\,dA\,dx \\ &= \frac{1}{2}\int_0^\ell\int_{A(x)}\rho\left[z^2\left(\frac{\partial\dot{w}}{\partial x}\right)^2+\dot{w}^2\right]\,dA\,dx \\ &= \frac{1}{2}\int_0^\ell\rho I\left(\frac{\partial\dot{w}}{\partial x}\right)^2 dx+\frac{1}{2}\int_0^\ell\rho A\dot{w}^2\,dx \end{aligned} \tag{5.48}$$

we obtain the expression

$$\mathcal{T}=\frac{1}{2}\int_0^\ell m\dot{w}^2\,dx+\frac{1}{2}\int_0^\ell mr^2\left(\frac{\partial\dot{w}}{\partial x}\right)^2 dx \tag{5.49}$$

The first term describes the kinetic energy for vertical translation, while the second is the rotational kinetic energy of the cross sections. The second term is thus often neglected for the Bernouilli beam as discussed above.

The potential associated with a bending moment M (figure 5.8) is computed as follows:

$$\begin{aligned}\mathcal{V}_{ext.M} &= -\int_A u\sigma_x\,dA \\ &= -\int_A\left(-z\frac{\partial w}{\partial x}\right)\sigma_x\,dA \\ &= -q\frac{\partial w}{\partial x}\end{aligned}$$

and the total potential of external loads is written

$$\begin{aligned}\mathcal{V}_{ext}=-\int_0^\ell pw\,dx &- \int_0^\ell q\frac{\partial w}{\partial x}\,dx+\overline{T}(0)w(0)-\overline{T}(\ell)w(\ell) \\ &+ \overline{M}(0)\left(\frac{\partial w}{\partial x}\right)_0-\overline{M}(\ell)\left(\frac{\partial w}{\partial x}\right)_\ell\end{aligned} \tag{5.50}$$

5.2 The Rayleigh–Ritz method

Among the problems of elastodynamics governed by a system of partial differential equations, some of which have been considered in the previous section, very few have a closed-form solution which simultaneously verifies the differential equations on the domain V and the boundary conditions on its external surface S.

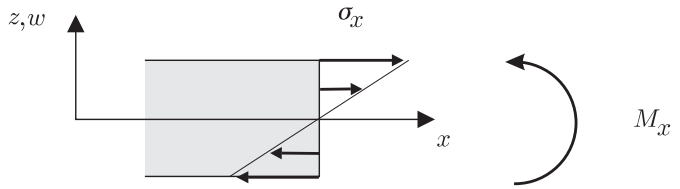

Figure 5.8: Bending moment from longitudinal stress

The need to find an exact closed-form solution may be overcome through the application of the Rayleigh–Ritz method. What results is a substitution problem which possesses a finite number n degrees of freedom and is described by ordinary differential equations similar to those of discrete systems. The Rayleigh–Ritz solution is seldom exact, but its quality improves with the number of degrees of freedom incorporated in its expression.

The Rayleigh–Ritz method dates back to 1870 and the study of vibration problems by Lord Rayleigh [11]: the displacement approximation was originally limited to one trial function (Rayleigh's method). In 1909 Ritz generalized this method by constructing an approximation of the displacement field in terms of several functions, each one associated with a different degree of freedom.

5.2.1 Choice of approximation functions

The Rayleigh–Ritz method for a problem of elastodynamics starts with the choice of approximation functions for the displacements. Each component u_i of the field $u_i(x_1, x_2, x_3, t)$, $i = 1, 2, 3$, is described by a series whose characteristic term is a function $f_{ij}(x_1, x_2, x_3)$ multiplied by a time-dependent amplitude, denoted $q_j(t)$. The components q_j play the role of generalized coordinates. The Rayleigh–Ritz approximation is written in the form

$$u_i(x_1, x_2, x_3, t) = \sum_{j=1}^{n} f_{ij}(x_1, x_2, x_3) q_j(t) \qquad i = 1, 2, 3 \tag{5.51}$$

where each set of functions describing a particular displacement field

$$\boldsymbol{f}_j(x_1, x_2, x_3) = \begin{bmatrix} f_{1j}(x_1, x_2, x_3) \\ f_{2j}(x_1, x_2, x_3) \\ f_{3j}(x_1, x_2, x_3) \end{bmatrix} \tag{5.52}$$

must be admissible, which means that **it must satisfy the internal compatibility conditions (C_0 continuity) and the essential boundary conditions, namely those related to imposed boundary displacements**. Conversely, they are not required to verify the natural conditions.

The degrees of freedom of the approximation are the n amplitudes $q_j(t)$ that are determined by application of the virtual work principle as outlined below.

5.2.2 Discretization of continuous linear dynamical systems

Let us express the approximation (5.51) in matrix form

$$\boldsymbol{u}(x_1, x_2, x_3, t) = \boldsymbol{F}(x_1, x_2, x_3)\boldsymbol{q}(t) \tag{5.53}$$

where

$$\boldsymbol{q}(t) = \left[\begin{array}{ccc} q_1 & \dots & q_n \end{array} \right] \tag{5.54}$$

represents the vector of generalized coordinates, and matrix $\boldsymbol{F}$ of dimension $3 \times n$ is the displacement interpolation matrix

$$\boldsymbol{F}(x_1, x_2, x_3) = \left[\begin{array}{ccc} f_{11}(x_1, x_2, x_3) & \dots & f_{1n}(x_1, x_2, x_3) \\ f_{21}(x_1, x_2, x_3) & \dots & f_{2n}(x_1, x_2, x_3) \\ f_{31}(x_1, x_2, x_3) & \dots & f_{3n}(x_1, x_2, x_3) \end{array} \right] \tag{5.55}$$

The strain components (5.1) are next evaluated by the relationship

$$\begin{aligned} \boldsymbol{\varepsilon}(\boldsymbol{x}, t) &= \boldsymbol{D}\boldsymbol{F}(x_1, x_2, x_3)\boldsymbol{q}(t) \\ &= \boldsymbol{B}(x_1, x_2, x_3)\boldsymbol{q}(t) \end{aligned} \tag{5.56}$$

where matrix $\boldsymbol{B}(x_1, x_2, x_3)$ of dimension $6 \times n$ is the strain interpolation matrix:

$$\boldsymbol{B}(x_1, x_2, x_3) = \boldsymbol{D}\boldsymbol{F}(x_1, x_2, x_3) \tag{5.57}$$

Let us now write the equilibrium equation (5.22) of a continuous system assuming the solution can be approximated by (5.53):

$$\boldsymbol{D}^T\boldsymbol{H}\boldsymbol{B}\boldsymbol{q} + \bar{\boldsymbol{X}} - \rho\boldsymbol{F}\ddot{\boldsymbol{q}} = \boldsymbol{0} \qquad \text{in} \quad V \tag{5.58}$$

$$\boldsymbol{N}^T\boldsymbol{H}\boldsymbol{B}\boldsymbol{q} = \bar{\boldsymbol{t}} \qquad \text{on} \quad S_\sigma \tag{5.59}$$

These equilibrium equations can in general not be satisfied exactly since not all possible solutions are allowed by the approximation (5.53). Hence, the solution considered in this approximation contains artificial constraints and the equilibrium equations can only be satisfied as

$$\boldsymbol{D}^T\boldsymbol{H}\boldsymbol{B}\boldsymbol{q} + \bar{\boldsymbol{X}} - \rho\boldsymbol{F}\ddot{\boldsymbol{q}} = \mathbf{res}_V \qquad \text{in} \quad V \tag{5.60}$$

$$\bar{\boldsymbol{t}} - \boldsymbol{N}^T\boldsymbol{H}\boldsymbol{B}\boldsymbol{q} = \mathbf{res}_S \qquad \text{on} \quad S_\sigma \tag{5.61}$$

where $\mathbf{res}_V$ and $\mathbf{res}_S$ are force residuals in the volume and on the surface boundary corresponding to the equilibrium default.

We therefore consider that the problem to solve has changed: we want to find the solution of the equilibrium equations which satisfies the constraints inherent to (5.53). The residual forces in (5.60) and (5.61) can then be seen as reaction forces associated to the constraints put on the solution field.

In that view, we can find the unknown amplitudes $\boldsymbol{q}$ of the shape functions by applying the virtual work principle, namely by requiring that the equilibrium equations (5.60) and (5.61) must be satisfied for any compatible displacements, namely displacements that can be represented by the expression (5.53). The residual forces (seen as reactions to the artificial constraints) cancel out for the admissible displacements. The virtual work principal thus yields

$$\int_V (\boldsymbol{F}\delta\boldsymbol{q})^T \left(\boldsymbol{D}^T\boldsymbol{H}\boldsymbol{B}\boldsymbol{q} + \bar{\boldsymbol{X}} - \rho\boldsymbol{F}\ddot{\boldsymbol{q}}\right) dV + \int_{S_\sigma} (\boldsymbol{F}\delta\boldsymbol{q})^T \left(\bar{\boldsymbol{t}} - \boldsymbol{N}^T\boldsymbol{H}\boldsymbol{B}\boldsymbol{q}\right) dS = 0 \tag{5.62}$$

Since the variations $\delta\boldsymbol{q}$ are arbitrary, one finds the projected equilibrium equations

$$\int_V \boldsymbol{F}^T \left(\boldsymbol{D}^T\boldsymbol{H}\boldsymbol{B}\boldsymbol{q} + \bar{\boldsymbol{X}} - \rho\boldsymbol{F}\ddot{\boldsymbol{q}}\right) dV + \int_{S_\sigma} \boldsymbol{F}^T \left(\bar{\boldsymbol{t}} - \boldsymbol{N}^T\boldsymbol{H}\boldsymbol{B}\boldsymbol{q}\right) dS = 0 \tag{5.63}$$

Let us then apply an integration by part in space for the first term in (5.63) and write

$$\begin{aligned}\int_V \boldsymbol{F}^T \left(\boldsymbol{D}^T\boldsymbol{H}\boldsymbol{B}\boldsymbol{q}\right) dV &= \int_S \boldsymbol{F}^T \left(\boldsymbol{N}^T\boldsymbol{H}\boldsymbol{B}\boldsymbol{q}\right) dV - \int_V (\boldsymbol{D}\boldsymbol{F})^T \boldsymbol{H} \left(\boldsymbol{B}\boldsymbol{q}\right) dV \\ &= \int_{S_\sigma} \boldsymbol{F}^T \left(\boldsymbol{N}^T\boldsymbol{H}\boldsymbol{B}\boldsymbol{q}\right) dS - \int_V \boldsymbol{B}^T\boldsymbol{H}\boldsymbol{B}\boldsymbol{q} dV \end{aligned} \tag{5.64}$$

Finally, substituting (5.64) into (5.63) one finds

$$\int_V \boldsymbol{B}^T\boldsymbol{H}\boldsymbol{B}\boldsymbol{q} dV + \int_V \rho\boldsymbol{F}^T\boldsymbol{F}\ddot{\boldsymbol{q}} dV = \int_V \boldsymbol{F}^T\bar{\boldsymbol{X}} dV + \int_{S_\sigma} \boldsymbol{F}^T\bar{\boldsymbol{t}} dS = \boldsymbol{0} \tag{5.65}$$

which can be put in matrix form as

$$\boxed{\boldsymbol{K}\boldsymbol{q} + \boldsymbol{M}\ddot{\boldsymbol{q}} = \boldsymbol{g}(t)} \tag{5.66}$$

where the discretized mass, stiffness and force matrices are

$$\boldsymbol{M} = \int_V \rho\boldsymbol{F}^T\boldsymbol{F}\, dV \tag{5.67}$$

$$\tag{5.68}$$

$$\boldsymbol{K} = \int_V \boldsymbol{B}^T\boldsymbol{H}\boldsymbol{B}\, dV \tag{5.69}$$

$$\boldsymbol{g} = \int_{S_\sigma} \boldsymbol{F}^T\, \overline{\boldsymbol{t}}\, dS + \int_V \boldsymbol{F}^T\, \overline{\boldsymbol{X}}\, dV \tag{5.70}$$

The discretized mass has dimension $n \times n$ and is necessarily symmetric and positive definite. The stiffness matrix is also symmetric and has dimension $n \times n$. It is, however,

not always positive definite. Indeed, if there exist *rigid-body modes* $\boldsymbol{u}$ that do not generate deformations, then

$$\boldsymbol{B}\boldsymbol{u} = \boldsymbol{0} \qquad \text{and} \qquad \boldsymbol{K}\boldsymbol{u} = \boldsymbol{0} \tag{5.71}$$

and the stiffness matrix is then semi-positive definite.

5.2.3 Interpretation in terms of minimum weighted residual

The discretized equations (5.66) derive directly from relation (5.63) and therefore expresses that

$$\int_V \boldsymbol{F}^T \mathbf{res}_V dV + \int_{S_\sigma} \boldsymbol{F}^T \mathbf{res}_S dS = \boldsymbol{0} \tag{5.72}$$

which can be interpreted as follows: *the approximate solution (5.53) is determined so as to minimize the error on the equilibrium equation weighted by the shape functions*. It is therefore a best solution to the equilibrium problem in a minimum weighted residual sense.

When the representation of the solution is improved, namely when the basis of shape functions $\boldsymbol{F}$ is enriched, the solution will converge towards the exact solution of the continuous problem.

5.2.4 Discretized equation from Lagrange's equation

Let us show how the discretized equations of motion can also be derived from Lagrange's equation of motion. When the displacement field is approximated by (5.53), the kinetic and potential energy of a continuous system are written as follows:

- Kinetic energy: by substitution of (5.53) into (5.23)

$$\mathcal{T} = \frac{1}{2}\int_V \rho \dot{\boldsymbol{q}}^T \boldsymbol{F}^T \boldsymbol{F} \dot{\boldsymbol{q}}\, dV = \frac{1}{2}\dot{\boldsymbol{q}}^T \boldsymbol{M} \dot{\boldsymbol{q}} \tag{5.73}$$

- Strain energy: through substitution of the discretized strain expression (5.56) for linear materials in (5.29)

$$\begin{aligned} \mathcal{V}_{int} &= \frac{1}{2}\int_V \boldsymbol{\varepsilon}^T \boldsymbol{H} \boldsymbol{\varepsilon}\, dV = \frac{1}{2}\int_V \boldsymbol{q}^T \boldsymbol{B}^T \boldsymbol{H} \boldsymbol{B} \boldsymbol{q}\, dV \\ &= \frac{1}{2}\boldsymbol{q}^T \boldsymbol{K} \boldsymbol{q} \end{aligned} \tag{5.74}$$

- External potential energy: substituting (5.53) into (5.30)

$$\mathcal{V}_{ext} = -\int_{S_\sigma} (\boldsymbol{F}\boldsymbol{q})^T\, \overline{\boldsymbol{t}}\, dS - \int_V (\boldsymbol{F}\boldsymbol{q})^T\, \overline{\boldsymbol{X}}\, dV \tag{5.75}$$

or

$$\mathcal{V}_{ext} = -\boldsymbol{q}^T \boldsymbol{g} \tag{5.76}$$

Applying then Lagrange's equation (1.26) for the degrees of freedom $\boldsymbol{q}$, one directly finds the discretized equilibrium (5.66)

5.2.5 Free vibration modes and frequencies

When no external forces are applied to a structure and all displacement boundary conditions are homogeneous, the dynamic equilibrium equations (5.22) write

$$\begin{cases} \boldsymbol{D}^T\boldsymbol{\sigma} - \rho\ddot{\boldsymbol{u}} = \boldsymbol{0} & \text{in} \quad V \\ \boldsymbol{N}^T\boldsymbol{\sigma} = \boldsymbol{0} & \text{on} \quad S_\sigma \\ \boldsymbol{u} = \boldsymbol{0} & \text{on} \quad S_u \end{cases} \tag{5.77}$$

It can be shown that there exist free vibration modes described by a spatial displacement $\boldsymbol{u}_i(x_j, t)$ and an harmonic time variation, i.e.

$$\boldsymbol{u}_i(x_j, t) = \boldsymbol{u}_i(x_j) \cos \omega_i t \tag{5.78}$$

satisfying the continuous equations (5.77), i.e.such that

$$\boldsymbol{D}^T\boldsymbol{H}\boldsymbol{D}\boldsymbol{u}_i + \omega_i^2 \rho \boldsymbol{u}_i = \boldsymbol{0} \qquad \text{in} \quad V \tag{5.79}$$

where ω_i are the corresponding free vibration frequencies and $i = 1, 2, \ldots \infty$.

The free vibration and harmonic motion assumptions yield the expression of the discretized eigenvalue problem

$$\boxed{\boldsymbol{K}\boldsymbol{q} = \omega^2 \boldsymbol{M}\boldsymbol{q}} \tag{5.80}$$

the solutions of which are approximations to the corresponding Sturm–Liouville problem (5.79).

Let us denote $\omega_{i,c}^2$ the approximate eigenvalues computed by the Rayleigh–Ritz method, and $\omega_{i,e}^2$ the exact eigenvalues of the original continuous problem (5.77). The following result allows us to qualify the type of convergence obtained to the exact solution:

> *Each eigenvalue $\omega_{i,c}^2$ resulting from the discretization of the displacement variational principle by the Rayleigh–Ritz method is an upper bound to the corresponding exact eigenvalue $\omega_{i,e}^2$*
>
> $$\omega_{i,e}^2 \leq \omega_{i,c}^2 \qquad\qquad i = 1, \ldots, n \tag{5.81}$$

The proof of this result will not be developed here. But intuitively, one can say that imposing to the system to behave according to the approximation (5.53) while in fact it has an infinity of degrees of freedom introduces artificial constraints and thus stiffens the model compared to reality.

Once the approximate solutions $\omega_{i,c}^2$ of eigenproblem (5.80) are known, the approximations $\boldsymbol{q}_{(i),c}$ to the associated eigenmodes verifying the relationship

$$\boldsymbol{K}\boldsymbol{q}_{(i),c} - \omega_{i,c}^2 \boldsymbol{M}\boldsymbol{q}_{(i),c} = 0 \tag{5.82}$$

are easily obtained. The approximate eigenmodes given by the Rayleigh–Ritz method are then written

$$\boldsymbol{u}_{(i),c} = \boldsymbol{F}(x_1, x_2, x_3)\boldsymbol{q}_{(i),c} \tag{5.83}$$

Example 1: the clamped–free uniform bar

Let us take the example of the clamped–free bar and express the displacement using a series of two kinematically admissible functions

$$u(x) = \frac{x}{\ell} q_1 + \frac{x^2}{\ell^2} q_2$$

extracted from the complete set of monomials

$$\left[1,\ \frac{x}{\ell},\ \frac{x^2}{\ell^2},\ \frac{x^3}{\ell^3},\ \ldots,\ \frac{x^n}{\ell^n},\ \ldots \right]$$

Let us compute successively the mass coefficients

$$\begin{aligned} m_{11} &= \int_0^\ell m \frac{x^2}{\ell^2} dx = \frac{m\ell}{3} \\ m_{12} &= \int_0^\ell m \frac{x^3}{\ell^3} dx = \frac{m\ell}{4} \\ m_{22} &= \int_0^\ell m \frac{x^4}{\ell^4} dx = \frac{m\ell}{5} \end{aligned}$$

and the stiffness coefficients

$$\begin{aligned} k_{11} &= \int_0^\ell EA \left(\frac{\partial f_1}{\partial x} \right)^2 dx \\ &= \int_0^\ell EA \frac{1}{\ell^2} dx = \frac{EA}{\ell} \\ k_{12} &= \int_0^\ell EA \frac{\partial f_1}{\partial x} \frac{\partial f_2}{\partial x} dx \\ &= \int_0^\ell EA \frac{2x}{\ell^3} dx = \frac{EA}{\ell} \\ k_{22} &= \int_0^\ell EA \left(\frac{\partial f_2}{\partial x} \right)^2 dx \\ &= \int_0^\ell EA \frac{4x^2}{\ell^4} dx = \frac{4}{3} \frac{EA}{\ell} \end{aligned}$$

Thus the eigenvalue problem is

$$\frac{EA}{\ell} \begin{bmatrix} 1 & 1 \\ 1 & \frac{4}{3} \end{bmatrix} \begin{bmatrix} q_1 \\ q_2 \end{bmatrix} - \omega^2 m\ell \begin{bmatrix} \frac{1}{3} & \frac{1}{4} \\ \frac{1}{4} & \frac{1}{5} \end{bmatrix} \begin{bmatrix} q_1 \\ q_2 \end{bmatrix} = \boldsymbol{0}$$

The frequency parameter defined as

$$\mu = \frac{\omega^2 m \ell^2}{EA} \tag{5.84}$$

verifies the quadratic equation

$$\begin{vmatrix} 1 - \frac{\mu}{3} & 1 - \frac{\mu}{4} \\ 1 - \frac{\mu}{4} & \frac{4}{3} - \frac{\mu}{5} \end{vmatrix} = 0$$

or

$$3\mu^2 - 104\mu + 240 = 0$$

One obtains the eigenvalues

$$\omega_{1,c2}^2 = 2.49\frac{EA}{m\ell^2} \quad \text{in place of} \quad 2.467\frac{EA}{m\ell^2}$$

$$\omega_{2,c2}^2 = 32.18\frac{EA}{m\ell^2} \quad \text{in place of} \quad 22.21\frac{EA}{m\ell^2}$$

It is thus observed that the set of admissible functions is appropriate to approximate the first mode $u_{(1)} = a\sin\frac{\pi x}{2\ell}$ but does not allow correct representation of the second one. Adding the cubic admissible function would give the new approximations

$$\omega_{1,c3}^2 = 2.47\frac{EA}{m\ell^2} \quad \text{in place of} \quad 2.467\frac{EA}{m\ell^2}$$

$$\omega_{2,c3}^2 = 23.4\frac{EA}{m\ell^2} \quad \text{in place of} \quad 22.21\frac{EA}{m\ell^2}$$

$$\omega_{3,c3}^2 = 109.2\frac{EA}{m\ell^2} \quad \text{in place of} \quad 61.68\frac{EA}{m\ell^2}$$

showing that the computed solutions converge to the exact ones as the trial function is completed.

Example2 : The simply supported uniform beam excited by external loading

Let consider the problem of the uniform simply supported beam (figure 5.9). A load

$$p(x,t) = p_0\frac{x}{\ell}$$

is suddenly applied. Let us seek an approximate solution by the Rayleigh–Ritz

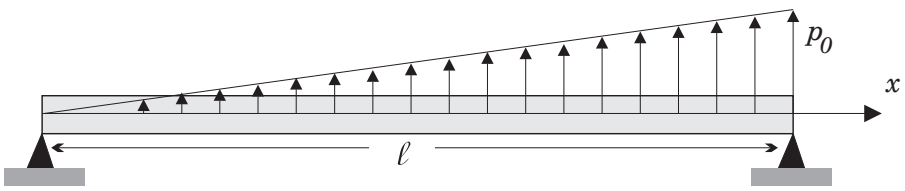

Figure 5.9: Excitation applied to a simply supported beam

method using as an admissible function to represent the eigenmodes a polynomial of general expression

$$w(x) = a_0 + a_1\frac{x}{\ell} + a_2\left(\frac{x}{\ell}\right)^2 + a_3\left(\frac{x}{\ell}\right)^3$$

In order to verify the boundary conditions

$$w(0) = w(\ell) = 0$$

the kinematically admissible trial function is written

$$w(x) = q_1 \left(\frac{x^2}{\ell^2} - \frac{x}{\ell} \right) + q_2 \left(\frac{x^3}{\ell^3} - \frac{x}{\ell} \right)$$

Let us next compute the approximations to the eigenfrequencies $\omega_{i,c}$ and mode shapes $w_{(i),c}$. The coefficients of the discretized mass and stiffness matrices are

$$\begin{aligned}
m_{11} &= \int_0^\ell m \left(\frac{x^2}{\ell^2} - \frac{x}{\ell} \right)^2 dx = \frac{m\ell}{30} \\
m_{12} &= \int_0^\ell m \left(\frac{x^2}{\ell^2} - \frac{x}{\ell} \right) \left(\frac{x^3}{\ell^3} - \frac{x}{\ell} \right) dx = \frac{m\ell}{20} \\
m_{21} &= m_{12} \\
m_{22} &= \int_0^\ell m \left(\frac{x^3}{\ell^3} - \frac{x}{\ell} \right)^2 dx = \frac{8m\ell}{105}
\end{aligned}$$

$$\begin{aligned}
k_{11} &= EI \int_0^\ell \left[\frac{d^2}{dx^2} \left(\frac{x^2}{\ell^2} - \frac{x}{\ell} \right) \right]^2 dx = 4\frac{EI}{\ell^3} \\
k_{12} &= EI \int_0^\ell \frac{d^2}{dx^2} \left(\frac{x^2}{\ell^2} - \frac{x}{\ell} \right) \frac{d^2}{dx^2} \left(\frac{x^3}{\ell^3} - \frac{x}{\ell} \right) dx = 6\frac{EI}{\ell^3} \\
k_{12} &= k_{21} \\
k_{22} &= EI \int_0^\ell \left[\frac{d^2}{dx^2} \left(\frac{x^3}{\ell^3} - \frac{x}{\ell} \right) \right]^2 dx = 12\frac{EI}{\ell^3}
\end{aligned}$$

The discretized eigenvalue problem is thus written

$$\frac{EI}{\ell^3} \begin{bmatrix} 4 & 6 \\ 6 & 12 \end{bmatrix} - \omega^2 m\ell \begin{bmatrix} \frac{1}{30} & \frac{1}{20} \\ \frac{1}{20} & \frac{8}{105} \end{bmatrix} = \boldsymbol{0}$$

By defining the non-dimensional parameter

$$\mu = \frac{\omega^2 m\ell^4}{EI}$$

the characteristic equation takes the form

$$\left(4 - \frac{\mu}{30} \right) \left(12 - \frac{8\mu}{105} \right) - \left(6 - \frac{\mu}{20} \right)^2 = 0$$

We obtain the approximate eigenvalues

$$\begin{aligned}
\omega_{1,c}^2 &= 120\frac{EI}{m\ell^4} \\
\omega_{2,c}^2 &= 2520\frac{EI}{m\ell^4}
\end{aligned}$$

to be compared to the exact ones

$$\begin{aligned} \omega_1^2 &= \pi^4 \frac{EI}{m\ell^4} = 97.41 \frac{EI}{m\ell^4} \\ \omega_2^2 &= (2\pi)^4 \frac{EI}{m\ell^4} = 1558.5 \frac{EI}{m\ell^4} \end{aligned}$$

Then replacing ω^2 by the computed values $\omega_{i,c}$ in the eigenvalue equation yields the associated eigenmodes with unit modal mass

$$\boldsymbol{q}_{(1),c} = \sqrt{\frac{30}{m\ell}} \begin{bmatrix} 1 \\ 0 \end{bmatrix} \qquad \boldsymbol{q}_{(2),c} = \sqrt{\frac{1890}{m\ell}} \begin{bmatrix} 1 \\ -\frac{2}{3} \end{bmatrix}$$

$$\begin{aligned} w_{(1),c} &= \sqrt{\frac{30}{m\ell}} \left(\frac{x^2}{\ell^2} - \frac{x}{\ell} \right) \\ w_{(2),c} &= \sqrt{\frac{1890}{m\ell}} \left(\frac{x}{3\ell} - \frac{x^2}{\ell^2} + \frac{2x^3}{3\ell^3} \right) \end{aligned}$$

These solutions are compared to the exact eigenshapes in figure 5.10

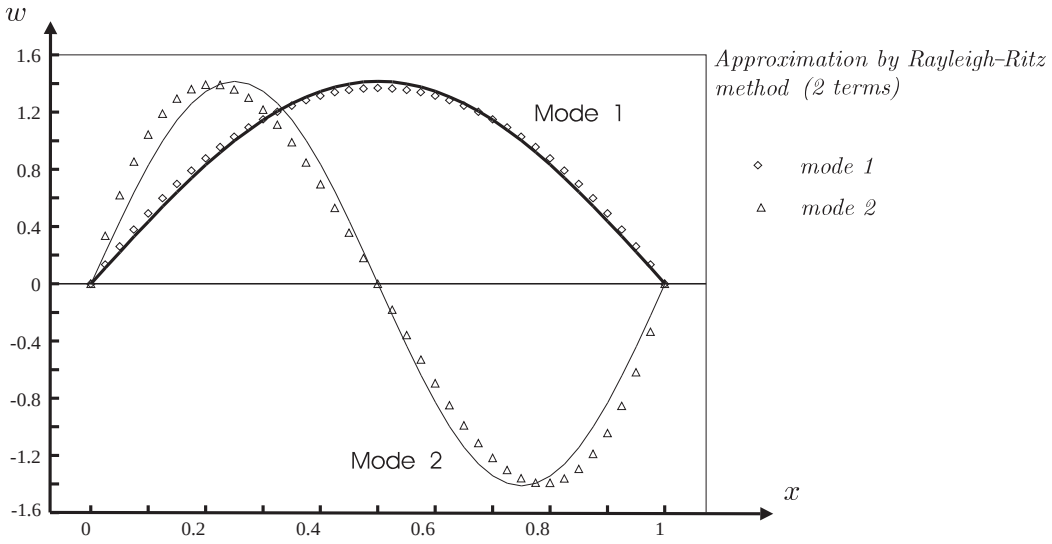

Figure 5.10: Eigenmodes of the simply supported beam

Let us then consider the external excitation

$$p(x,t) = p_0 \frac{x}{\ell}$$

The different terms of the load vector $\boldsymbol{g}$ take the values

$$\begin{aligned} g_1 &= \int_0^\ell p(x,t)\left(\frac{x^2}{\ell^2}-\frac{x}{\ell}\right)dx \\ &= -\frac{p_0\ell}{12} \\ g_2 &= \int_0^\ell p(x,t)\left(\frac{x^3}{\ell^3}-\frac{x}{\ell}\right)dx \\ &= -\frac{2p_0\ell}{15} \end{aligned}$$

We next perform the modal superposition

$$\boldsymbol{q}_c(t) = \eta_1(t)\boldsymbol{q}_{(1),c} + \eta_2(t)\boldsymbol{q}_{(2),c}$$

The load participation factors may be written

$$\begin{aligned} \phi_1 &= \boldsymbol{q}_{(1),c}^T\boldsymbol{g} \\ &= p_0\sqrt{\frac{30\ell}{m}}\begin{bmatrix}1 & 0\end{bmatrix}\begin{bmatrix}-\frac{1}{12}\\ -\frac{2}{15}\end{bmatrix} \\ &= -\frac{p_0}{12}\sqrt{\frac{30\ell}{m}} \\ \phi_2 &= \boldsymbol{q}_{(2),c}^T\boldsymbol{g} \\ &= p_0\sqrt{\frac{1890\ell}{m}}\begin{bmatrix}1 & -\frac{2}{3}\end{bmatrix}\begin{bmatrix}-\frac{1}{12}\\ -\frac{2}{15}\end{bmatrix} \\ &= \frac{p_0}{60}\sqrt{\frac{210\ell}{m}} \end{aligned}$$

Supposing that the beam is at rest before applying the excitation, the normal equations admit the solutions

$$\begin{aligned} \eta_1 &= \frac{p_0}{12\ \omega_{1,c}^2}\sqrt{\frac{30\ell}{m}}\left(\cos\omega_{1,c}t - 1\right) \\ \eta_2 &= \frac{p_0}{60\ \omega_{2,c}^2}\sqrt{\frac{210\ell}{m}}\left(1-\cos\omega_{2,c}t\right) \end{aligned}$$

The approximation to the response computed through superposition of computed eigenmodes is thus

$$\boldsymbol{q}_c = \frac{p_0\ell^4}{EI}\begin{bmatrix}\frac{\cos\omega_{1,c}t}{48} - \frac{\cos\omega_{2,c}t}{240} - \frac{1}{60} \\ -\frac{1-\cos\omega_{2,c}t}{360}\end{bmatrix}$$

or

$$\begin{aligned} w_c(x) &= \left(\frac{x^2}{\ell^2}-\frac{x}{\ell}\right)\left[\frac{\cos\omega_{1,c}t}{48} - \frac{\cos\omega_{2,c}t}{240} - \frac{1}{60}\right] \\ &\quad -\left(\frac{x^3}{\ell^3}-\frac{x}{\ell}\right)\frac{1-\cos\omega_{2,c}t}{360} \end{aligned}$$

Figure 5.11 compares the approximate solution computed from a discretization with two degrees of freedom to the exact one obtained by solving the continuous problem. It is observed that the approximation correctly represents the first eigenmode which is symmetric, but does a poor job of representing the participation to mode 2. This could have been expected because of the relatively large discrepancy between the computed and exact eigenfrequencies. Moreover, the plots clearly illustrate the fact that the Rayleigh–Ritz approximation always leads to an overestimate of the structural stiffness.

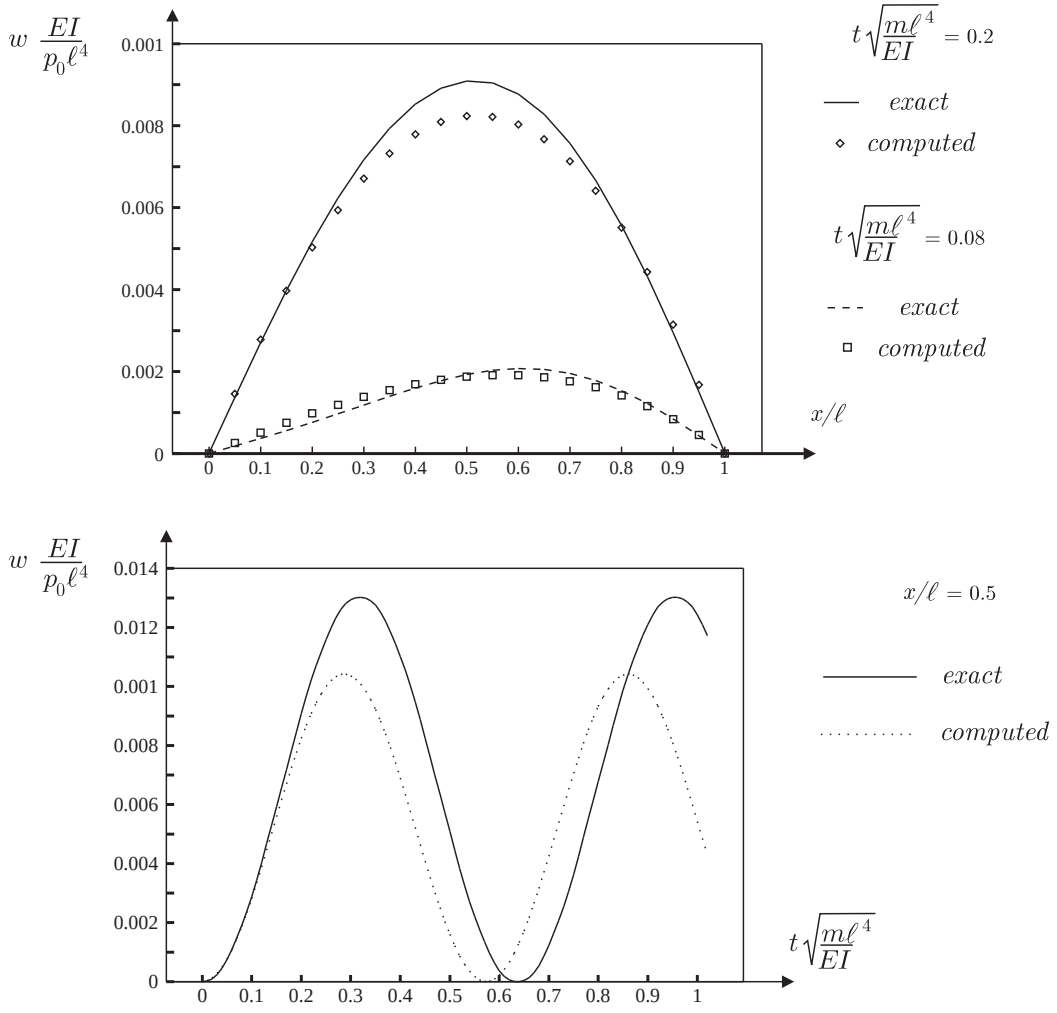

Figure 5.11: Response of the simply supported beam

5.3 Finite Element method in linear dynamics

A complete course should be dedicated to a systematic discussion of the *finite element method*. It is thus not our objective to make a complete presentation of it here. Our purpose is simply to show its potential and mode of application in the context of elastodynamics: therefore this discussion will be limited to the cases of the bar element in extension, the beam element in bending.

The finite element method may be regarded as a particular application procedure of the Rayleigh–Ritz method. It consists of subdividing the deformable body or the structure into a finite number of elements (figure 5.12) of simple geometry (line segment in the one-dimensional case, triangle or quadrangle in two dimensions, tetrahedron or hexahedron in three dimensions) with well-identified structural behavior (bar, beam, membrane, plate, shell, 3-D solid, etc.).

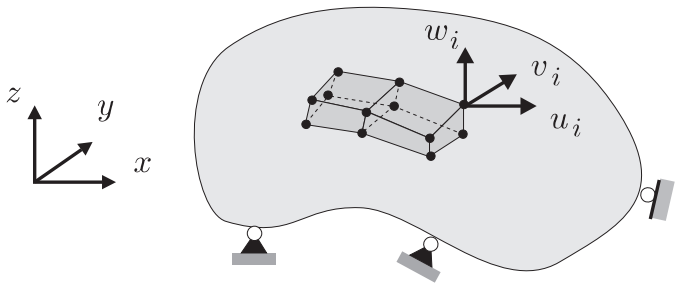

Figure 5.12: The finite element method

The interpolation functions of the displacement field are chosen next in order to fulfill the following requirements:

1. Interpolation is performed in terms of *piecewise continuous* functions. Inside each element, the displacement field is represented by a superposition of a small number of functions which are chosen to be simple but representative of the element's structural behavior in the global structure. They are generally of polynomial type.

2. These functions are also chosen in such a way that their intensity parameters, which are the *generalized coordinates* of the Rayleigh–Ritz method, are *local values of the displacement field* (see figure 5.12) in the structure. In this way, the continuity of the global displacement field may be achieved at the structural level through simple identification of the parameters.

If both conditions are strictly satisfied, the approximation obtained is kinematically admissible in the sense of the Rayleigh–Ritz method: indeed, the displacement field is then integrable over each element domain, and imposing equal values of the generalized

coordinates at element interfaces allows us to keep the continuity of the displacement field at the global level.

A finite element respecting both conditions is said to be *kinematically admissible* and *co-deformable* or, simply speaking, *conforming*.

5.3.1 The bar in extension

Generation of a bar element

Let us consider the case of a bar in extension possibly subjected to distributed loads $p(t)$. The bar is first divided into N elements of length ℓ as sketched in figure 5.13. Next, the displacement field in the element is linearly interpolated by the formula

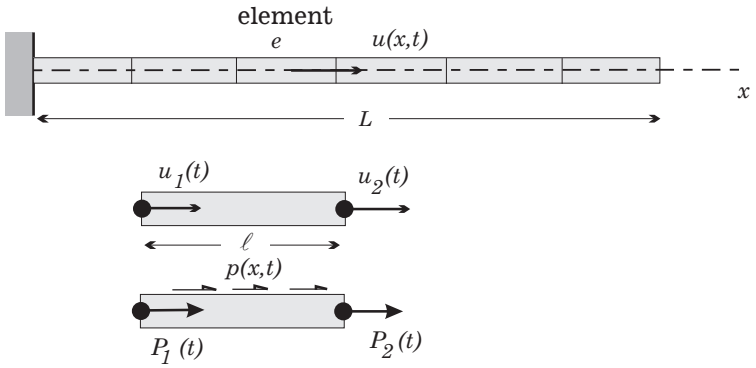

Figure 5.13: Bar in extension modeled by N finite elements

$$u(x,t) = u_1(t)\phi_1(x) + u_2(t)\phi_2(x) \tag{5.85}$$

where

- $u_1(t)$, $u_2(t)$ are the *connector* degrees of freedom, namely the axial displacements at both element ends, also called *nodes*

- $\phi_1(x)$, $\phi_2(x)$ are the *shape functions* of the element, chosen in such a way that

$$u(0,t) = u_1(t) \qquad\qquad u(\ell,t) = u_2(t)$$

  If no internal parameter is introduced, they result from a linear interpolation

$$\phi_1(x) = 1 - \frac{x}{\ell} \qquad\qquad \phi_2(x) = \frac{x}{\ell} \tag{5.86}$$

Equation (5.85) may be put in matrix form

$$u(x,t) = \boldsymbol{F}_e(x)\boldsymbol{q}_e(t) \qquad\qquad x \in \text{element } e \tag{5.87}$$

where

$\boldsymbol{F}_e(x) = [\phi_1(x) \;\; \phi_2(x)]$ is the shape function matrix of element e

$\boldsymbol{q}_e^T(t) = [u_1(t) \;\; u_2(t)]$ is the set of degrees of freedom of element e

We may then compute successively

- the element kinetic and strain energies as quadratic forms of the mass and stiffness *elementary matrices*

$$\mathcal{T}_e = \frac{1}{2}\dot{\boldsymbol{q}}_e^T \boldsymbol{M}_e \dot{\boldsymbol{q}}_e \qquad \text{and} \qquad \mathcal{V}_{int,e} = \frac{1}{2}\boldsymbol{q}_e^T \boldsymbol{K}_e \boldsymbol{q}_e \tag{5.88}$$

  given by

$$\boldsymbol{M}_e = \int_0^\ell m \boldsymbol{F}_e^T \boldsymbol{F}_e \, dx \tag{5.89}$$

$$\boldsymbol{K}_e = \int_0^\ell EA \frac{d\boldsymbol{F}_e^T}{dx}\frac{d\boldsymbol{F}_e}{dx} \, dx \tag{5.90}$$

- the virtual work of external forces in the form

$$\delta\mathcal{V}_{ext,e} = -\delta\boldsymbol{q}_e^T \boldsymbol{g}_e(t) \tag{5.91}$$

  with the *generalized loads* $\boldsymbol{g}_e(t)$ conjugated to displacements $\boldsymbol{q}_e(t)$

$$\boldsymbol{g}_e(t) = \int_0^\ell \boldsymbol{F}_e^T p(x,t)\, dx + \begin{bmatrix} P_1(t) \\ P_2(t) \end{bmatrix} \tag{5.92}$$

  The first term results from the discretization of the load per unit length and the second one contains the end loads of the element. The latter are themselves made of two contributions: the reaction forces with adjacent elements and the eventual external loads.

In particular, for the bar element of uniform characteristics modeled using linear interpolation functions, we obtain the *elementary stiffness and mass matrices*

$$\boldsymbol{K}_e = \frac{EA}{\ell}\begin{bmatrix} 1 & -1 \\ -1 & 1 \end{bmatrix} \qquad\qquad \boldsymbol{M}_e = \frac{m\ell}{6}\begin{bmatrix} 2 & 1 \\ 1 & 2 \end{bmatrix} \tag{5.93}$$

and the discretized force vector representing a uniform load p per unit length over the element

$$\boldsymbol{g}_e^{(1)} = \frac{p\ell}{2}\begin{bmatrix} 1 \\ 1 \end{bmatrix} \tag{5.94}$$

We notice that summing up the elements of the mass matrix restores the total mass of the element: $\sum_{k,s} [\boldsymbol{M}]_{ks} = m\ell$. It is also observed that the stiffness matrix of the bar element has one translational rigid body mode.

The mass matrix constructed in this way is said to be *consistent* in the sense that it is obtained from the same displacement approximation as the stiffness matrix.

Assembly process

In order to express dynamic equilibrium for the global system of figure 5.13, let us construct the matrix of structural displacements $\boldsymbol{q}$ collecting the $(N+1)$ nodal displacements (figure 5.14).

Figure 5.14: Nodal displacements of the system

The transpose of this matrix is

$$\boldsymbol{q}^T = \left[\begin{array}{cccccc} u_0 & u_1 & u_2 & u_3 & \dots & u_N \end{array} \right]$$

so that

$$\boldsymbol{q}_e = \boldsymbol{L}_e \boldsymbol{q} \tag{5.95}$$

where the localization operator $\boldsymbol{L}_e$ is a Boolean matrix, here with dimension $2 \times (N+1)$, and containing only 1 and 0 terms. For instance, for elements 1 and 2 of figure 5.14 [2]

$$\boldsymbol{L}_1 = \left[\begin{array}{cccccc} 0 & 0 & 0 & 0 & \dots & 0 \\ 0 & 1 & 0 & 0 & \dots & 0 \end{array} \right] \tag{5.96}$$

$$\boldsymbol{L}_2 = \left[\begin{array}{cccccc} 0 & 1 & 0 & 0 & \dots & 0 \\ 0 & 0 & 1 & 0 & \dots & 0 \end{array} \right] \tag{5.97}$$

By summing all the elements of the system, the total kinetic and potential enrgy of the

[2] With the notation adopted, the localization operators implicitly fix the degrees of freedom implied in the boundary conditions. The latter could also be kept in the assembly process and fixed later on.

system can be written as

$$\mathcal{T} = \frac{1}{2}\sum_{e=1}^{N} \dot{\boldsymbol{q}}_e^T \boldsymbol{M}_e \dot{\boldsymbol{q}}_e \tag{5.98}$$

$$\mathcal{V}_{int} = \frac{1}{2}\sum_{e=1}^{N} \boldsymbol{q}_e^T \boldsymbol{K}_e \boldsymbol{q}_e \tag{5.99}$$

$$\mathcal{V}_{ext} = \sum_{e=1}^{N} \boldsymbol{q}_e^T \boldsymbol{g}_e \tag{5.100}$$

and they may be expressed in terms of structural displacements through substitution of (5.95)

$$\mathcal{T} = \frac{1}{2}\sum_{e=1}^{N} \dot{\boldsymbol{q}}^T \boldsymbol{L}_e^T \boldsymbol{M}_e \boldsymbol{L}_e \dot{\boldsymbol{q}} \tag{5.101}$$

$$\mathcal{V}_{int} = \frac{1}{2}\sum_{e=1}^{N} \boldsymbol{q}^T \boldsymbol{L}_e^T \boldsymbol{K}_e \boldsymbol{L}_e \boldsymbol{q} \tag{5.102}$$

$$\mathcal{V}_{ext} = \sum_{e=1}^{N} \boldsymbol{q}^T \boldsymbol{L}_e^T \boldsymbol{g}_e \tag{5.103}$$

We then define

- the mass matrix of the assembled system, or *structural mass matrix*

$$\boldsymbol{M} = \sum_{e=1}^{N} \boldsymbol{L}_e^T \boldsymbol{M}_e \boldsymbol{L}_e \tag{5.104}$$

- the *structural stiffness matrix*

$$\boldsymbol{K} = \sum_{e=1}^{N} \boldsymbol{L}_e^T \boldsymbol{K}_e \boldsymbol{L}_e \tag{5.105}$$

- the *structural load vector*

$$\boldsymbol{g} = \sum_{e=1}^{N} \boldsymbol{L}_e^T \boldsymbol{g}_e \tag{5.106}$$

It is important to note that expressions (5.104-5.106) simply correspond to a formal representation of the assembly operation. In practice, structural assembly may be performed much more simply by addressing correctly the matrices $\boldsymbol{K}_e$ and $\boldsymbol{M}_e$ in the structural matrices $\boldsymbol{K}$ and $\boldsymbol{M}$ (figure 5.15).

The following observations can be made on figure 5.15:

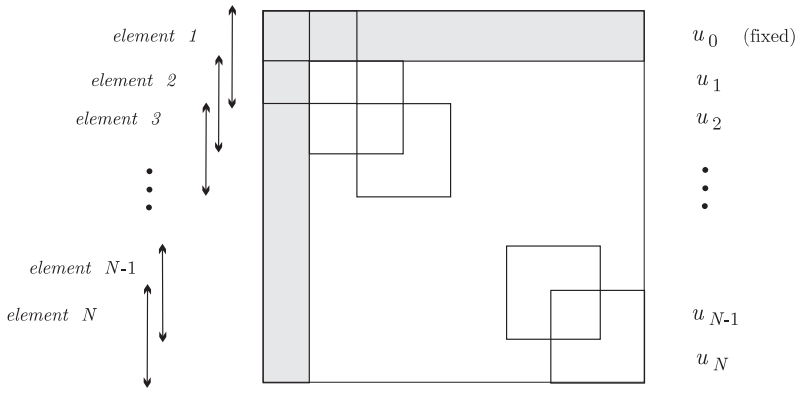

Figure 5.15: Assembly of structural matrices

- The shaded zone corresponds to the clamped end of the bar and must therefore be wiped out.
- The diagonal mass and stiffness terms add two by two on the diagonal of the structural matrix.
- Owing to the system topology (chain-type system or simply connected form) and the sequential numbering of the degrees of freedom, both $\boldsymbol{K}$ and $\boldsymbol{M}$ have tridiagonal form.

When all finite elements have the same length $\ell = \frac{L}{N}$, one obtains for the clamped–free bar

$$\boldsymbol{K} = \frac{EA}{\ell} \begin{bmatrix} 2 & -1 & & & & \\ -1 & 2 & -1 & & \boldsymbol{0} & \\ & -1 & 2 & \ddots & & \\ & & \ddots & \ddots & -1 & \\ & \boldsymbol{0} & & -1 & 2 & -1 \\ & & & & -1 & 1 \end{bmatrix} \tag{5.107}$$

$$\boldsymbol{M} = \frac{m\ell}{6} \begin{bmatrix} 4 & 1 & & & & \\ 1 & 4 & 1 & & \boldsymbol{0} & \\ & 1 & 4 & \ddots & & \\ & & \ddots & \ddots & 1 & \\ & \boldsymbol{0} & & 1 & 4 & 1 \\ & & & & 1 & 2 \end{bmatrix} \tag{5.108}$$

For the structural load vector $\boldsymbol{g}$, the assembly operation (5.106) corresponds to the sum at each node of the contributions of the connecting elements. The reaction forces between

elements are eliminated by the assembly process: the forces applied externally are the only ones to remain in the structural load vector $\boldsymbol{g}$.

By taking the variation of the final discretized expression of the energies, one obtains the discretized structural equations in the usual form

$$\boldsymbol{K}\boldsymbol{q} + \boldsymbol{M}\ddot{\boldsymbol{q}} = \boldsymbol{g}(t) \tag{5.109}$$

5.3.2 Truss frames

Let us consider the case of a structure made of bars, like the frame of figure 5.16. The members are hinged at joints in such a way that they contribute to the global stiffness only through their extension stiffness. The structural mass and stiffness matrices are thus very easily constructed by using the bar element developed above, provided that *all elementary matrices describing individual members are expressed in a common axis system.*

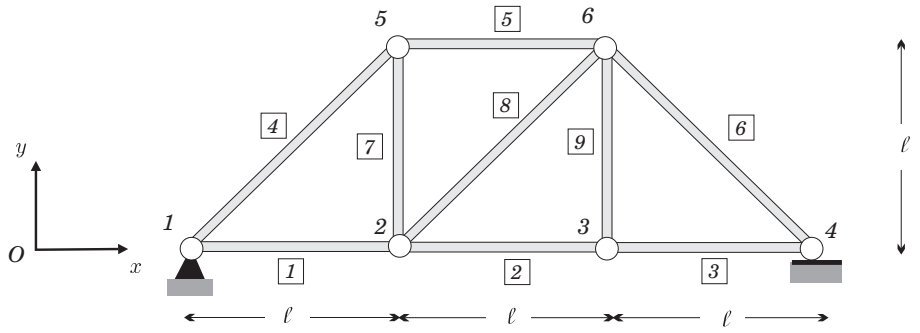

Figure 5.16: Truss frame structure

Let us thus consider the case of an element making an angle α with the x axis (figure 5.17). Passing from the local axial displacements u_i $(i = 1, 2)$ to the structural displacements U_i, V_i is expressed by the transformation

$$u_i = U_i \cos\alpha + V_i \sin\alpha \qquad\qquad i = 1, 2 \tag{5.110}$$

which gives rise to the matrix transformation

$$\begin{bmatrix} u_1 \\ u_2 \end{bmatrix} = \begin{bmatrix} \cos\alpha & \sin\alpha & 0 & 0 \\ 0 & 0 & \cos\alpha & \sin\alpha \end{bmatrix} \begin{bmatrix} U_1 \\ V_1 \\ U_2 \\ V_2 \end{bmatrix} \tag{5.111}$$

or

$$\boldsymbol{q}_{eL} = \boldsymbol{R}\boldsymbol{q}_{eS} \tag{5.112}$$

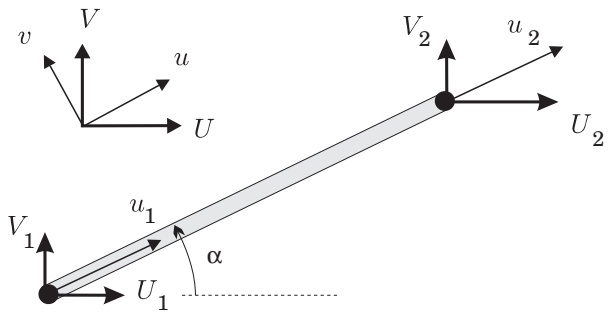

Figure 5.17: Bar element in arbitrary axes

where $\boldsymbol{q}_{eL}$ and $\boldsymbol{q}_{eS}$ represent respectively the element degrees of freedom in local and structural axes, and $\boldsymbol{R}$, the corresponding rotation operation.

The strain energy of the element may now be written as

$$\mathcal{V}_{int,e} = \frac{1}{2}\boldsymbol{q}_{eL}^T \boldsymbol{K}_{eL} \boldsymbol{q}_{eL} = \frac{1}{2}\boldsymbol{q}_{eS}^T \boldsymbol{K}_{eS} \boldsymbol{q}_{eS} \tag{5.113}$$

The transformation on the stiffness matrix is thus

$$\boldsymbol{K}_{eS} = \boldsymbol{R}^T \boldsymbol{K}_{eL} \boldsymbol{R} \tag{5.114}$$

In order to compute the kinetic energy, we have to observe that *its expression must be completed by the transverse kinetic energy term*:

$$\begin{aligned} \mathcal{T}_e &= \frac{1}{2}\int_0^\ell m\left(\dot{u}^2 + \dot{v}^2\right) dx \\ &= \frac{1}{2}\int_0^\ell m\left(\dot{U}^2 + \dot{V}^2\right) dx \end{aligned} \tag{5.115}$$

It can be observed that the elementary mass matrix also becomes invariant under frame transformation.

Explicitly, using the same linear shape functions for v and u as before, we obtain for the element of uniform properties

$$\boldsymbol{K}_{eS} = \frac{EA}{\ell}\begin{bmatrix} \cos^2\alpha & & \text{Sym.} & \\ \cos\alpha\sin\alpha & \sin^2\alpha & & \\ -\cos^2\alpha & -\cos\alpha\sin\alpha & \cos^2\alpha & \\ -\cos\alpha\sin\alpha & -\sin^2\alpha & \cos\alpha\sin\alpha & \sin^2\alpha \end{bmatrix} \tag{5.116}$$

and

$$\boldsymbol{M}_{eS} = \frac{m\ell}{6}\begin{bmatrix} 2 & & \text{Sym.} & \\ 0 & 2 & & \\ 1 & 0 & 2 & \\ 0 & 1 & 0 & 2 \end{bmatrix} \tag{5.117}$$

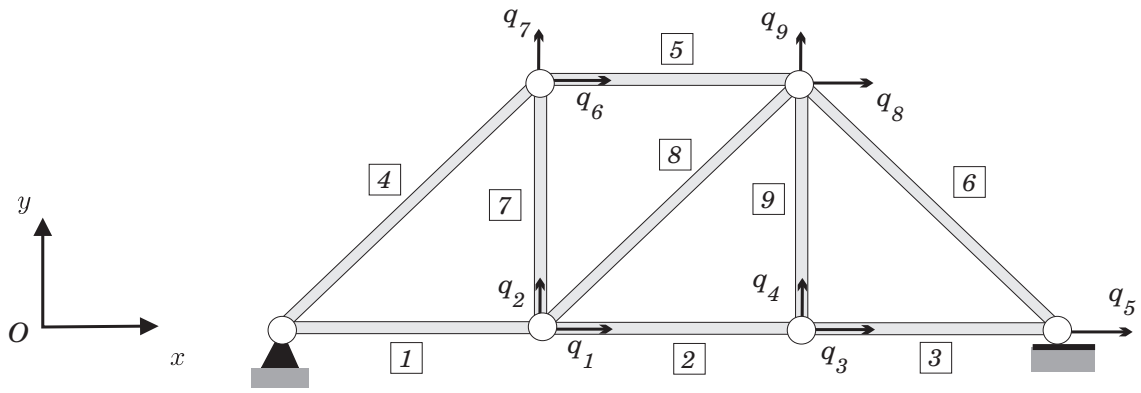

Figure 5.18: Truss frame degrees of freedom

The assembly process of the structural stiffness and mass matrices may then be organized as follows:

a. The structural degrees of freedom are identified while taking account of the boundary conditions and are collected in the vector of structural displacements (see figure 5.18)

$$\begin{aligned} \boldsymbol{q}^T &= \left[\begin{array}{ccccccccc} U_2 & V_2 & U_3 & V_3 & U_4 & U_5 & V_5 & U_6 & V_6 \end{array}\right] \\ &= \left[\begin{array}{ccccccccc} q_1 & q_2 & q_3 & q_4 & q_5 & q_6 & q_7 & q_8 & q_9 \end{array}\right] \end{aligned} \tag{5.118}$$

b. The *localization vector* of each element is constructed by establishing the correspondence between elementary degrees of freedom and structural degrees of freedom:

$$\text{locel}_j^e = \left\{ \begin{array}{l} \text{position of degree of freedom} \\ q_j^e \text{ in structural vector } \boldsymbol{q} \end{array} \right. \tag{5.119}$$

The same operation is done for each element while respecting the numbering of the degrees of freedom (figure5.18).

c. The elementary stiffness and mass matrices are constructed through application of (5.116) and (5.117). Owing to repetitions and symmetries, we have

– for elements 1, 2, 3 and 5

$$\boldsymbol{K}_{eS} = \frac{EA}{\ell} \left[\begin{array}{cccc} 1 & 0 & -1 & 0 \\ 0 & 0 & 0 & 0 \\ -1 & 0 & 1 & 0 \\ 0 & 0 & 0 & 0 \end{array}\right] \qquad \boldsymbol{M}_{eS} = \frac{m\ell}{6} \left[\begin{array}{cccc} 2 & 0 & 1 & 0 \\ 0 & 2 & 0 & 1 \\ 1 & 0 & 2 & 0 \\ 0 & 1 & 0 & 2 \end{array}\right]$$

element e	locel^e vector
1	$\begin{pmatrix} 0 & 0 & 1 & 2 \end{pmatrix}$
2	$\begin{pmatrix} 1 & 2 & 3 & 4 \end{pmatrix}$
3	$\begin{pmatrix} 3 & 4 & 5 & 0 \end{pmatrix}$
4	$\begin{pmatrix} 0 & 0 & 6 & 7 \end{pmatrix}$
5	$\begin{pmatrix} 6 & 7 & 8 & 9 \end{pmatrix}$
6	$\begin{pmatrix} 8 & 9 & 5 & 0 \end{pmatrix}$
7	$\begin{pmatrix} 1 & 2 & 6 & 7 \end{pmatrix}$
8	$\begin{pmatrix} 1 & 2 & 8 & 9 \end{pmatrix}$
9	$\begin{pmatrix} 3 & 4 & 8 & 9 \end{pmatrix}$

Table 5.1: Localization vectors of the truss frame bar elements

– for elements 7 and 9

$$\boldsymbol{K}_{eS} = \frac{EA}{\ell}\begin{bmatrix} 0 & 0 & 0 & 0 \\ 0 & 1 & 0 & -1 \\ 0 & 0 & 0 & 0 \\ 0 & -1 & 0 & 1 \end{bmatrix} \qquad \boldsymbol{M}_{eS} = \frac{m\ell}{6}\begin{bmatrix} 2 & 0 & 1 & 0 \\ 0 & 2 & 0 & 1 \\ 1 & 0 & 2 & 0 \\ 0 & 1 & 0 & 2 \end{bmatrix}$$

– for elements 4 and 8

$$\boldsymbol{K}_{eS} = \frac{EA}{2\ell\sqrt{2}}\begin{bmatrix} 1 & 1 & -1 & -1 \\ 1 & 1 & -1 & -1 \\ -1 & -1 & 1 & 1 \\ -1 & -1 & 1 & 1 \end{bmatrix} \qquad \boldsymbol{M}_{eS} = \frac{m\ell\sqrt{2}}{6}\begin{bmatrix} 2 & 0 & 1 & 0 \\ 0 & 2 & 0 & 1 \\ 1 & 0 & 2 & 0 \\ 0 & 1 & 0 & 2 \end{bmatrix}$$

– for element 6

$$\boldsymbol{K}_{eS} = \frac{EA}{2\ell\sqrt{2}}\begin{bmatrix} 1 & -1 & -1 & 1 \\ -1 & 1 & 1 & -1 \\ -1 & 1 & 1 & -1 \\ 1 & -1 & -1 & 1 \end{bmatrix} \qquad \boldsymbol{M}_{eS} = \frac{m\ell\sqrt{2}}{6}\begin{bmatrix} 2 & 0 & 1 & 0 \\ 0 & 2 & 0 & 1 \\ 1 & 0 & 2 & 0 \\ 0 & 1 & 0 & 2 \end{bmatrix}$$

d. The use of the localization operator obtained in step b allows assembly of the structural mass and stiffness matrices according to the following procedure (of C^{++} type):

```
Matrix K, M; int N;
for(int e=0; e<N ; ++e)                                   // loop over elements
{
            /* reading of localization vectors and elementary matrices */
   read_element(Matrix_el kel, Matrix_el mel, Vector locel);
      for( int i=0; i<4 ; ++i)                            // loop over rows
      {
         for( int j=0; j<4 ; ++j)                         // loop over columns
         {
               int ii = locel[i];                         // localization of rows
               int jj = locel[j];                         // localization of columns
               K[ii][jj] + = kel[i][j];                   // assembly of K
               M[ii][jj] + = Mel[i][j];                   // assembly of M
         }}}
```

As an exercise it can be verified that the following stiffness and mass matrices are obtained

$$\frac{\ell \boldsymbol{K}_S}{EA} = \begin{bmatrix} 2+\frac{1}{2\sqrt{2}} & & & & & & & & \\ \frac{1}{2\sqrt{2}} & 1+\frac{1}{2\sqrt{2}} & & & & & & & \\ -1 & 0 & 2 & & & & \text{Sym.} & & \\ 0 & 0 & 0 & 1 & & & & & \\ 0 & 0 & -1 & 0 & 1+\frac{1}{2\sqrt{2}} & & & & \\ 0 & 0 & 0 & 0 & 0 & 1+\frac{1}{2\sqrt{2}} & & & \\ 0 & -1 & 0 & 0 & 0 & \frac{1}{2\sqrt{2}} & 1+\frac{1}{2\sqrt{2}} & & \\ \frac{-1}{2\sqrt{2}} & \frac{-1}{2\sqrt{2}} & 0 & 0 & \frac{-1}{2\sqrt{2}} & -1 & 0 & 1+\frac{1}{\sqrt{2}} & \\ \frac{-1}{2\sqrt{2}} & \frac{-1}{2\sqrt{2}} & 0 & -1 & \frac{1}{2\sqrt{2}} & 0 & 0 & 0 & 1+\frac{1}{\sqrt{2}} \end{bmatrix}$$

$$\frac{6\boldsymbol{M}_S}{m\ell} = \begin{bmatrix} 2(3+\sqrt{2}) & & & & & & & & \\ 0 & 2(3+\sqrt{2}) & & & & & & & \\ 1 & 0 & 6 & & & & \text{Sym.} & & \\ 0 & 1 & 0 & 6 & & & & & \\ 0 & 0 & 1 & 0 & 2(1+\sqrt{2}) & & & & \\ 1 & 0 & 0 & 0 & 0 & 2(2+\sqrt{2}) & & & \\ 0 & 1 & 0 & 0 & 0 & 0 & 2(2+\sqrt{2}) & & \\ \sqrt{2} & 0 & 1 & 0 & \sqrt{2} & 1 & 0 & 4(1+\sqrt{2}) & \\ 0 & \sqrt{2} & 0 & 1 & 0 & 0 & 1 & 0 & 4(1+\sqrt{2}) \end{bmatrix}$$

e. The solution of the resulting eigenvalue problem

$$\boldsymbol{K}\boldsymbol{q} = \omega^2 \boldsymbol{M}\boldsymbol{q} \tag{5.120}$$

can only be performed numerically. It yields the nine eigenfrequencies given in table 5.2. The first three eigenmodes are represented in figure 5.19.

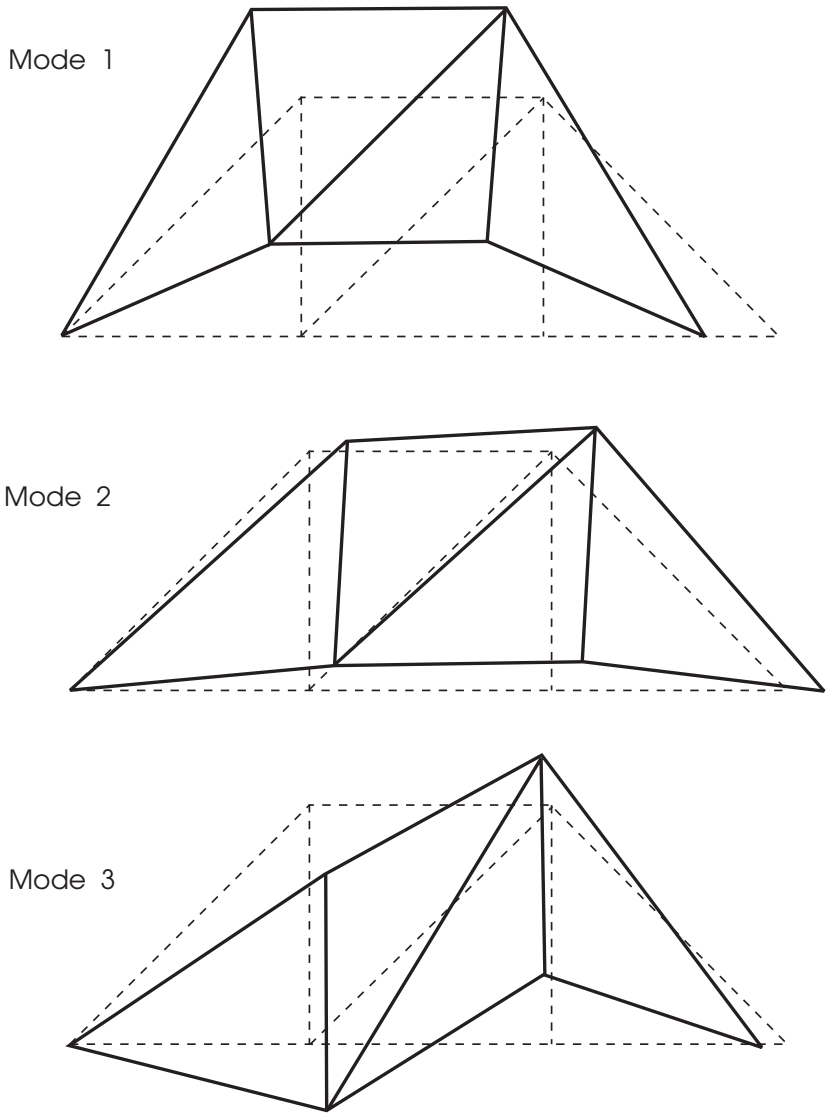

Figure 5.19: Eigenmodes of the truss frame structure

r	$\frac{\omega_r}{2\pi}\sqrt{\frac{m\ell^2}{EA}}$	
1	3.428	10^{-2}
2	5.810	10^{-2}
3	8.901	10^{-2}
4	12.15	10^{-2}
5	19.47	10^{-2}
6	23.42	10^{-2}
7	23.96	10^{-2}
8	24.67	10^{-2}
9	33.27	10^{-2}

Table 5.2: Eigenfrequencies of the truss frame structure by finite elements

5.3.3 Beams in bending without shear deflection

Generation of a beam element

Consider the case of the beam in bending represented in figure 5.20, excited by a distributed load $p(x,t)$.

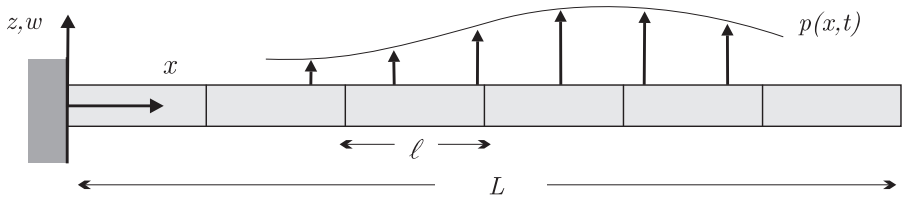

Figure 5.20: Beam in bending modeled by N finite elements

Integration of the strain energy over the beam

$$\mathcal{V}_{int} = \int_0^L EI \left(\frac{\partial^2 w}{\partial x^2}\right)^2 dx \tag{5.121}$$

implies that the function $w(x,t)$ and its first derivative are continuous (C_1 continuity). Therefore, to obtain a finite element approximation of pure displacement type in the Rayleigh–Ritz sense, the interpolation of the bending deflection must be at least cubic in order to maintain continuity of the deflection w and of the cross section rotation (or slope) $\psi = \frac{\partial w}{\partial x}$ through nodal identification. The connectors of the element are the deflection and slope values at both ends (see figure 5.21). In terms of the non-dimensional variable $\xi = \frac{x}{\ell}$

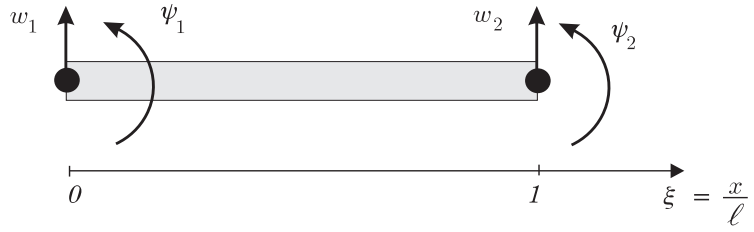

Figure 5.21: Connectors of the beam element in bending

over the element domain, the cubic approximation to the deflection may be written in the form

$$\begin{aligned} w(\xi) &= w_1 F_1(\xi) + \psi_1 F_2(\xi) + w_2 F_3(\xi) + \psi_2 F_4(\xi) \\ &= \boldsymbol{F}_e(\xi)\boldsymbol{q}_e(t) \end{aligned} \tag{5.122}$$

where the shape functions $F_i(\xi)$, $(i = 1, \ldots, 4)$ are the third-order *Hermitian polynomials*, matching the conditions

$$\begin{array}{lll} F_1(0) = 1 & F_1'(0) = 0 & F_1(1) = F_1'(1) = 0 \\ F_2(0) = 0 & F_2'(0) = \ell & F_2(1) = F_2'(1) = 0 \end{array}$$

$$\begin{aligned} F_3(\xi) &= F_1(1-\xi) \\ F_4(\xi) &= -F_2(1-\xi) \end{aligned} \tag{5.123}$$

where the notation F_i' is used for $\frac{dF}{d\xi}$ (see figure 5.22). In this manner one obtains the matrix of shape functions

$$\boldsymbol{F}_e^T(\xi) = \begin{bmatrix} 1 - 3\xi^2 + 2\xi^3 \\ \ell\xi(1-\xi)^2 \\ \xi^2(3-2\xi) \\ \ell\xi^2(\xi-1) \end{bmatrix} \tag{5.124}$$

associated with the element degrees of freedom

$$\boldsymbol{q}_e^T = \begin{bmatrix} w_1 & \psi_1 & w_2 & \psi_2 \end{bmatrix} \tag{5.125}$$

One computes successively

- the kinetic energy of the element

$$\mathcal{T}_e = \frac{1}{2}\dot{\boldsymbol{q}}_e^T \boldsymbol{M}_e \dot{\boldsymbol{q}}_e \tag{5.126}$$

with the elementary mass matrix

$$\boldsymbol{M}_e = \int_0^1 m(\xi)\boldsymbol{F}_e^T(\xi)\boldsymbol{F}_e(\xi)\ell\, d\xi \tag{5.127}$$

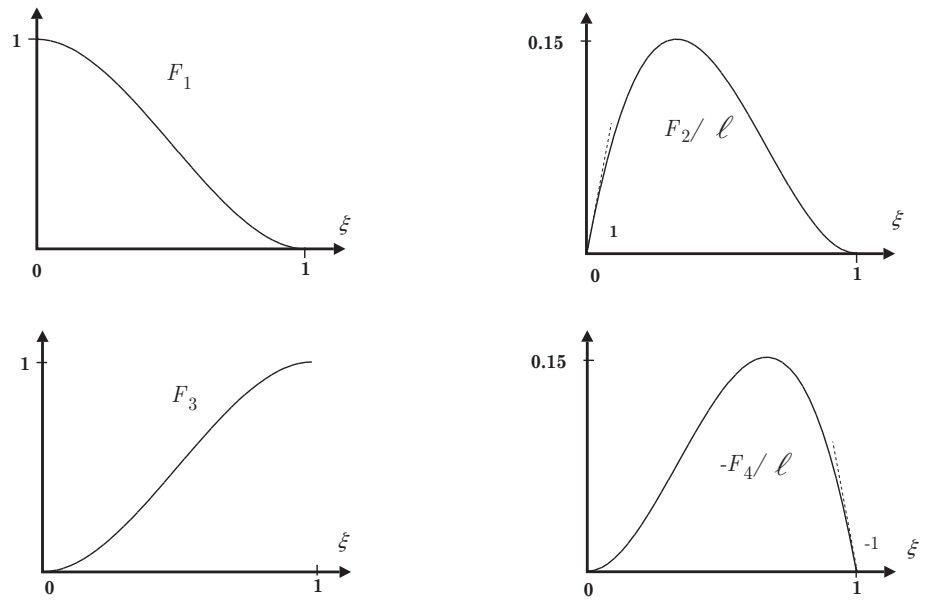

Figure 5.22: Shape functions: Hermitian polynomials of the third order

- the strain energy of the element

$$\mathcal{V}_{int,e} = \frac{1}{2}\boldsymbol{q}_e^T \boldsymbol{K}_e \boldsymbol{q}_e \tag{5.128}$$

with the elementary stiffness matrix

$$\boldsymbol{K}_e = \int_0^1 EI(\xi) \left(\frac{d^2\boldsymbol{F}_e}{d\xi^2}\right)^T \left(\frac{d^2\boldsymbol{F}_e}{d\xi^2}\right) \frac{d\xi}{\ell^3} \tag{5.129}$$

- the virtual work of external loads

$$\delta\mathcal{V}_{ext,e} = -\delta\boldsymbol{q}_e^T \boldsymbol{g}_e(t) \tag{5.130}$$

with the vector of external loads

$$\boldsymbol{g}_e(t) = \int_0^1 \boldsymbol{F}_e^T(\xi) p(x,t) \ell \, d\xi \tag{5.131}$$

For an element of uniform characteristics excited by a constant distributed load p_0 we

explicitly obtain

$$\boldsymbol{K}_e = \frac{EI}{\ell^3}\begin{bmatrix} 12 & 6\ell & -12 & 6\ell \\ 6\ell & 4\ell^2 & -6\ell & 2\ell^2 \\ -12 & -6\ell & 12 & -6\ell \\ 6\ell & 2\ell^2 & -6\ell & 4\ell^2 \end{bmatrix} \tag{5.132}$$

$$\boldsymbol{M}_e = \frac{m\ell}{420}\begin{bmatrix} 156 & 22\ell & 54 & -13\ell \\ 22\ell & 4\ell^2 & 13\ell & -3\ell^2 \\ 54 & 13\ell & 156 & -22\ell \\ -13\ell & -3\ell^2 & -22\ell & 4\ell^2 \end{bmatrix} \tag{5.133}$$

$$\boldsymbol{g}_e = \frac{p_0\ell}{2}\begin{bmatrix} 1 \\ \frac{\ell}{6} \\ 1 \\ \frac{-\ell}{6} \end{bmatrix} \tag{5.134}$$

One can verify that the stiffness matrix has one translational rigid body mode

$$\boldsymbol{u}_{trans}^T = [1 \;\; 0 \;\; 1 \;\; 0]$$

and one rotational rigid body mode about the center of mass

$$\boldsymbol{u}_{rot}^T = [\frac{-\ell}{2} \;\; 1 \;\; \frac{\ell}{2} \;\; 1]$$

It is easily verified that the quadratic form $\boldsymbol{u}_{trans}^T \boldsymbol{M} \boldsymbol{u}_{trans}$ is equal to the translation inertia $m\ell$ and that $\boldsymbol{u}_{rot}^T \boldsymbol{M} \boldsymbol{u}_{rot}$ yields the rotatory inertia $\frac{m\ell^3}{12}$.

Example: the beam clamped at both ends

Because the number of degrees of freedom of a finite element model rapidly becomes too large to allow for explicit calculations, only a very limited number of examples can be treated if one does not make use of numerical solution methods. The beam clamped at both ends is one of the few cases well suited to calculation by hand: we will treat it successively with a two-element mesh and a three-element mesh to obtain quantitative information on the convergence of the method.

Two finite element model

After application of the boundary conditions, only two degrees of freedom are left in the model: displacement w_2 and slope ψ_2 at the center of the beam. The localization vectors of these elements are

$$\begin{array}{ll} \text{element 1 :} & \begin{pmatrix} 0 & 0 & 1 & 2 \end{pmatrix} \\ \text{element 2 :} & \begin{pmatrix} 1 & 2 & 0 & 0 \end{pmatrix} \end{array}$$

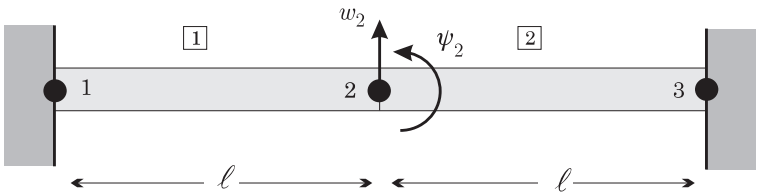

Figure 5.23: Modeling of the clamped–clamped beam using two finite elements

giving the assembled mass and stiffness matrices

$$\boldsymbol{K} = \frac{EI}{\ell^3}\begin{bmatrix} 24 & 0 \\ 0 & 8\ell^2 \end{bmatrix} \qquad \boldsymbol{M} = \frac{m\ell}{420}\begin{bmatrix} 312 & 0 \\ 0 & 8\ell^2 \end{bmatrix}$$

It can be observed that, owing to symmetry, the eigensolutions contained in the model are directly uncoupled.

The solution of the eigenvalue problem yields

$$\begin{aligned} \omega_1^2 &= \frac{24\times 420}{312}\,\frac{EI}{m\ell^4} = 32.31\frac{EI}{m\ell^4} \\ & \quad \boldsymbol{q}_{(1)}^T = \begin{bmatrix} 1 & 0 \end{bmatrix} \\ \omega_2^2 &= 420\frac{EI}{m\ell^4} \\ & \quad \boldsymbol{q}_{(2)}^T = \begin{bmatrix} 0 & 1 \end{bmatrix} \end{aligned} \tag{5.135}$$

The first eigenmode is *symmetric* while the second one is *antisymmetric*. This approximate result may be compared to the exact closed-form solution

$$\begin{aligned} \omega_1^2 &= 516.92\frac{EI}{mL^4} \qquad \text{in place of } 500.55\frac{EI}{mL^4} \\ \omega_2^2 &= 6720.0\frac{EI}{mL^4} \qquad \text{in place of } 3803.1\frac{EI}{mL^4} \end{aligned}$$

It is thus observed that the two-element model restores with acceptable accuracy the first frequency, but that the approximation adopted is not able to represent the second eigenmode correctly.

Three finite element model

This time, four degrees of freedom are left in the structural model (figure 5.24)

$$\boldsymbol{q}^T = \begin{bmatrix} w_2 & \psi_2 & w_3 & \psi_3 \end{bmatrix}$$

and the three elements of the model have the localization vectors

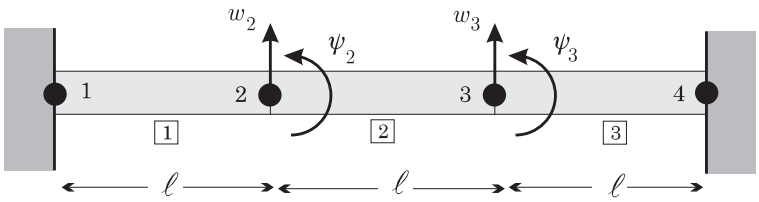

Figure 5.24: Modeling of the clamped-clamped beam using three finite elements

$$\begin{array}{ll} \text{element } 1: & \left(\begin{array}{cccc} 0 & 0 & 1 & 2 \end{array} \right] \\ \text{element } 2: & \left(\begin{array}{cccc} 1 & 2 & 3 & 4 \end{array} \right] \\ \text{element } 3: & \left(\begin{array}{cccc} 3 & 4 & 0 & 0 \end{array} \right] \end{array}$$

giving the assembled stiffness and mass matrices

$$\boldsymbol{K} = \frac{EI}{\ell^3} \begin{bmatrix} 24 & 0 & -12 & 6\ell \\ 0 & 8\ell^2 & -6\ell & 2\ell^2 \\ -12 & -6\ell & 24 & 0 \\ 6\ell & 2\ell^2 & 0 & 8\ell^2 \end{bmatrix}$$

$$\boldsymbol{M} = \frac{m\ell}{420} \begin{bmatrix} 312 & 0 & 54 & -13\ell \\ 0 & 8\ell^2 & 13\ell & -3\ell^2 \\ 54 & 13\ell & 312 & 0 \\ -13\ell & -3\ell^2 & 0 & 8\ell^2 \end{bmatrix}$$

Although the resulting model has four degrees of freedom this time, it is still possible to compute its eigensolutions explicitly by taking advantage of symmetry of the system.

- *Symmetric modes :* The symmetric modes must satisfy the conditions

  $$w_3 = w_2 \qquad\qquad \psi_3 = -\psi_2$$

  and therefore by setting $\boldsymbol{y}^T = [w_2 \;\; \psi_2]$ we can change the variables

  $$\boldsymbol{q} = \boldsymbol{C}\boldsymbol{y}$$

  with the matrix of constraints

  $$\boldsymbol{C}^T = \begin{bmatrix} 1 & 0 & 1 & 0 \\ 0 & 1 & 0 & -1 \end{bmatrix}$$

  We transform the eigenvalue problem into a problem of dimension 2×2

  $$\boldsymbol{K}^*\boldsymbol{y} = \omega^2 \boldsymbol{M}^*\boldsymbol{y}$$

  with $\boldsymbol{K}^* = \boldsymbol{C}^T\boldsymbol{K}\boldsymbol{C}$ and $\boldsymbol{M}^* = \boldsymbol{C}^T\boldsymbol{M}\boldsymbol{C}$. The reduced matrices are

  $$\boldsymbol{K}^* = \frac{EI}{\ell^3} \begin{bmatrix} 24 & -12\ell \\ -12\ell & 12\ell^2 \end{bmatrix} \qquad\qquad \boldsymbol{M}^* = \frac{m\ell}{210} \begin{bmatrix} 366 & 13\ell \\ \ell & 11\ell^2 \end{bmatrix}$$

By setting $\lambda = \dfrac{\omega^2 m\ell^4}{210EI}$ we then obtain the eigenvalue problem

$$\begin{bmatrix} 24-366\lambda & -12\ell-13\ell\lambda \\ -12\ell-13\ell\lambda & 12\ell^2-11\ell^2\lambda \end{bmatrix} \begin{bmatrix} w_2 \\ \psi_2 \end{bmatrix} = \boldsymbol{0}$$

and its characteristic equation

$$3857\lambda^2 - 4968\lambda + 144 = 0$$

The solutions are $\lambda = 0.02967$ and $\lambda = 1.2584$; they correspond to the first and third modes of the complete system, giving the approximate eigenvalues

$$\begin{aligned} \omega_1^2 &= 6.2305\frac{EI}{m\ell^4} \\ \omega_3^2 &= 264.26\frac{EI}{m\ell^4} \end{aligned}$$

or, in terms of the total beam length $L = 3\ell$

$$\begin{aligned} \omega_1^2 &= 504.67\tfrac{EI}{mL^4} \\ \omega_3^2 &= 21\,405\tfrac{EI}{mL^4} \end{aligned} \tag{5.136}$$

The associated eigenmodes are

$$\begin{aligned} \boldsymbol{q}_{(1)}^T &= \begin{bmatrix} 1 & \frac{1.061}{\ell} & 1 & \frac{-1.061}{\ell} \end{bmatrix} \\ \boldsymbol{q}_{(3)}^T &= \begin{bmatrix} 1 & \frac{-15.39}{\ell} & 1 & \frac{15.39}{\ell} \end{bmatrix} \end{aligned} \tag{5.137}$$

- *Antisymmetric eigenmodes:* Similarly, the antisymmetric modes obey

$$w_3 = -w_2 \qquad\qquad \psi_3 = \psi_2$$

The matrix of constraints is thus

$$\boldsymbol{C}^T = \begin{bmatrix} 1 & 0 & -1 & 0 \\ 0 & 1 & 0 & 1 \end{bmatrix}$$

and yields the reduced stiffness and mass matrices

$$\boldsymbol{K}^* = \frac{EI}{\ell^3}\begin{bmatrix} 72 & 12\ell \\ 12\ell & 20\ell^2 \end{bmatrix} quad \boldsymbol{M}^* = \frac{m\ell}{210}\begin{bmatrix} 258 & -13\ell \\ -13\ell & 5\ell^2 \end{bmatrix}$$

By setting also $\lambda = \dfrac{\omega^2 m\ell^4}{210EI}$, we obtain the eigenvalue problem

$$\begin{bmatrix} 72-258\lambda & 12\ell+13\ell\lambda \\ 12\ell+13\ell\lambda & 20\ell^2-5\ell^2\lambda \end{bmatrix} \begin{bmatrix} w_2 \\ \psi_2 \end{bmatrix} = \boldsymbol{0}$$

and the characteristic equation

$$1121\lambda^2 - 5832\lambda + 1296 = 0$$

with the roots $\lambda = 0.2326$ and $\lambda = 4.9699$, which correspond to eigenmodes 2 and 4 of the complete system. The eigenvalues are

$$\begin{aligned} \omega_2^2 &= 3\,956.9\frac{EI}{mL^4} \\ \omega_4^2 &= 84\,537\frac{EI}{mL^4} \end{aligned} \tag{5.138}$$

The eigenmode associated with eigenvalue ω_2^2 is

$$\boldsymbol{q}_{(2)}^T = \left[\begin{array}{cccc} 1 & \frac{-0.798}{\ell} & -1 & \frac{-0.798}{\ell} \end{array}\right] \tag{5.139}$$

Gathering the results, the numerical values are compared to the exact ones in table 5.3.

$\omega_r^2 \frac{mL^4}{EI}$			
r	2 elements	3 elements	exact
1	516.92	504.67	500.55
2	6720.0	3956.9	3803.1
3	—	21405.	14620.
4	—	84537.	39944.

Table 5.3: Beam clamped at both ends: eigenvalues computed by finite elements

It can be observed that the number of nearly converged eigenvalues is equal to half the number of degrees of freedom in the model: it results from the aptitude of the model to represent the corresponding mode shape correctly.

It can also be observed that all approximations obtained are upper bounds to the exact ones, a property resulting from the conformity of the displacement field used to construct the finite element model.

5.3.4 Three-dimensional beam element without shear deflection

Element generation

In many problems of structural dynamics, beam behavior has to be described with arbitrary orientation in space when the beam is subjected to combined loading (bending in two orthogonal directions, extension and torsion). Such general behavior may be modeled as follows.

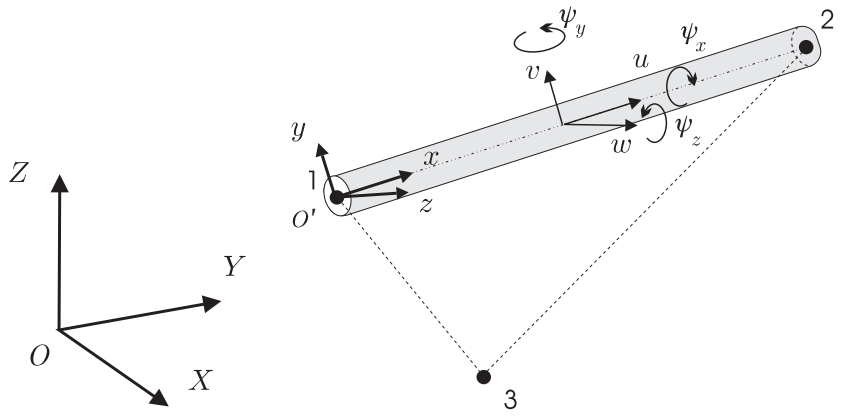

Figure 5.25: Three-dimensional beam element

Let $OXYZ$ be a structural axis frame and $O'xyz$ be a local frame attached to the beam element.

Let us make the following assumptions:

1. Axis $O'x$ is the beam neutral axis, chosen in such a way that a bending moment does not produce any axial deformation. Conversely, an axial load induces only axial deformation.

2. Axes $O'y$ and $O'z$ are the principal inertia axes for bending, defined in such a way that a bending moment about $O'y$ produces no bending about $O'z$, and conversely.

In the context of the kinematic Bernoulli assumptions for beams with no shear deflection, let us express the strain energy of the beam element in the form

$$\mathcal{V}_{int,e} = \frac{1}{2}\int_0^\ell \left[EI_z \left(\frac{\partial^2 v}{\partial x^2}\right)^2 + EI_y \left(\frac{\partial^2 w}{\partial x^2}\right)^2 + EA\left(\frac{\partial u}{\partial x}\right)^2 + GJ_x \left(\frac{\partial \psi_x}{\partial x}\right)^2 \right] dx \qquad (5.140)$$

where

- The first term represents the bending energy in plane $O'xy$. It is computed in terms of the displacement field $v(x)$ and of the bending stiffness about the local axis $O'z$

$$EI_z = \int_A E(y,z) y^2 \, dA$$

- The second term represents the bending energy in plane $O'xz$. It is computed in terms of the displacement field $w(x)$ and of the bending stiffness about the local axis $O'y$

$$EI_y = \int_A E(y,z) z^2 \, dA$$

- The third term represents the extension energy of the beam. It is computed in terms of the axial displacement $u(x)$ and of the axial stiffness

$$EA = \int_A E(y,z) \, dA$$

- The fourth term represents the torsional deformation energy of the beam. It is computed in terms of the local rotation ψ_x and the torsional stiffness GJ_x, the latter being evaluated following the classical techniques used in strength of materials with the assumption of free cross-sectional warping.

The elementary stiffness matrix is computed in terms of the element degrees of freedom expressed in local axes

$$\boldsymbol{q}_{eL}^T = \left[\begin{array}{cccccccccccc} u_1 & v_1 & w_1 & \psi_{x_1} & \psi_{y_1} & \psi_{z_1} & u_2 & v_2 & w_2 & \psi_{x_2} & \psi_{y_2} & \psi_{z_2} \end{array} \right] \tag{5.141}$$

noting that the rotations ψ_y and ψ_z are linked to deflections by

$$\psi_z = \frac{\partial v}{\partial x} \qquad\qquad \psi_y = -\frac{\partial w}{\partial x} \tag{5.142}$$

For the torsion term, we assume linear variation of the torsion angle: it thus takes the same form as the extension term.

By taking account of the results (5.140), the discretized strain energy of the beam element may be expressed in the form

$$\mathcal{V}_{int,e} = \frac{1}{2} \boldsymbol{q}_{eL}^T \boldsymbol{K}_{eL} \boldsymbol{q}_{eL} \tag{5.143}$$

where the elementary stiffness matrix in local axes is given by

$$\boldsymbol{K}_{eL} = \left[\begin{array}{cccccccccccc} \frac{EA}{\ell} & & & & & & & & & & & \\ 0 & \frac{12EI_z}{\ell^3} & & & & & & & & & & \\ 0 & 0 & \frac{12EI_y}{\ell^3} & & & & & & \text{Sym.} & & & \\ 0 & 0 & 0 & \frac{GJ_x}{\ell} & & & & & & & & \\ 0 & 0 & \frac{-6EI_y}{\ell^2} & 0 & \frac{4EI_y}{\ell} & & & & & & & \\ 0 & \frac{6EI_z}{\ell^2} & 0 & 0 & 0 & \frac{4EI_z}{\ell} & & & & & & \\ \frac{-EA}{\ell} & 0 & 0 & 0 & 0 & 0 & \frac{EA}{\ell} & & & & & \\ 0 & \frac{-12EI_z}{\ell^3} & 0 & 0 & 0 & \frac{-6EI_z}{\ell^2} & 0 & \frac{12EI_z}{\ell^3} & & & & \\ 0 & 0 & \frac{-12EI_y}{\ell^3} & 0 & \frac{6EI_y}{\ell^2} & 0 & 0 & 0 & \frac{12EI_y}{\ell^3} & & & \\ 0 & 0 & 0 & \frac{-GJ_x}{\ell} & 0 & 0 & 0 & 0 & 0 & \frac{GJ_x}{\ell} & & \\ 0 & 0 & \frac{-6EI_y}{\ell^2} & 0 & \frac{2EI_y}{\ell} & 0 & 0 & 0 & \frac{6EI_y}{\ell^2} & 0 & \frac{4EI_y}{\ell} & \\ 0 & \frac{6EI_z}{\ell^2} & 0 & 0 & 0 & \frac{2EI_z}{\ell} & 0 & \frac{-6EI_z}{\ell^2} & 0 & 0 & 0 & \frac{4EI_z}{\ell} \end{array} \right] \tag{5.144}$$

The kinetic energy is computed in a similar manner

$$\mathcal{T}_e = \frac{1}{2}\int_0^\ell m\left(\dot{u}^2 + \dot{v}^2 + \dot{w}^2\right)\,dx + \frac{1}{2}\int_0^\ell mr^2\dot{\psi}_x^2\,dx \tag{5.145}$$

The first three terms represent the translational kinetic energy and the last one describes the rotational kinetic energy about the longitudinal axis, with r being the gyration radius about $O'x$ defined by

$$mr^2 = \int_A \rho\left(y^2 + z^2\right)\,dA$$

It is worthwhile to notice that the rotational kinetic energy about axes $O'y$ and $O'z$ is implicitly contained in the translation terms: the only contribution neglected in (5.145) is the rotational energy of the cross section which always remains very low for a slender beam.

Expression (5.145) may be discretized in the form

$$\mathcal{T}_e = \frac{1}{2}\dot{\boldsymbol{q}}_{eL}^T\boldsymbol{M}_{eL}\dot{\boldsymbol{q}}_{eL} \tag{5.146}$$

where the elementary mass matrix computed in local axes from the displacement approximations adopted is given by

$$\frac{\boldsymbol{M}_{eL}}{m\ell} = \begin{bmatrix}
\frac{1}{3} & & & & & & & & & & & \\
0 & \frac{13}{35} & & & & & & & & & & \\
0 & 0 & \frac{13}{35} & & & & & & \text{Sym.} & & & \\
0 & 0 & 0 & \frac{r^2}{3} & & & & & & & & \\
0 & 0 & \frac{-11\ell}{210} & 0 & \frac{\ell^2}{105} & & & & & & & \\
0 & \frac{11\ell}{210} & 0 & 0 & 0 & \frac{\ell^2}{105} & & & & & & \\
\frac{1}{6} & 0 & 0 & 0 & 0 & 0 & \frac{1}{3} & & & & & \\
0 & \frac{9}{70} & 0 & 0 & 0 & \frac{13\ell}{420} & 0 & \frac{13}{35} & & & & \\
0 & 0 & \frac{9}{70} & 0 & \frac{-13\ell}{420} & 0 & 0 & 0 & \frac{13}{35} & & & \\
0 & 0 & 0 & \frac{r^2}{6} & 0 & 0 & 0 & 0 & 0 & \frac{r^2}{3} & & \\
0 & 0 & \frac{13\ell}{420} & 0 & \frac{-\ell^2}{140} & 0 & 0 & 0 & \frac{11\ell}{210} & 0 & \frac{\ell^2}{105} & \\
0 & \frac{-13\ell}{420} & 0 & 0 & 0 & \frac{-\ell^2}{140} & 0 & \frac{-11\ell}{210} & 0 & 0 & 0 & \frac{\ell^2}{105}
\end{bmatrix} \tag{5.147}$$

Coordinate transformations

In order to express the elementary stiffness and mass matrices in structural axes, the rotation operator from local frame to structural frame is constructed as follows (figure 5.26).

Let $P_i = (X_i, Y_i, Z_i)$, $(i = 1, 2)$ be the end nodes of the beam element.

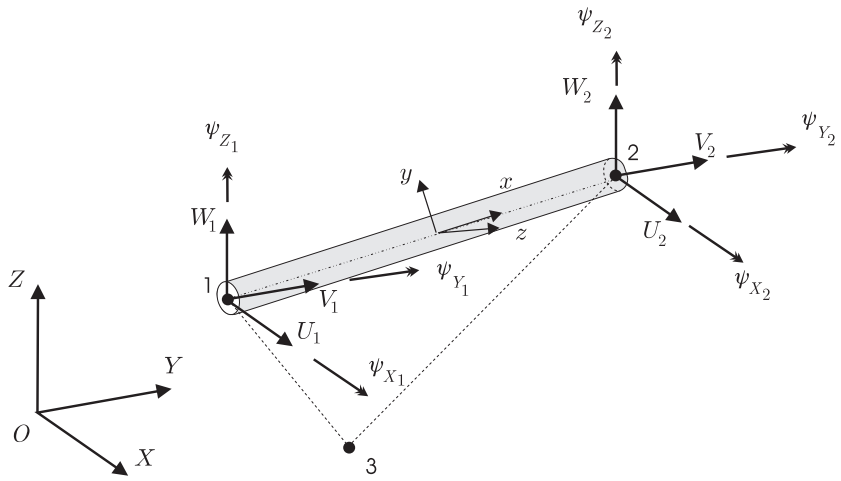

Figure 5.26: Three-dimensional beam element in arbitrary axes

1. The direction $\vec{e}_x$ of the element's neutral axis is defined in the structural frame by the components

$$\vec{e}_x = \left[\begin{array}{ccc} \dfrac{X_2 - X_1}{\ell} & \dfrac{Y_2 - Y_1}{\ell} & \dfrac{Z_2 - Z_1}{\ell} \end{array} \right]$$

2. Directions $\vec{e}_y$ and $\vec{e}_z$ corresponding to the principal axes of the cross section are constructed from the knowledge of a third point $P_3 = (X_3, Y_3, Z_3)$ contained in the plane Oxz. Noting

$$\vec{d}_i = [X_i - X_1 \;\; Y_i - Y_1 \;\; Z_i - Z_1]$$

direction $\vec{e}_y$ is obtained from the vector operation

$$\vec{e}_y = \frac{\vec{d}_3 \times \vec{d}_2}{\| \vec{d}_3 \times \vec{d}_2 \|}$$

3. Direction $\vec{e}_z$ results from the cross product

$$\vec{e}_z = \vec{e}_x \times \vec{e}_y$$

4. The rotation operator $\boldsymbol{R}$ describing the frame transformation

$$\left[\begin{array}{c} x \\ y \\ z \end{array} \right] = \boldsymbol{R} \left[\begin{array}{c} X \\ Y \\ Z \end{array} \right]$$

is next constructed in terms of dot products of the base vectors

$$\boldsymbol{R} = \left[\begin{array}{ccc} \vec{e}_X \cdot \vec{e}_x & \vec{e}_Y \cdot \vec{e}_x & \vec{e}_Z \cdot \vec{e}_x \\ \vec{e}_X \cdot \vec{e}_y & \vec{e}_Y \cdot \vec{e}_y & \vec{e}_Z \cdot \vec{e}_y \\ \vec{e}_X \cdot \vec{e}_z & \vec{e}_Y \cdot \vec{e}_z & \vec{e}_Z \cdot \vec{e}_z \end{array} \right]$$

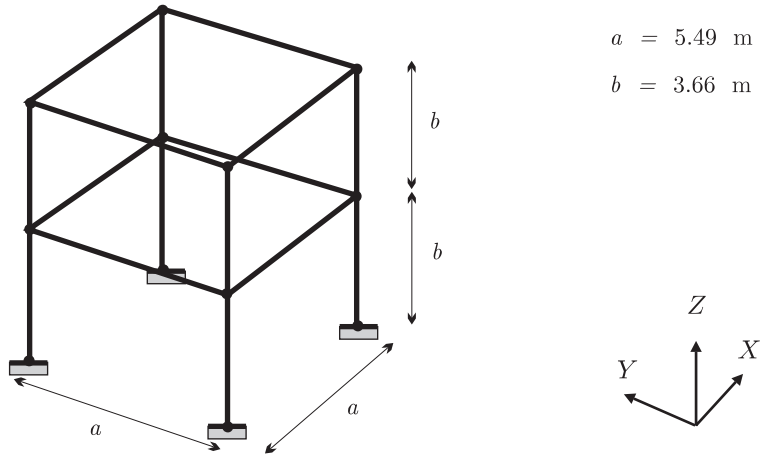

Figure 5.27: Three-dimensional portal frame

5. Displacements and rotations in local and in structural axes are linked respectively by

$$\begin{bmatrix} u \\ v \\ w \end{bmatrix} = \boldsymbol{R} \begin{bmatrix} U \\ V \\ W \end{bmatrix} \qquad \begin{bmatrix} \psi_x \\ \psi_y \\ \psi_z \end{bmatrix} = \boldsymbol{R} \begin{bmatrix} \psi_X \\ \psi_Y \\ \psi_Z \end{bmatrix}$$

from which we deduce the transformation to structural degrees of freedom for the element

$$\boldsymbol{q}_{eS}^T = \begin{bmatrix} U_1 & V_1 & W_1 & \psi_{X_1} & \psi_{Y_1} & \psi_{Z_1} & U_2 & V_2 & W_2 & \psi_{X_2} & \psi_{Y_2} & \psi_{Z_2} \end{bmatrix} \tag{5.148}$$

$$\boldsymbol{q}_{eL} = \boldsymbol{T}\boldsymbol{q}_{eS} \tag{5.149}$$

with

$$\boldsymbol{T} = \begin{bmatrix} \boldsymbol{R} & \boldsymbol{0} & \boldsymbol{0} & \boldsymbol{0} \\ \boldsymbol{0} & \boldsymbol{R} & \boldsymbol{0} & \boldsymbol{0} \\ \boldsymbol{0} & \boldsymbol{0} & \boldsymbol{R} & \boldsymbol{0} \\ \boldsymbol{0} & \boldsymbol{0} & \boldsymbol{0} & \boldsymbol{R} \end{bmatrix}$$

The resulting stiffness and mass matrices of the element expressed in structural axes are

$$\boldsymbol{K}_{eS} = \boldsymbol{T}^T \boldsymbol{K}_{eL} \boldsymbol{T} \qquad \boldsymbol{M}_{eS} = \boldsymbol{T}^T \boldsymbol{M}_{eL} \boldsymbol{T} \tag{5.150}$$

Example: analysis of a three-dimensional portal frame

Let us consider the portal frame of figure 5.27, composed of beams with the following characteristics:

- Properties of vertical beams $A = 5.14\ 10^{-3}\ \mathrm{m}^2$ $J_x = 1.73\ 10^{-7}\ \mathrm{m}^4$ $I_y = 6.9\ 10^{-6}\ \mathrm{m}^4$ $I_z = 8.49\ 10^{-5}\ \mathrm{m}^4$
- Properties of horizontal beams: $A = 5.68\ 10^{-3}\ \mathrm{m}^2$ $J_x = 1.76\ 10^{-7}\ \mathrm{m}^4$ $I_y = 1.2\ 10^{-4}\ \mathrm{m}^4$ $I_z = 7.3\ 10^{-6}\ \mathrm{m}^4$

The material is steel

$$E = 2.1\ 10^{11}\ \mathrm{N/m}^2 \qquad \nu = 0.3 \qquad \rho = 7.8\ 10^3\ \mathrm{kg/m}^3$$

The column bases are clamped to the ground and the local axes are defined as follows:

- Vertical beams
$$\vec{e}_x = \vec{e}_Z \qquad \vec{e}_y = \vec{e}_X \qquad \vec{e}_z = \vec{e}_Y$$
- Horizontal beams parallel to OX
$$\vec{e}_x = \vec{e}_X \qquad \vec{e}_y = \vec{e}_Y \qquad \vec{e}_z = \vec{e}_Z$$
- Horizontal beams parallel to OY
$$\vec{e}_x = \vec{e}_Y \qquad \vec{e}_y = -\vec{e}_X \qquad \vec{e}_z = \vec{e}_Z$$

Let us model the structure with sixteen 3-D beam elements of the type developed above. Each mesh intersection being a node, the model has 12 nodes and 72 degrees of freedom, 24 of them being fixed. The eigenfrequencies and mode shapes are then computed numerically and the results are presented on figure 5.28.

It is observed that modes 1 and 3 are the first bending modes in the planes OYZ and OXZ respectively. Mode 2 is the first torsion mode, and mode 4 is the second bending mode in plane OYZ.

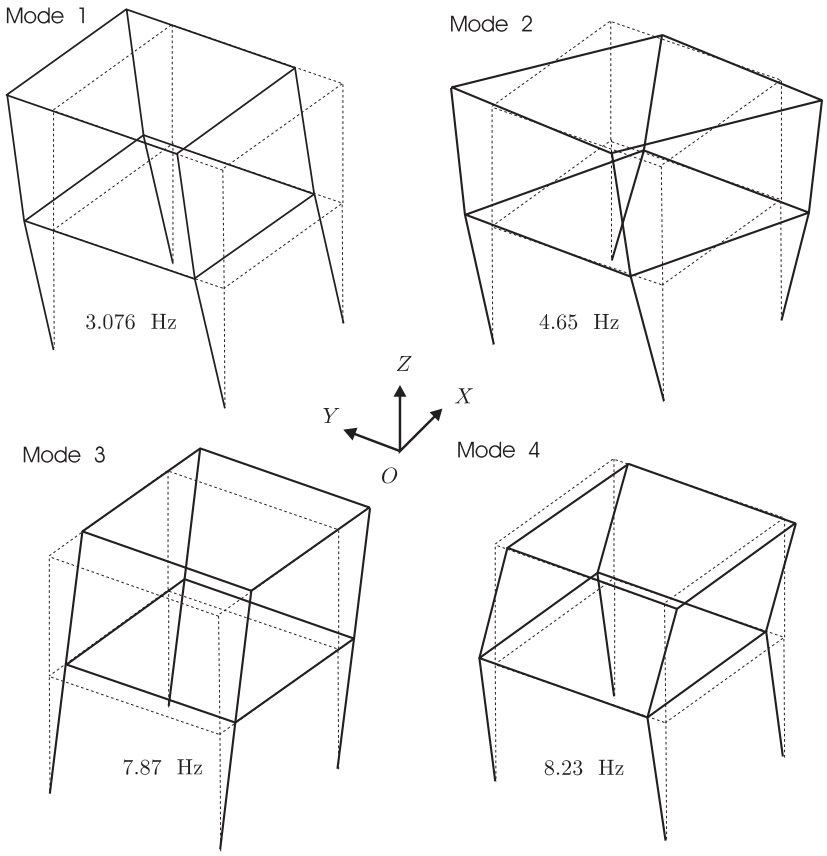

Figure 5.28: Mode shapes and eigenfrequencies of the portal frame

Bibliography

[1] C. Courant and D. Hilbert. *Methods of Mathematical Physics, vol. 1.* Interscience Publishers, New-York, 1953.

[2] D.J. Ewins. *Modal Testing: theory, practice and application.* Research Studies Press LTD, 2000. ISBN 0 86380 218 4.

[3] M. Géradin and D. Rixen. *Mechanical Vibrations. Theory and Application to Structural Dynamics.* Wiley & Sons, Chichester, 2d edition, 1997.

[4] J.L. Lagrange. *Méchanique Analytique.* Desaint, Paris, 1788. re-edited in 1811 under the title *Mécanique Analytique*, Courcier, Paris.

[5] M. Lalanne and G. Ferraris. *Rotor Prediction in Engineering.* John Wiley and Sons, Chichester, 1990.

[6] C. Lanczos. *The Variational Principles of Mechanics.* Mathematical Expositions, No. 4. University of Toronto Press, Toronto, Canada, 1949.

[7] N.M.M. Maia and J.M.M. Silva, editors. *Theoretical and Experimental Modal Analsysis.* Research Studies Press Ltd., Somerser, England, 1997. ISBN 0 86380 208 7.

[8] K.J. McConnel. *Vibration Testing: theory and practice.* John Wiley & Sons, 1995. ISBN 0 471 30435 2.

[9] L. Meirovitch. *Methods of Analytical Dynamics.* Mc Graw Hill Book Co, New-York, 1970.

[10] L. Meirovitch. *Computational Methods in Structural Dynamics.* Sijthoff and Noordhoff, 1980.

[11] J.W.S. Rayleigh. *The Theory of Sound, second edition.* Dover, 1896.

[12] V. Rochus, D.J. Rixen, and J.-C. Golinval. Monolithic modeling of electro-mechanical coupling in micro-structures. *Int. J. Num. Meth. Eng.* submitted.

[13] R.M. Rosenberg. *Analytical Dynamics of Discrete Systems.* Plenum Press, New York, 1977.

[14] N. Rouche, P. Habets, and M. Laloy. *Stability Theory by Liapunov's Direct Method*. Applied Mathematical Sciences, 22. Springer-Verlag, New-York, 1977.

[15] E.T. Whittaker. *A treatise on the Analytical Dynamics of Particles and Rigid Bodies*. Cambridge University Press, 1965.

[16] K. Zaveri. *Modal Analysis of Large Structures – Multiple Exciter Systems*. Brüel & Kjær, 1984. BT 0001-11.